The main objective of this PhD project is to contribute to the development of a quantitative model of *S.accharomyces cerevisiae* metabolism in winemaking conditions. This model would allow to assess the effect of different environmental variables and of a particular starter yeast strain not only on fermentation kinetics but also on the production of relevant fermentation products (such as ethanol, glycerol, acetic acid, or some volatile compounds). This model would be useful in the improvement and control of the fermentation process, as well as in the definition of a rational use of enological additives and starter cultures, in order to ensure and improve wine quality.

The research presented in this thesis has been performed in close collaboration with the Universitat Autònoma de Barcelona (Barcelona, Spain) in the context of the **Deméter** project (**D**esarrollo de **E**strategias y **M**étodos vitícolas y **E**nológicos frente al cambio climático. **A**plicación de nuevas **T**ecnologías que mejoren la **E**ficiencia de los procesos **R**esultantes). The Deméter project (http://www.cenitdemeter.es/) deals with the study of wine and winemaking adaptation to the new scenario produced by global warming.

upna Universidad Pública de Navarra
Nafarroako Unibertsitate Publikoa

Instituto de Ciencias de la Vid y del Vino

Gobierno de La Rioja

CSIC CONSEJO SUPERIOR DE INVESTIGACIONES CIENTÍFICAS

UNIVERSIDAD DE LA RIOJA

Tesis Doctoral - Rubén Martínez Moreno

RUBÉN MARTÍNEZ MORENO - TESIS DOCTORAL

Universidad Pública de Navarra
Instituto de ciencias de la Vid y del Vino

Departamento de Producción Agraria
Universidad Pública de Navarra

Laboratorio de Enología
Instituto de Ciencias de la Vid y del Vino

$$r_s = \begin{pmatrix} \mu \\ r_P \\ -r_S \end{pmatrix} = (\mu, r_{P_1}, \ldots, r_{S_i}, \ldots)^T$$

$$r_{S_i} = \mu \cdot Y_{XS_i} = \frac{\mu}{Y_{S_iX}} = \frac{1}{X}\frac{dS_i}{dt}$$

$$r_{P_i} = \mu \cdot Y_{XP_i} = \frac{\mu}{Y_{P_iX}} = \frac{1}{X}\frac{dP_i}{dt}$$

$$X + \sum_{i=1}^{M} Y_{XP_i} P_i - \sum_{i=1}^{N} Y_{XS_i} S_i = 0$$

$$r_{S_i} = Y_{XS_i}^{true}\mu + m_S; \quad Y_{SX} = \frac{\mu}{Y_{XS_i}^{true}\mu + m_S}$$

ADVANCED STUDIES OF YEAST METABOLISM UNDER WINEMAKING CONDITIONS. PAVING THE WAY FOR A PREDICTIVE MODEL.

RUBÉN MARTÍNEZ MORENO

Pamplona - Iruña, 2014

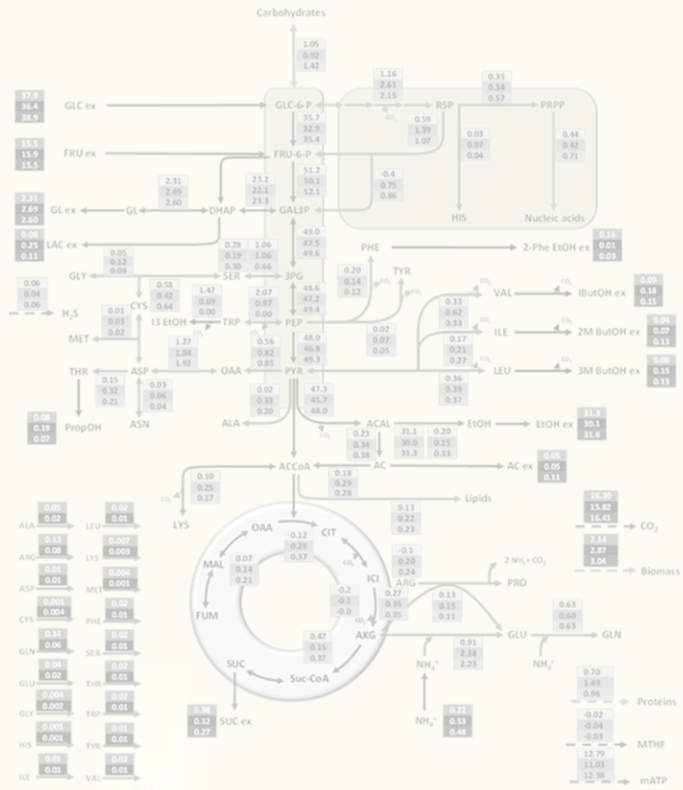

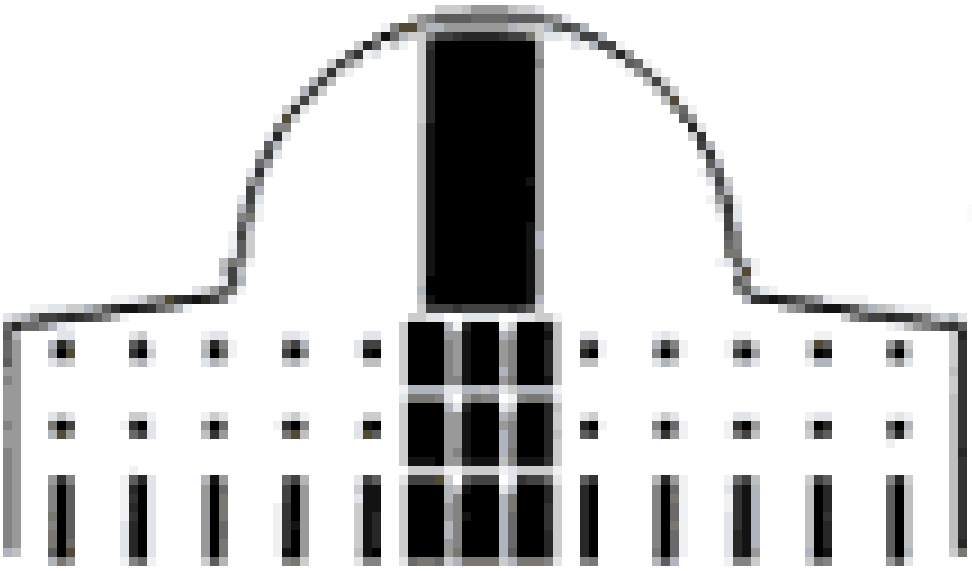

Departamento de Producción Agraria

Universidad Pública de Navarra

upna

Universidad Pública de Navarra
Nafarroako Unibertsitate Publikoa

ADVANCED STUDIES OF YEAST METABOLISM UNDER WINEMAKING CONDITIONS. PAVING THE WAY FOR A PREDICTIVE MODEL.

Trabajo presentado para optar al grado de Doctor (a través del programa de doctorado en biotecnología) por la Universidad Pública de Navarra por parte de

Rubén Martínez Moreno

Máster en Enología por la Universitat Rovira i Virgili
Licenciado en Biología por la Universidad de Salamanca
Licenciado en Bioquímica por la Universidad de Salamanca

upna
Universidad Pública de Navarra
Nafarroako Unibertsitate Publikoa

Directores de tesis:

Dr. D. Ramón González García (Profesor de investigación del CSIC)

Dra. Dª. Pilar Morales Calvo (Científico titular del CSIC)

Dr. D. Manuel Quirós Asensio (Contratado JAE-Doc del CSIC)

Tutor de la Universidad Pública de Navarra:

Antonio Gerardo Pisabarro de Lucas (Catedrático de universidad)

Los trabajos de investigación que conforman esta tesis doctoral han sido desarrollados en el Departamento de enología del Instituto de Ciencias de la Vid y el Vino (ICVV), España, apoyados por la financiación del Centro para el Desarrollo Tecnológico Industrial (CDTI). El doctorando, Rubén Martínez Moreno, ha sido beneficiario de una beca pre-doctoral del programa JAE del Consejo Superior de Investigaciones Científicas (CSIC) para desarrollar dichos trabajos.

The research described in this thesis was performed at the Department of Oenology, Research Centre of Vine-and- Wine-related Science (ICVV), Spain. Financial support was provided by the Centre for Industrial Technological Development (CDTI). Rubén Martínez Moreno was recipients of a pre-doctoral fellowship in the JAE program from the Spanish Council for Scientific Research (CSIC).

Tribunal de tesis

Presidente:
Dr. D. José Martínez Peinado
Catedrático de Universidad
Departamento de Microbiología
Universidad complutense de Madrid

Secretaria:
Dra. Dña. María Carmen Ancín Azpilicueta
Catedrático de Universidad
Departamento de Química Aplicada
Universidad Pública de Navarra

Vocal:
Dr. D. José Manuel Guillamón Navarro
Científico Titular
Instituto de Agroquímica y Tecnología de los Alimentos
Consejo Superior de Investigaciones científicas

Suplente:
Dr. D. Jesús Murillo Martínez
Catedrático de Universidad
Departamento de Producción Agraria
Universidad Pública de Navarra

Revisor externo:
Dr. D. Enrico Vaudano
Investigador
Dipartimento Microbiologia e Biologia Moleculare
Centro di Ricerca per L'Enologia

Revisor externo:
Dr. D. Ramón Mira de Orduña
Investigador
Ecole d'ingénieurs de Changins
Haute Ecole Spécialisée de Suisse Occidentale

Suplente:
Dra. Dña. Gemma Beltrán i Caselles
Profesor Adjunto
Departamento de Biotecnología
Universitat Rovira i Virgili

Dr. RAMÓN GONZÁLEZ GARCÍA, Profesor de Investigación del Consejo Superior de Investigaciones Científicas,

Dra. PILAR MORALES CALVO, Científico Titular del Consejo Superior de Investigaciones Científicas, y

Dr. MANUEL QUIRÓS ASENSIO, contratado JAE-Doc del Consejo Superior de Investigaciones Científicas

CERTIFICAN,

que la presente memoria de Tesis Doctoral titulada "**Advanced studies of yeast metabolism under winemaking conditions. Paving the way for a predictive model.**", elaborada por D. Rubén Martínez Moreno, ha sido realizada bajo su dirección y cumple las condiciones exigidas por la legislación vigente para optar al grado de Doctor.

Y para que así conste, firman el presente documento.

En Logroño a 10 de enero de 2014

Fdo. Dr. Ramón González García

Fdo. Dra. Pilar Morales Calvo

Fdo. Dr. Manuel Quirós Asensio

"Se templado en el beber, considerando que el vino demasiado ni guarda secreto ni cumple palabra"

Miguel de Cervantes Saavedra. 1615.
El ingenioso caballero Don Quijote de la Mancha. Cap. XLIII.

Contents

SUMMARY

Study of yeast physiology during the alcoholic fermentation in winemaking

A new approach to study yeast physiology during wine fermentation has been developed in this thesis. This methodology consists on mimicking a phase, period or event of wine fermentation in continuous culture after an exhaustive and detailed characterization of the alcoholic fermentation, a typical batch process. This technique has shown a high reproducibility and allowed obtaining accurate data for further analysis. On the other hand, a new metabolic model has been designed for metabolic flux analysis of yeast during wine fermentation. This model considers not only the central carbon and nitrogen metabolism but also incorporated reactions for the uptake of the main nitrogen sources present in wine as well as those involved in the synthesis of important volatile compounds, including acetic acid and fusel alcohols.

The strategy developed has been used for studying the effect of sugar content of grape must, fermentation temperature and growth rate on yeast physiology during the exponential growth phase of wine fermentation.

The study of the exponential growth phase of yeast during wine fermentation has allowed drawing different conclusions. Conversion rates were mainly affected by temperature and growth rate. The distribution of carbon fluxes during this period was not drastically modified by none of the variables studies, i.e. sugar content, temperature or dilution rate. However, pathways such as glycerol synthesis and the pentose phosphate pathway presented higher sensitivity to changes in the variables studied than others.

Correction of nitrogen deficiencies in grape must

Nitrogen deficiency in must is a frequent problem in wineries since low nitrogen content in grape juice could result in sluggish and/or stuck fermentations. In order to avoid these problems, different commercial products, mainly based on ammonium salts, are normally added during the early stages on the fermentative process. For these and other reasons, yeast nitrogen metabolism during wine fermentation has been a hot research topic for the last decades. Additionally,

several studies have pointed out the relevant role played by the nitrogen composition of must on the organoleptic properties of wine.

Our results have shown the simultaneous consumption of both ammonium and amino acids during the exponential growth phase of yeast. On the other hand, we have also demonstrated how temperature and growth rate modify the proportions of organic/inorganic nitrogen uptake. Both the concentration and nature of the nitrogen sources present in the medium have been shown to affect yeast metabolism. We have observed that the latter exerts a strong influence on carbon flux distribution of yeast during the transition from exponential growth phase to stationary phase, particularly on those pathways related to the production of volatile compounds, such as fusel alcohols, since this type of compounds are synthetized both catabolically from amino acids and anabolically from sugars.

As mentioned before, ammonium salts are used as a nitrogen supplement in order to solve nitrogen deficiencies in grape must. Nevertheless, the use of ammonium as additive has been reported to cause some problems related to volatile acidity. For this reason, several companies have developed other nutritional supplements based on organic nitrogen sources, such as amino acids or inactive dry yeast. However, we have demonstrated that the appropriate use of ammonium not only solves nitrogen deficiencies but also reduces volatile acidity and increases glycerol content in wine. Furthermore, our results have also shown that a clear increase in volatile acidity occurs when a grape must is over-supplemented with ammonium. An accurate knowledge about the content and composition of nitrogen sources in grape must together with specific nitrogen requirements of the yeast strain is therefore required for an optimal design of ammonium supplementation protocols. These would take into account both the amount of compound to be used and the timing of addition.

Future perspectives

The study presented in this thesis should be extended to the last phases of wine fermentation. These stages are characterized by very low growth rate (very close to zero or zero), high ethanol content in the medium, the absence of nitrogen sources and the presence of fructose as main carbon source. Although a first approach to the study of these stages has been shown in Chapter II, chemostat

cultures, necessarily performed at very low dilution rates, do not seem to be an ideal tool for mimicking these phases.

new studies should be developed. So, other cultivation tools such as retentostats could be tested in order to obtain more detailed results in the future. In our opinion, the best approach to study low–growth rate phases would be the use batch culture. However, certain assumptions, such as the constant value of the biomass, should be taken into account in order to simplify the subsequent mathematical analysis of data.

The methodology proposed in this thesis could be used for analyzing the effects of other environmental factors such as pH, acidity or oxygen on yeast physiology. Results obtained in Chapter V provide the basis for studying the effect of nitrogen supplementation on the distribution of metabolic flux distribution in yeast. Indeed, generated data are currently being used to refine models expanded to genome-scale that would allow for an accurate prediction of the production of key metabolites (i.e. ethanol, glycerol, acetic acid) in industrial batch fermentations. These studies could be extended with the use of ^{13}C and ^{15}N. As described in Chapter I, the use of isotope-labeled carbon (and/ or nitrogen) allows a more accurate determination of flux distribution through metabolic pathways with higher complexity by analyzing ^{13}C (^{15}N) enrichment patterns of intracellular metabolites.

Further studies should be developed in order to determine how nutritional supplementation during alcoholic fermentation could work as a flavor modulator. This would allow for the formulation and design of new supplementation protocols attending the particular needs of specific grape musts.

Chapter I

♦

General introduction

CHAPTER I

General introduction

Contents

Saccharomyces cerevisiae in winemaking

A historical overview

In 6000 BC, the horse had not yet been domesticated, but civilized nations from Caucasus and Mesopotamia already exploited yeast for the production of alcoholic beverages and bread (Cavalieri et al. 2003). Archeological evidences of wine production have also been found in Egypt, Phoenicia, Greece and Crete from 5000 to 2000 BC. Romans were responsible for spreading wine production all around the Mediterranean (in 500 BC, wine was being produced in Sicily, Italy, France, Spain, Portugal and northern Africa) and the north of Europe (including Balkan States, Germany or Britain). In the 16th century, European explorers introduced the vine culture into the New World (mainly in Mexico, Argentina, Peru and Chile). In the 18th century, viticulture and winemaking were present in all continents except for Oceania. It was during the 19th century when Australia and New Zealand imported vine cultivation and wine production (Pretorius 2000).

Although the origin of wine history is dated around 8000 years ago, the transformation of grape juice into wine has only been studied during the last two centuries. It was not until the second half of the 19th century that Louis Pasteur unequivocally established the key role of living yeast in alcoholic fermentation (Pasteur 1857). This acceptance was preceded by an intense scientific debate in which the most accepted idea postulated was a chemical process and that yeast was a non-living catalyst (Barnett 2003a). In the 20th century, yeast has contributed to the extensive development of biology and other bio-sciences (biochemistry, biotechnology…) due to its role as a model organism (Barnett 2003a). Nowadays, the genome sequence of different yeast strains, including the wine strain *Saccharomyces cerevisiae* EC1118 (Novo et al. 2009), is available. However, the complexity arising from the genome sequencing projects did not fulfill the expectations for whole network comprehension. For that reason, new global approaches have been developed during the last decades in order to extend our knowledge about the internal working of biological systems integrating transcriptomic, proteomic, fluxomic or metabolomic data (Pizarro et al. 2007a).

The alcoholic fermentation I: carbon metabolism

Fermentation (from the Latin verb *fervere*; which means to boil) is a metabolic process whereby electrons released from nutrients are ultimately transferred to molecules obtained from the breakdown of those same nutrients, and energy (ATP) is obtained by substrate-level phosphorylation. The same word is used in industrial microbiology to define any large-scale microbial process (usually driven by bacteria or fungi; or in some cases by biochemical catalyzers) to make products useful to human beings. Both meanings could be applied to wine fermentation. Briefly, in winemaking, sugar (glucose and fructose) is converted by a series of metabolic steps into carbon dioxide (CO_2), ethanol and other minor, but important, metabolites such as glycerol, acetic, lactic, pyruvic or succinic acid, among others (Pretorius 2000, Bell and Henschke 2005). This process is driven by yeast and is performed in fermentation tanks in wineries.

Glycolysis is the central pathway for carbon and energy metabolism under anaerobic conditions in yeast (Figure 1). One molecule of glucose or fructose is taken up by the yeast and consecutively broken down by glycolysis into two molecules of pyruvate. The result of this process is the net formation of two ATP molecules (from ADP and inorganic phosphate), along with the reduction of two molecules of NAD^+ to NADH. During alcoholic fermentation, pyruvate is then mainly converted into ethanol and carbon dioxide and the NADH previously produced during glycolysis is re-oxidized to NAD^+ in order to maintain the redox balance (Barnett 2003b).

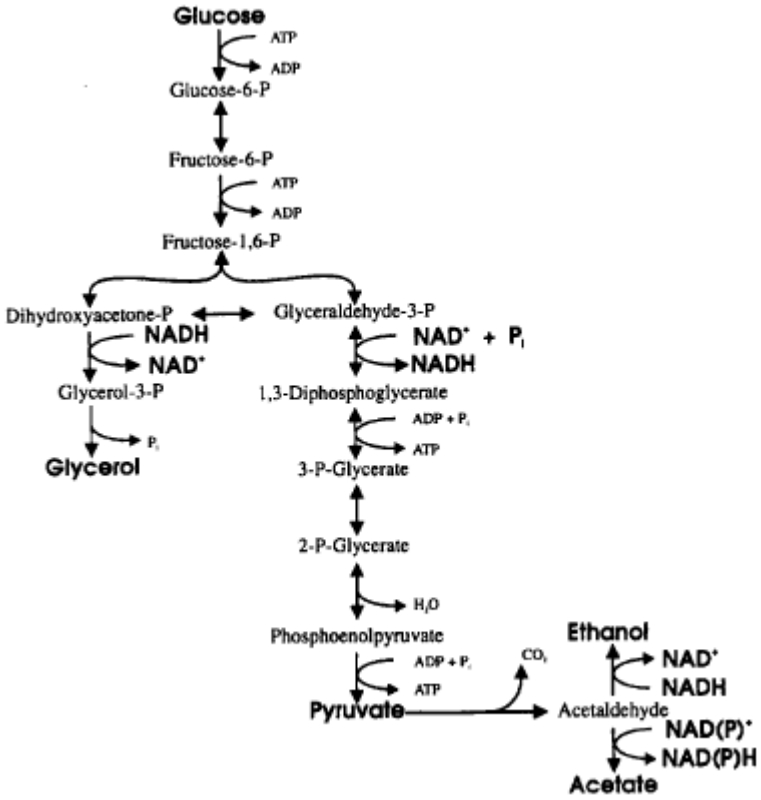

Figure 1. Catabolic pathways of S. cerevisiae for the fermentative metabolism of glucose. Adapted from Schulze et al. (1996b).

In contrast to fermentative metabolism, the major fate of pyruvate in respiratory metabolism (that requires aerobic conditions) is the synthesis of acetyl-coenzyme A, the “fuel” for the Tri-Carboxylic Acid cycle (TCA cycle). The main products formed throughout this mitochondrial pathway are oxaloacetate (OAA), alpha-ketoglutarate (AKG) and reduction equivalents, NADH and FADH (Figure 2). This reduction equivalents are used for ATP production in the mitochondrial electron-chain, where electrons are transferred to oxygen. From an energetic point of view, respiration (which involves the total degradation of sugars into water and carbon dioxide) is more efficient than fermentation, up to 36 ATP molecules are produced per glucose while only 2 ATP molecules are synthetized during fermentation. Under anaerobic conditions, the TCA cycle does not work as such but it presents a two-branch operating mode and only a basal activity is maintained in

order to produce oxaloacetate and alpha-ketoglutarate (Camarasa et al. 2003). Under aerobic conditions, *S. cerevisae* shows a respiro-fermentative metabolism. In fact, sugar is mainly catabolized by a fermentative process even under aerobic conditions. This phenomenon is known as the Crabtree effect (Swanson and Clifton 1948). After several decades of research (De Deken 1966, Petrik et al. 1983, Käppeli 1986), the Crabtree effect is currently defined as "the occurrence of alcoholic fermentation under aerobic conditions" according to Pronk et al. (1996). Käppeli (1986) argue that the Crabtree effect is due to an "overflow of the limited respiratory capacities" in the branching point of pyruvate metabolism.

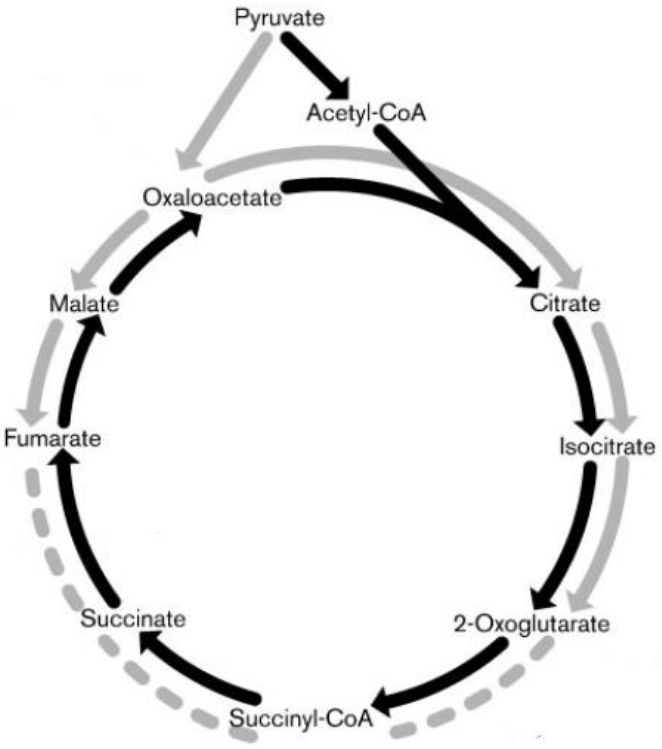

Figure 2. Tri-Carboxylic Acid cycle during fermentation and respiration. Black arrows: the TCA pathway works as a cycle during respiration. Solid grey arrows: the TCA pathway operates as an oxidative branch and a reductive branch during fermentative metabolism. Broken grey line: the point at which the cycle is interrupted during fermentation has not yet been identified. Adapted from Camarasa et al. (2003).

As mentioned above, apart from ethanol and CO_2, relatively minor but relevant products are also formed during the alcoholic fermentation of grape must. These include succinic acid, the main by-product from the TCA cycle that is released into wine, acetic acid, glycerol, biomass, and may other molecules in even lower amounts.

Acetic acid derives from acetaldehyde, which is also the intermediate between pyruvate and ethanol (Figure 1). Although lipid metabolism under anaerobic conditions has some peculiarities (extensively reviewed by Belviso et al. (2004)), the biosynthesis of acetic acid is important in anaerobic metabolism both for maintaining redox balance and for lipid formation (Pigeau and Inglis 2005, Vilanova et al. 2007). In addition, this acid has an important impact on the final aroma profile of wine and is the main contributor to volatile acidity (Barnett 2003b). In fact, an excess of acetic acid in wine produces a characteristic and undesirable vinegar aroma.

Glycerol production branches off from glycolysis at the level of dihydroxyacetone phosphate (DHAP). In this pathway, glycerol is formed by the reduction of DHAP to glycerol 3-phosphate (G3P) and the subsequent dephosphorylation of G3P to glycerol (Figure 1). The main role of glycerol biosynthesis in the anaerobic growth of yeast is the regeneration of NAD^+ for maintaining internal redox balance. Moreover, the final product of the pathway, glycerol, has a key role as a compatible solute in conditions of high extracellular osmolarity and as precursor of acyl-glycerol lipids. Glycerol also has an impact on the organoleptic properties of wine. An adequate content of this polyol (5-14 g L^{-1} according to Swiegers et al. (2005)) has a noticeable effect on apparent sweetness, wine viscosity and/or oily mouth-feel (Bell and Henschke 2005, Styger et al. 2011, Jain et al. 2012).

Lactic acid is also produced from the glycolytic intermediate DHAP through the methyl-glyoxal bypass. This minor pathway only works under overflow metabolism (Pronk et al. 1996). However, most lactic acid present in wine does not derive from yeast metabolism, but is produced during malo-lactic fermentation by the metabolism of lactic acid bacteria (Novo et al. 2012).

Glucose 6-phosphate is not only the starting-point of glycolysis but also the entry point for the biosynthesis of structural and reserve carbohydrates and the

pentose phosphate pathway (PPP). PPP provides key precursors for the synthesis of biomass, specifically amino acids (histidine), nucleotides and redox equivalents in the form of NADPH (Rodrigues et al. 2006, Villadsen et al. 2011).

The alcoholic fermentation II: nitrogen metabolism

Although grape must is a very complex medium containing carbon sources (glucose and fructose), nitrogen sources (amino acids and ammonium), vitamins and other trace elements, it sometimes does not provide the amounts of all nutrients that yeast requires for the complete conversion of sugars into ethanol and CO_2. Specifically, nitrogen is often the limiting-nutrient during wine fermentation. Insufficient nitrogen in must, which can be due to several factors such as timing of harvest, grape ripeness or vineyard fertilization practices, could be the reason for sluggish or stuck fermentations (Bisson and Butzke 2000). Nitrogen is not only important for fermentation performance but also plays a crucial role in the final organoleptic characteristics of wine (Rapp and Versini 1991, Swiegers et al. 2005, Styger et al. 2011). For these reasons, nitrogen metabolism of yeast in winemaking has become an important research topic during the last decades (see Bell and Henschke (2005) for an extensive review).

The amino acids and ammonium present in the medium are internalized into the cell and metabolized during the first 24-48 hours of fermentation. Nitrogen sources are uptaken through (specific or unspecific) membrane permeases whose presence and activity are regulated by specific and/or general regulatory mechanisms such as SPS system (whose name derives from the three components involved: SSY1, PTR3 and SSY5), Nitrogen Catabolite Repression (NCR) and general amino acid control (Boer 2005). These regulatory systems have thoroughly been studied in wine fermentation during the last decades (Beltran et al. 2004, Beltran et al. 2005, Beltran et al. 2007, Godard et al. 2007, Crépin et al. 2012). According to the last studies published, the direct contribution of exogenous amino acids to protein biosynthesis is limited. Amino acids are mainly channeled throughout the nitrogen metabolism pathways (Crépin 2012). Most of them are catabolized via transamination reactions, where the amino group of the amino acid is transferred directly to alpha-ketoglutarate to yield glutamate and the cognate alpha-ketoacid. Amino acids can also be catabolized via deamination reactions with

the production of free ammonium. This free ammonium together with ammonium directly incorporated from the medium are used for the synthesis of glutamic acid and/or glutamine (Figure 3). In contrast, proline, the most abundant amino acid in grape juice, follows a completely different assimilation pathway (actually proline is not an amino acid but an imino acid). However, *S. cerevisiae* is not able to use it as nitrogen source under winemaking conditions since oxygen is needed for proline conversion into glutamate (Ingledew et al. 1987).

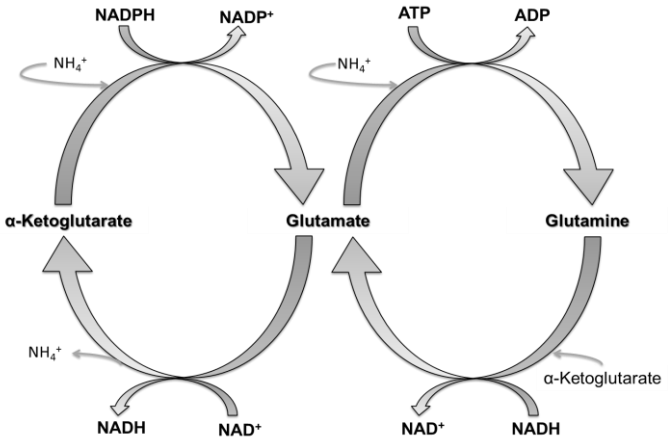

Figure 3. Enzymatic reactions involved in central nitrogen metabolism.

Nitrogen composition of grape must plays a significant role in the release of glycerol (Albers et al. 1996, Remize et al. 2000, Erasmus et al. 2004). Depending on the degree of reduction of the nitrogen incorporated, nitrogen metabolism could function as a net producer of NAD^+ or as a net producer of NADH. Ammonium assimilation could be considered as NADH producer since ammonium is more reduced than the amino group from amino acids. Accordingly, when yeasts are growing in ammonium as the sole or the main nitrogen source, an increase on glycerol production is observed (Albers et al. 1996, Schulze et al. 1996a, Bakker et al. 2001).

The production of volatile compounds important for the final aroma profile of wine is also affected by the nitrogen composition of must and nitrogen metabolism (Morakul et al. 2011). This is the case of the aroma compounds produced through

the Ehrlich pathway (Ehrlich (1904), extensively reviewed by Hazelwood et al. (2008)), the main dissimilatory pathway for branched-chain amino acids (leucine, isoleucine and valine), aromatic amino acids (pheylalanine, tyrosine and tryptophan) and sulfur-containing amino acids such as methionine (Figure 4). Under winemaking conditions, this catabolic pathway leads to the formation of fusel alcohols since the reductive branch of the pathway is not functional under anaerobic conditions. These volatile compounds could have a positive or negative impact on the final aroma of wine, depending on its concentration. On the other hand, fusel alcohols could also be synthetized from sugars (Figure 4). Both the anabolic and the catabolic pathways for fusel alcohols production could play a role in the maintenance of internal redox balance.

Yeasts are also able to synthetize and release esters, which can contribute to the fruity and floral aroma of wines. The most common esters present in wine are the ethyl esters and the esters of acetate, including ethyl-acetate. The production of aroma compounds (fusel alcohols, esters and fatty acids) derived from yeast metabolism is strain-dependent (Bell and Henschke 2005).

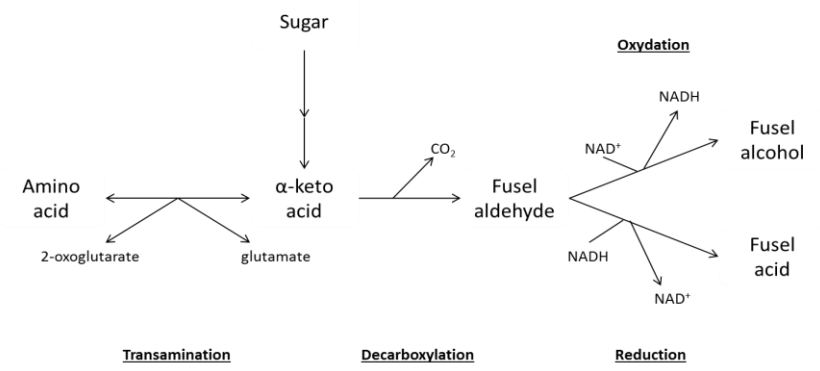

Figure 4. The Ehrlich pathway for the synthesis of fusel alcohols.

Wine fermentation in the 21st century: the effect of global warming

As documented in the last issue of the report of the Intergovernmental Panel on Climate Change (IPCC), prepared under the aegis of the United Nations Environment Program (UNEP) and the World Meteorological Organization (WMO), the average global temperature has increased by 0.6 °C during the 20th century (GIEC 2001). The effects of global warming in the melting of the ice polar caps, the rising of sea levels or the changes in the global distribution of certain organism (including vectors of diseases) are well known by public opinion. However, global warming, one of the major challenges in the history of mankind (Grassl 2011), affects other human activities like agriculture (Lavalle et al. 2009, Trnka et al. 2011). The effects of climate change in vine cultivation and wine production is a current research topic in wine-producing countries like Spain, South Africa, Italy, Australia or France (Battaglini et al. 2009, Mira de Orduña 2010, Salazar-Parra et al. 2010, Alonso and O'Neill 2011). Nowadays, viticultural regions are located in relatively narrow geographical areas between 30° to 50° N and 30° to 40° S with growing season average temperatures between 12 and 22 °C (Schultz and Jones 2010). As a consequence of global warming, wine region climate suitability was shown to shift upward in elevation and/or poleward, while southern European regions are expected to become progressively unsuitable for grapevine cultivation because of increasing temperatures and water deficit (Moriondo et al. 2013).

The quality of wine is strongly influenced by the chemical composition of grape berries at harvest time. This berry composition is affected by several factors such as climate, vine genotype, management, or soil type, among others. According to recent studies, climate is the dominant factor that influences berry and wine quality (Storchmann 2005, Makra et al. 2009, Barnuud et al. 2013). Although climate presents several variables (temperature, precipitations, solar radiation…), temperature has been recognized as a primary driver of vine growth and berry composition (Jones et al. 2005, Soar et al. 2008). For example, a higher average temperature during the growing season results in increased rates of sugar accumulation and advanced fruit maturity dates (Petrie and Sadras 2008, Bock et al. 2013). This elevated sugar content in must results in a higher osmotic pressure and an increase on the carbon/nitrogen sources ratio, which produce changes in yeast physiology during wine fermentation. On the one hand, this higher osmotic

pressure increases the risk of sluggish or stuck fermentation. On the other hand, as a consequence of a high sugar content in grape must, wine presents a higher content of ethanol and low acidity. Moreover, the content of other fermentation by-products such as glycerol and acetic acid could also increase (Erasmus et al. 2004, Pigeau and Inglis 2005).

Metabolic flux analysis (MFA)

Principle

One of the more powerful approaches to determine the *in vivo* physiological status of a cell consists in the determination of its intracellular reaction rates. The complexity of cellular systems and the lack of a direct method to measure all those rates have derived in a number of different approaches for its determination. One of the most extended experimental approaches requires the establishment of a (pseudo) steady state in the metabolic system were the reaction rates can be considered stable. In those conditions, metabolic reaction rates are known as metabolic fluxes and their determination and study has been termed fluxomics. Together with other 'omics' approaches (i.e. transcriptomics, metabolomics…) they provide a solid basis towards understanding, and ultimately modifying, the behavior or biological systems.

Metabolic flux analysis is based on the stoichiometry of the metabolic reactions and the global mass balances under (pseudo) steady state assumption. In MFA, metabolite balances of intracellular reactions are coupled to the conversion rate of products and substrates measured extracellularly (Ostergaard et al. 2000, Iwatani et al. 2008). The result is a flux map that shows the distribution of anabolic and catabolic fluxes over the described metabolic network (Figure 5).

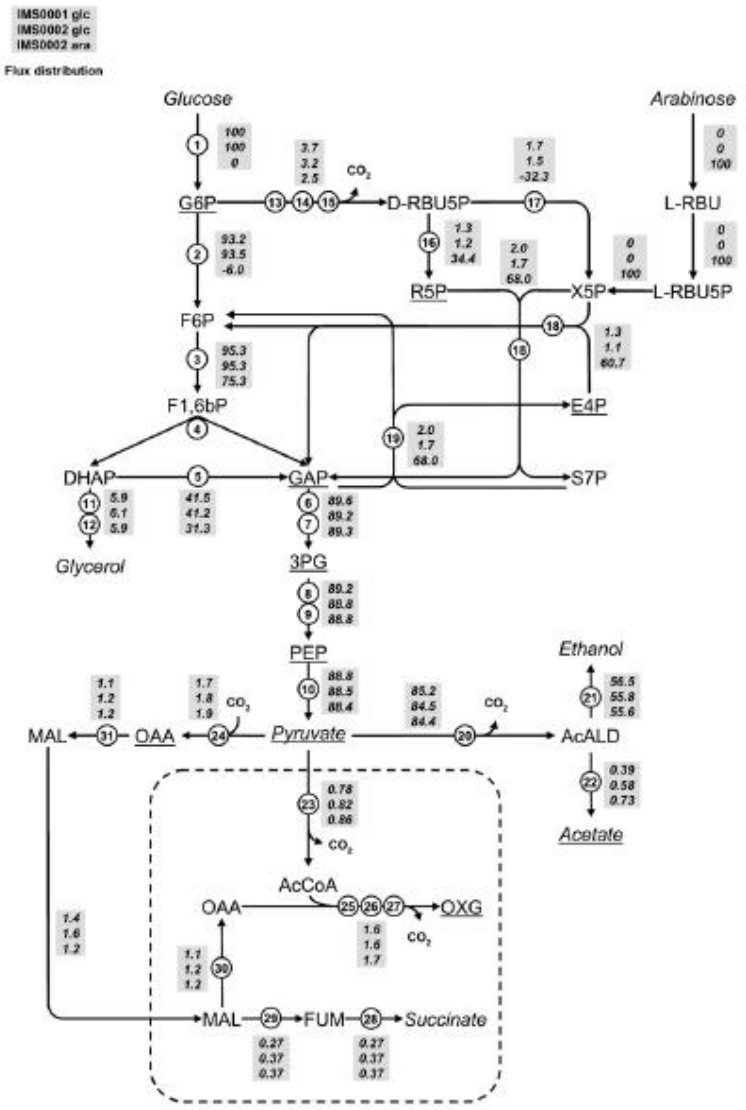

Figure 5. Example of flux map from Wisselink et al. (2010).

Two main different approaches have been used to study the metabolic flux distribution in biological systems: metabolic flux analysis (MFA) and constraints-based flux analysis (Lee et al. 2011) also known as metabolic flux balancing (MFB). In the first approach, the metabolic network model is first reduced in complexity so that it can be solved using the available experimental data. If the data includes only extracellular input-output information it is known as classic MFA. This approach

allows analyzing only low complexity networks but a unique solution, or metabolic flux distribution, is obtained. Nevertheless it has been traditionally applied with notable success in a number of systems usually including only central carbon metabolism reactions. This approach is usually extended by including carbon labeling data (usually ^{13}C) and therefore it is known as ^{13}C-MFA. In this way networks of a higher degree of complexity can be solved. ^{13}C-based flux analysis utilizes an isotope-labeled carbon substrate and allows the determination of intracellular fluxes in metabolic networks by analyzing ^{13}C enrichment patterns of intracellular metabolites with nuclear magnetic resonance or gas chromatography–mass spectrometry (Wiechert 2001, Sauer 2006). ^{13}C-MFA will not be further described in this chapter; for an extensive review see Wiechert (2001). The second approach allows to use metabolic networks of genome scale complexity. The constraint-based flux analysis is a general mathematical method using optimization-based simulation techniques to analyze cellular metabolism under a specified environmental or genetic condition (Park et al. 2009). The solutions derive from the optimization (maximization or minimization) of a certain objective function (maximization of biomass production, minimization of resources required…) while, at the same time, certain constraints must be obeyed (ex. the direction of certain fluxes or the maximum flux a certain step can reach…). This method is also frequently referred to as Flux Balancing Analysis (FBA) or Metabolic Flux Balancing (MFB), in the bibliography.

According to Visser (2002), MFA has several useful applications: i) calculation of the intracellular flux distribution from extracellular measurements (Vallino and Stephanopoulos 1993), ii) calculation of extracellular fluxes that have not been measured iii) calculation of theoretical yields (van Gulik and Heijnen 1995), iv) calculation of the optimal pathway configuration for production of a novel compound, v) evaluation of the possible effects of the introduction of new pathways, vi) identification of new metabolic pathways (Nissen et al. 1997), vii) prediction of genotype-phenotype relationships (Schuster et al. 1999), viii) identification of rigid and flexible nodes (Stephanopoulos and Vallino 1991) and ix) localization of metabolic bottlenecks (van Gulik et al. 2000).

Experimental framework: cultivation systems

MFA has been applied to study the metabolism of cells growing in three different cultivation systems: batch cultures, fed-batch cultures and continuous cultures (Table 1).

Table 1. Types of cultivation.

Cultivation system	Characteristics	Sub-type of cultivation	Characteristics
Batch	$F_{in} = F_{out} = 0$ Volume is constant		
Fed-batch	$F_{in} \neq 0$; $F_{out} = 0$ Volume increases		
Continuous	$F_{in} = F_{out} \neq 0$ Volume is constant	Chemostat	Growth rate (μ) is limited by the rate of nutrients supply
		Turbidostat	The organism grows reaching a steady state of fixed turbidity
		Auxostat	D changes to maintain a certain factor constant, for example, pH.

F: Flow; D: Dilution rate (h^{-1})

Batch culture is the most commonly applied cultivation form for microorganisms, and is the traditional way for producing fermented foods such as beer or wine. In batch cultivation, no substrate is added to the initial charge and no product is removed until the process is finished. Initially, all the nutrients are present in excess amounts and do not restrict the specific growth rate of the culture. The

main characteristic of this kind of culture is a very high glycolytic activity and a specific growth rate that reach its maximum level ($\mu = \mu_{max}$) under the existing environmental conditions during the exponential growth phase. Classically, anaerobic yeast growth in a batch culture has been divided into four phases: i) lag phase, ii) exponential growth phase, iii) stationary phase and iv) death phase. This mode of cultivation has a very dynamic nature due to the progressive depletion of carbon sources and accumulation of fermentation products and by-products that involve quasi-instantaneous variations on its composition. This fact complicates the study of metabolic fluxes of cells growing in a batch mode.

Fed-batch cultivations could be considered as a variation of batch cultures, whereby after the initial exponential growth period, the limiting substrate is added to the fermenter in a controlled way to enable optimal formation of biomass and/or product at a rate sustainable by the fermentation set-up. This cultivation technique has been broadly applied in industry for the large-scale production of biomass and different compounds (antibiotics, among others). The product accumulates in high concentration in the reactor and is harvested after the process is stopped (Roubos 2002). Fed-batch cultivations are used for the production of Active Dry Wine Yeast (ADWY), usually utilized as starter cultures in wineries (González et al. 2011).

Continuous culture is based on a constant feeding and product removal at the same rate, therefore keeping the volume of the fermentation vessel constant. The preferred choice of microbial cultivations for quantitative physiology research is the chemostat. Other types of continuous cultivation are described in Table 1. A diagrammatic representation of a chemostat set-up is shown in Figure 6. The theory of chemostat proposed by Monod (1950) (extensively reviewed by Hoskisson and Hobbs (2005)) is based on the fact that the specific growth rate of a biological system is governed by the external concentration of a limiting nutrient. Chemostat is the method of cultivation allowing for the highest degree of control over environmental parameters. In this way, all relevant parameters, including the specific growth rate, can be kept constant. The time period when growth rate, conversion rates of metabolites and concentration of metabolites and biomass in the broth are constant is known as steady-state. Under steady-state conditions the specific growth rate μ (h^{-1}) equals the dilution rate. It is generally accepted that (pseudo) steady state can be assumed after five residence times (one residence

time is the time required to replace a volume of growth medium equivalent to the working volume of the bioreactor). One of the main advantages of chemostat is that it provides appropriate and "user-friendly" data for the mathematical development of MFA.

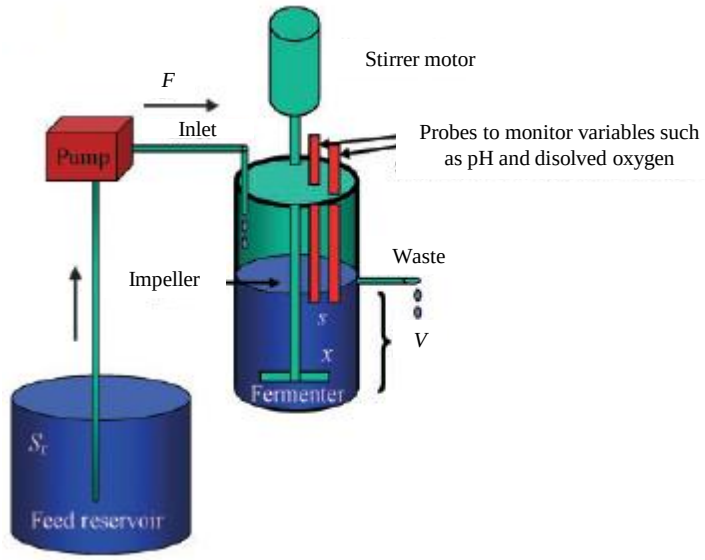

Figure 6. Diagrammatic representation of a continuous culture set-up from Hoskisson and Hobbs (2005). The arrow indicate the direction of medium flow. The pump regulates medium flow rate (F) in relation to the working volume (V) of the vessel to determine the dilution rate (D) and hence the specific growth rate of the culture (μ). S_r represents the concentration of the limiting nutrient in the feed reservoir, x is the concentration of biomass in the fermenter and s represents the concentration of the residual limiting nutrient in the fermenter.

Bioprocess modeling

Different approaches for bioprocess modeling have been followed during the last decades (Table 2). In this chapter, only black-box models and stoichiometric models are considered since both of them have been used in wine research. Figure 7 shows a schematic comparison of these two types of models. For an extensive review see Stephanopoulos et al. (1998).

Table 2. Approaches for bioprocess modeling according to Roubos (2002).

Knowledge- and data- based models (mathematical models)	White-box models
	Semi-mechanistics models
	Grey-box models
	Black-box models
Operating-regime models	Global models
	Multiple local models
Structured models	Unstructured models
	Structured models
Metabolic network models	Stoichiometric models
	Dynamic models

Black-box models apply a model structure and derive the corresponding equations and parameters with the purpose to reproduce experimental data but ignoring the internal operation. Reasonably accurate models are generally easy to obtain even without a detailed knowledge of the system, but they may suffer from weak extrapolation properties. Therefore, three main characteristics could be associated to black-box models: data-dependent, low extrapolation power and easy construction from a limited knowledge of the process (Roubos 2002). Black-box models are usually used as a first step in MFA. They have been applied for closing elemental and redox balances and for checking the robustness of the data obtained from experiments in combination with methods proposed by Wang and Stephanopoulos (1983) and Lange and Heijnen (2001) for experimental data reconciliation.

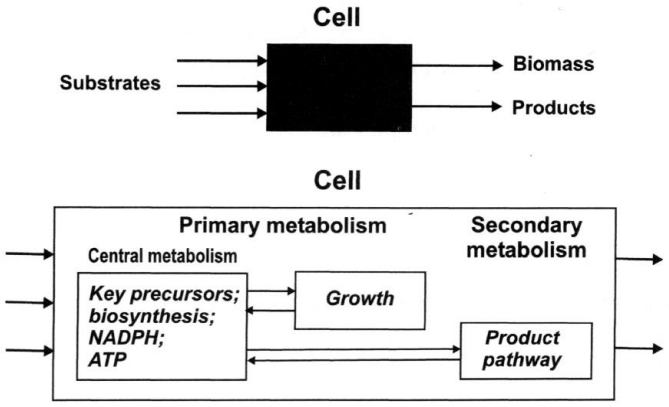

Figure 7. Comparison between black-box models and stoichiometric models from Roubos (2002).

Stoichiometric models are one of the two major classes of metabolic network models. In general, metabolic network models are based on a description of the biochemical reactions that take place inside the cell (Bailey 1991), as shown in Figure 7. Fortunately, biochemistry of *S. cerevisiae* has been extensively studied during the last century and, nowadays, this information has been made available through web platforms (KEGG: Kyoto Encyclopedia of Genes and Genomes - http://www.genome.jp/kegg/- or SGD: Saccharomyces Genome Database - http://pathway.yeastgenome.org/-). A stoichiometric model considers the uptake of extracellular substrates (by passive or active transport mechanisms), their channeling through primary metabolism and the consequent production of key precursors, energy (ATP) and reducing equivalents (NADH). Cell growth is taken into account trough the incorporation of reactions leading to the formation of building blocks (nucleotides, amino acids, sugars and fatty acids) from the key precursors and its polymerization into the biomass (nucleic acids, protein, lipids and carbohydrates). Traditionally, these models are characterized by a relative low number of reactions and metabolites (usually lower than 100 in both cases) and finding a unique solution is usually possible. During the last decade different genome scale stoichiometric mathematical models have been proposed. The existence of different models for the same organisms fostered the development of a consensus model publicly available which is being periodically upgraded (Herrgard

et al. 2008, Heavner et al. 2012). In the case of *S. cerevisiae*, it has reached version 7 at present time.

Although stoichiometric models have been applied to batch and fed-batch experiments (assuming that the biomass composition does not change within a fixed time period), they are in general applied to flux analysis of cells growing in continuous culture under (pseudo) steady state conditions (Roubos 2002). According to Nielsen (2001), metabolic network models are useful for i) identification of metabolic network structure (biochemical reaction), ii) quantification of the fluxes through the branches or the network and iii) identification of the control steps within the metabolic network.

Mathematical framework

Metabolism can be mathematically represented by means of a (stoichiometric) matrix (**S**) of size *m* x *n*. Rows of this matrix represent one unique compound and columns one reaction (for a system with *m* compounds and *n* reactions). The entries in each column are the stoichiometric coefficients of the metabolites participating in a reaction. In a metabolic reaction, a negative coefficient indicates the consumption of a metabolite while a positive coefficient indicates the production of a certain metabolite. A zero value is used for every metabolite that does not participate in the reaction. The flux through all of the reactions in a network is represented by the vector **v**, which has a length of *n*. The concentrations of all metabolites are represented by the vector **x**, with length *m*. Under steady state conditions $d\mathbf{x}/d\mathbf{t} = \mathbf{0}$ and $\mathbf{S}\cdot\mathbf{v} = \mathbf{0}$ (Orth et al. 2010).

Any **v** that satisfies this equation is said to be in the null space of **S**. In any realistic metabolic model, there are more reactions than compounds (n > m), in other words, there are more unknown variables than equations. This fact implies that there is no unique solution to this system of equations. For this reason, constraints are usually utilized to solve this mathematical systems since they define a range of solutions and allow to identify and analyze single points within the solution space. For example, we may be interested in identifying which point corresponds to the maximum growth rate or to maximum ATP production of an organism, given its particular set of constraints. MFB is one method for identifying such optimal points within a constrained space (Figure 8).

MFB seeks to maximize or minimize an objective function $Z = \mathbf{c}^T\mathbf{v}$, which can be any linear combination of fluxes, where **c** is a vector of weights indicating how much each reaction (such as the biomass reaction when simulating maximum growth) contributes to the objective function. In practice, when only one reaction is desired for maximization or minimization, **c** is a vector of zeros with a value of 1 at the position of the reaction of interest (Calik and Ozdamar 2002, Orth et al. 2010).

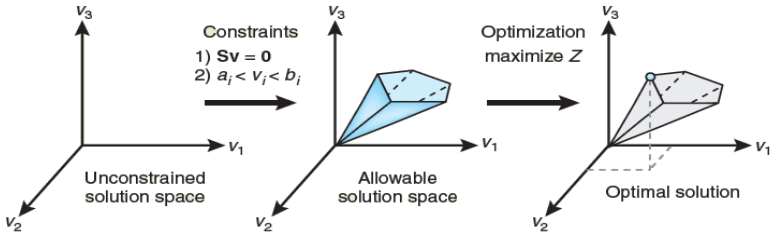

Figure 8. The conceptual basis of constraint-based modeling from Orth et al. (2010). With no constraints, the flux distribution of a biological network may lie at any point in a solution space. When mass balance constraints imposed by the stoichiometric matrix S (labeled 1) and capacity constraints imposed by the lower and upper bounds (a_i and b_i) (labeled 2) are applied to a network, it defines an allowable solution space. The network may acquire any flux distribution within this space. Through optimization of an objective function, MFA can identify a single optimal flux distribution that lies on the edge of the allowable solution space.

Optimization of such a system is accomplished by linear programming. MFA can thus be defined as the use of linear programming to solve the equation $\mathbf{S}\cdot\mathbf{v} = \mathbf{0}$, given a set of upper and lower bounds on **v** and a linear combination of fluxes as an objective function. The output of MFA is a particular flux distribution, **v**, which maximizes or minimizes the objective function (Orth et al. 2010, Lee et al. 2011).

Quantitative physiology in wine research

Although MFA was mainly developed in the 70's-80's (Otero and Nielsen 2010), this tool was not applied to wine research until the first decade of the 21st century. Modeling of wine process is a challenge for the current research in winemaking (Borneman et al. 2007). According to Charnomordic et al. (2010), the specific challenge is to provide a software with the ability to simultaneously handle

enough fermentations to be usable in practice for a winemaker in charge of a cellar. For that reason, new strategies for studying wine fermentation have been developed. Clement et al. (2011) proposed a new approach to study wine fermentation by using a continuous multistage bioreactor system. In this system, the first reactor was connected to the feeding tank containing sterile medium for mimicking the exponential growth phase of wine fermentation. The rest of tanks were connected in tandem as illustrated Figure 9 for mimicking the remaining stages of wine fermentation. This approach is currently being applied for studying yeast physiology during stationary phase in wine fermentations (Clement et al. 2013).

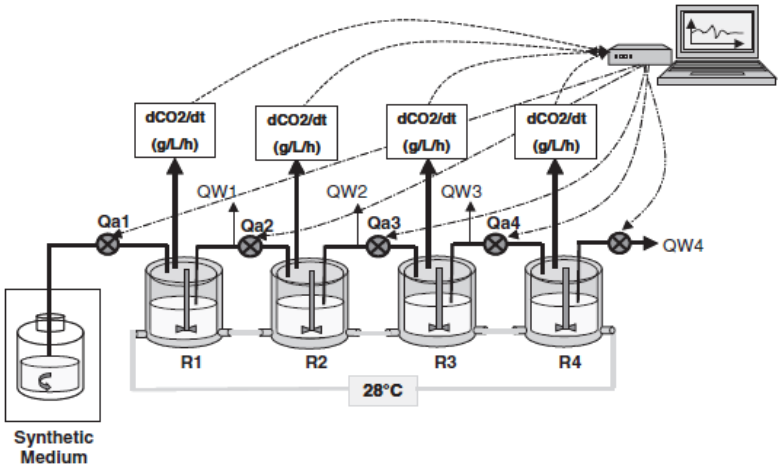

Figure 9. Multistage bioreactor system developed by Clement et al. (2012).

Studies of quantitative physiology have also been important to investigate how certain pathways operate in yeast during winemaking. For example, the work developed by Camarasa and co-workers (2003) showed the operating mode of the TCA cycle under winemaking conditions. In addition, this work also contributed to elucidate the importance of nitrogen sources for succinic acid production. Cadiere et al. (2011) demonstrated that evolutionary engineering techniques could be used for reshaping the central metabolism and could contribute to generate strains with new properties that could be potentially used in the wine industry. Moreover, this

study provided novel information about the operation mode of the pentose phosphate pathway (Nidelet et al. 2013).

One of the most interesting studies of MFA in wine yeast was developed by Varela et al. (2004). This work provided a stoichiometric model and the MFA of yeast at different time-points during alcoholic fermentation and showed that viable cell concentration governs the fermentation rates. In addition, the authors proposed two approaches for solving deficiencies in biomass: the early supplementation of must with nitrogen sources and the addition of biomass from other fermentation tanks. However, the stoichiometric model established in this work did not include all the amino acids present in grape must. Expanding the model to all amino acids would contribute to an accurate determination of metabolic fluxes throughout nitrogen metabolism pathways and also a more detailed analysis of redox metabolism of yeast growing under winemaking conditions.

Additional studies on wine fermentation modeling have been developed during the last decade. The model developed by Sainz et al. (2003) allowed the representation of long-term cell adaptation to environmental changes throughout the fermentation process and the subsequent physiological study of this process. On the other hand, the work by Raghunathan et al. (2006) presented a framework for parameter estimation of fermentation dynamics with metabolic flux balance models. The kinetic model developed by Pizarro et al. (2007b) was one of the most accurate for predicting glucose, fructose, and ethanol concentrations at various temperatures and with different initial assimilable nitrogen concentrations both in laboratory and industrial fermentations. This model could be useful for predicting the time required to complete the process. Vargas et al. (2011) described the first experimentally validated GS-DFBA model (Genome Scale-Dynamic Flux Balancing Analysis) for alcoholic fermentations. Finally, David et al. (2013) reported a comprehensive dynamic model of winemaking fermentation including the specific effect of nitrogen supplementation on hexose transporters.

Research aim

The main objective of this PhD project is to contribute to the development of a quantitative model of *S. cerevisiae* metabolism in winemaking conditions. This model would allow to assess the effect of different environmental variables and of a particular starter yeast strain not only on fermentation kinetics but also on the production of relevant fermentation products (such as ethanol, glycerol, acetic acid, or some volatile compounds). This model would be useful in the improvement and control of the fermentation process, as well as in the definition of a rational use of enological additives and starter cultures, in order to ensure and improve wine quality.

Specific objectives:

- ✓ To generate a new strategy for studying yeast physiology under winemaking conditions.
- ✓ To generate a comprehensive and quantitative model for *S. cerevisiae* main metabolic pathways under winemaking conditions.
- ✓ To describe the metabolic response of *S. cerevisiae* to variations in must composition.

Outline of this thesis

This thesis is the compilation of the work developed during the last four years in order to achieve the objectives described in the previous section. It contains four chapters consisting of journal papers that have been published or have been submitted to international peer reviewed journals included in the JCR (ISI-WOK). These chapters are self-contained and can be read independently of each other.

The research presented in this thesis has been performed in close collaboration with the group of Pau Ferrer at the Universitat Autònoma de Barcelona (Barcelona, Spain). This collaboration was established in the context of the Deméter project (**D**esarrollo de **E**strategias y **M**étodos vitícolas y **E**nológicos frente al cambio climático. Aplicación de nuevas **T**ecnologías que mejoren la **E**ficiencia de los procesos **R**esultantes). The Deméter project

(http://www.cenitdemeter.es/) deals with the study of wine and winemaking adaptation to the new scenario produced by global warming.

Chapter 2 provides a global overview of wine fermentation and the proof of concept of the work developed in this thesis. A new approach based on continuous culture for studying the flux distribution of yeast growing under winemaking conditions has been developed.

In chapter 3, the exponential growth phase of yeast during wine fermentation (both in white and red wines) is mimicked in continuous culture for studying the flux distribution in yeast growing in must with different sugar content.

An exhaustive analysis of the effect of must supplementation with ammonium salts (a common practice in wineries) on yeast physiology, fermentation kinetics and final chemical composition of wine is described in chapter 4. This study includes the impact of this practice in the final aroma profile of wine.

Finally, Chapter 5 shows the effect of must supplementation with ammonium salts on carbon flux distribution and macromolecular composition of yeast by the end of the exponential growth phase.

References

Albers, E., C. Larsson, G. Liden, C. Niklasson, and L. Gustafsson. 1996. Influence of the nitrogen source on *Saccharomyces cerevisiae* anaerobic growth and product formation. Appl. Environ. Microb. 62: 3187-3195.

Alonso, A. D., and M. A. O'Neill. 2011. Climate change from the perspective of Spanish wine growers: A three-region study. Brit. Food J. 113: 205-221.

Bailey, J. E. 1991. Toward a science of metabolic engineering. Science 252: 1668-1675.

Bakker, B. M., K. M. Overkamp, A. J. A. van Maris, P. Kotter, M. A. H. Luttik, J. P. van Dijken, and J. T. Pronk. 2001. Stoichiometry and compartmentation of NADH metabolism in *Saccharomyces cerevisiae*. FEMS Microbiol. Rev. 25: 15-37.

Barnett, J. A. 2003a. Beginnings of microbiology and biochemistry: The contribution of yeast research. Microbiology 149: 557-567.

Barnett, J. A. 2003b. A history of research on yeasts 5: The fermentation pathway. Yeast 20: 509-543.

Barnuud, N. N., A. Zerihun, M. Gibberd, and B. Bates. 2013. Berry composition and climate: Responses and empirical models. Int. J. Biometeorol.

Battaglini, A., G. Barbeau, M. Bindi, and F. W. Badeck. 2009. European winegrowers' perceptions of climate change impact and options for adaptation. Reg. Environ. Change. 9: 61-73.

Beltran, G., N. Rozes, A. Mas, and J. M. Guillamon. 2007. Effect of low-temperature fermentation on yeast nitrogen metabolism. World J. Microb. Biot. 23: 809-815.

Beltran, G., M. Novo, N. Rozes, A. Mas, and J. M. Guillamon. 2004. Nitrogen catabolite repression in *Saccharomyces cerevisiae* during wine fermentations. FEMS Yeast Res. 4: 625-632.

Beltran, G., B. Esteve-Zarzoso, N. Rozes, A. Mas, and J. M. Guillamon. 2005. Influence of the timing of nitrogen additions during synthetic grape must fermentations on fermentation kinetics and nitrogen consumption. J. Agric. Food Chem. 53: 996-1002.

Belviso, S., L. Bardi, A. B. Bartolini, and M. Marzona. 2004. Lipid nutrition of *Saccharomyces cerevisiae* in winemaking. Can. J. Microbiol. 50: 669-674.

Bell, S. J., and P. A. Henschke. 2005. Implications of nitrogen nutrition for grapes, fermentation and wine. Aust. J. Grape Wine Res. 11: 242-295.

Bisson, L. F., and C. E. Butzke. 2000. Diagnosis and rectification of stuck and sluggish fermentations. Am. J. Enol. Vitic. 51: 168-177.

Bock, A., T. H. Sparks, N. Estrella, and A. Menzel. 2013. Climate-induced changes in grapevine yield and must sugar content in Franconia (Germany) between 1805 and 2010. PLOS ONE 8: e69015.

Boer, V. M. 2005. Physiological and transcriptional responses of *Saccharomyces cerevisiae* to nutrient limitation. PhD Thesis. Delft University of Technology. Delft, The Nederlands.

Borneman, A. R., P. J. Chambers, and I. S. Pretorius. 2007. Yeast systems biology: Modelling the winemaker's art. Trends Biotechnol. 25: 349-355.

Cadiere, A., A. Ortiz-Julien, C. Camarasa, and S. Dequin. 2011. Evolutionary engineered *Saccharomyces cerevisiae* wine yeast strains with increased in vivo flux through the pentose phosphate pathway. Metab. Eng. 13: 263-271.

Calik, P., and T. H. Ozdamar. 2002. Bioreaction network flux analysis for industrial microorganisms: A review. Rev. Chem. Eng. 18: 553-596.

Camarasa, C., J. P. Grivet, and S. Dequin. 2003. Investigation by 13C-NMR and tricarboxylic acid (TCA) deletion mutant analysis of pathways for succinate formation in *Saccharomyces cerevisiae* during anaerobic fermentation. Microbiology 149: 2669-2678.

Cavalieri, D., P. E. McGovern, D. L. Hartl, R. Mortimer, and M. Polsinelli. 2003. Evidence for *S. cerevisiae* fermentation in ancient wine. J. Mol. Evol. 57 Suppl 1: S226-232.

Clement, T., M. Perez, J. R. Mouret, J. M. Sablayrolles, and C. Camarasa. 2011. Use of a continuous multistage bioreactor to mimic winemaking fermentation. Int. J. Food Microbiol. 150: 42-49.

Clement, T., I. Sanchez, M. Perez, J. M. Sablayrolles, and C. Camarasa. 2013. Metabolic and transcriptomic response of yeast to nitrogen additions during the stationary phase of four-stages continuous fermentation, 5th Conference on Physiology of Yeast and Filamentous Fungi, Montpellier, France.

Crépin, L. 2012. Variabilité dans l'utilixation de l'azote chez *Saccharomices cerevisae* et cónsequences sur la production de biomasse en fermentation oenologique. PhD Thesis. Université Montpellier II. Montpellier.

Crépin, L., T. Nidelet, I. Sanchez, S. Dequin, and C. Camarasa. 2012. Sequential use of nitrogen compounds by *Saccharomyces cerevisiae* during wine fermentation: a model based on kinetic and regulation characteristics of nitrogen permeases. Appl. Environ. Microb. 78: 8102-8111.

Charnomordic, B., R. David, D. Dochain, N. Hilgert, J. R. Mouret, J. M. Sablayrolles, and A. Vande Wouwer. 2010. Two modelling approaches of winemaking: First principle and metabolic engineering. Math. Comp. Model Dyn. 16: 535-553.

David, R., D. Dochain, J. R. Mouret, A. van De Wouwer, and J. M. Sablayrolles. 2013. Nitrogen-backboned modeling of wine-making in standard and nitrogen-added fermentations. Bioprocess. Biosyst. Eng.

De Deken, R. H. 1966. The Crabtree Effect: A Regulatory System in Yeast. J. Gen. Microbiol. 44: 149-156.

Ehrlich, F. 1904. Ueber das natürliche Isomere des Leucins. Ber. Dtsch. Chem. Ges. 37: 1809-1840.

Erasmus, D. J., M. Cliff, and H. J. J. van Vuuren. 2004. Impact of yeast strain on the production of acetic acid, glycerol, and the sensory attributes of icewine. Am. J. Enol. Vitic. 55: 371-378.

GIEC. 2001. Bilan 2001 des changements climatiques : Les éléments scientifiques, OMM-PNUE.

Godard, P., A. Urrestarazu, S. Vissers, K. Kontos, G. Bontempi, J. van Helden, and B. Andre. 2007. Effect of 21 different nitrogen sources on global gene expression in the yeast *Saccharomyces cerevisiae*. Mol. Cell Biol. 27: 3065-3086.

González, R., R. Muñoz, and A. V. Carrascosa. 2011. Production of wine starter cultures, pp. 279-302, Molecular Wine Microbiology. Academic Press, San Diego, USA.

Grassl, H. 2011. Climate change challenges. Surv. Geophys. 32: 319-328.

Hazelwood, L. A., J. M. Daran, A. J. A. van Maris, J. T. Pronk, and J. R. Dickinson. 2008. The ehrlich pathway for fusel alcohol production: A century of research on *Saccharomyces cerevisiae* metabolism. Appl. Environ. Microb. 74: 2259-2266.

Heavner, B., K. Smallbone, B. Barker, P. Mendes, and L. Walker. 2012. Yeast 5 - an expanded reconstruction of the Saccharomyces cerevisiae metabolic network. BMC Syst. Biol. 6: 55.

Herrgard, M. J., N. Swainston, P. Dobson, W. B. Dunn, K. Y. Arga, M. Arvas, N. Bluthgen, S. Borger, R. Costenoble, M. Heinemann, M. Hucka, N. Le Novere, P. Li, W. Liebermeister, M. L. Mo, A. P. Oliveira, D. Petranovic, S. Pettifer, E. Simeonidis, K. Smallbone, I. Spasic, D. Weichart, R. Brent, D. S. Broomhead, H. V. Westerhoff, B. Kirdar, M. Penttila, E. Klipp, B. O. Palsson, U. Sauer, S. G. Oliver, P. Mendes, J. Nielsen, and D. B. Kell. 2008. A consensus yeast metabolic network reconstruction obtained from a community approach to systems biology. Nat. Biotechnol. 26: 1155-1160.

Hoskisson, P. A., and G. Hobbs. 2005. Continuous culture - making a comeback? Microbiol.-Sgm 151: 3153-3159.

Ingledew, W. M., C. A. Magnus, and F. W. Sosulski. 1987. Influence of oxygen on proline utilization during the wine fermentation. Am. J. Enol. Vitic. 38: 246-248.

Iwatani, S., Y. Yamada, and Y. Usuda. 2008. Metabolic flux analysis in biotechnology processes. Biotechnol. Lett. 30: 791-799.

Jain, V. K., B. Divol, B. A. Prior, and F. F. Bauer. 2012. Effect of alternative NAD(+)-regenerating pathways on the formation of primary and secondary aroma compounds in a *Saccharomyces cerevisiae* glycerol-defective mutant. Appl. Microbiol. Biot. 93: 131-141.

Jones, G., M. White, O. Cooper, and K. Storchmann. 2005. Climate change and global wine quality. Climatic Change 73: 319-343.

Käppeli, O. 1986. Regulation of carbon metabolism in *Saccharomyces cerevisiae* and related yeasts. Adv. Microb. Physiol. 28: 181-209.

Lange, H. C., and J. J. Heijnen. 2001. Statistical reconciliation of the elemental and molecular biomass composition of *Saccharomyces cerevisiae*. Biotechnol. Bioeng. 75: 334-344.

Lavalle, C., F. Micale, T. D. Houston, A. Camia, R. Hiederer, C. Lazar, C. Conte, G. Amatulli, and G. Genovese. 2009. Climate change in Europe. 3. Impact on agriculture and forestry. A review (Reprinted). Agron. Sustain. Dev. 29: 433-446.

Lee, S. Y., J. M. Park, and T. Y. Kim. 2011. Application of metabolic flux analysis in metabolic engineering, pp. 67-93, Methods in Enzymology. Academic Press, San Diego, USA.

Makra, L., B. Vitányi, A. Gál, J. Mika, I. Matyasovszky, and T. Hirsch. 2009. Wine quantity and quality variations in relation to climatic factors in the Tokaj (Hungary) winegrowing region. Am. J. Enol. Vitic. 60: 312-321.

Mira de Orduña, R. 2010. Climate change associated effects on grape and wine quality and production. Food Res. Int. 43: 1844-1855.

Monod, J. 1950. La technoque de culture continue: Theorie et applications. Ann. Inst. Pasteur 79: 390-410.

Morakul, S., J.-R. Mouret, P. Nicolle, I. C. Trelea, J.-M. Sablayrolles, and V. Athes. 2011. Modelling of the gas-liquid partitioning of aroma compounds

during wine alcoholic fermentation and prediction of aroma losses. Process Biochem. 46: 1125-1131.

Moriondo, M., G. V. Jones, B. Bois, C. Dibari, R. Ferrise, G. Trombi, and M. Bindi. 2013. Projected shifts of wine regions in response to climate change. Climatic Change 119: 825-839.

Nidelet, T., A. Goelzer, C. Camarasa, and S. Dequin. 2013. Constrain-based modeling of yeast fermentative metabolism, 5th Conference on Physiology of Yeast and Filamentous Fungi, Montpellier, France.

Nielsen, J. 2001. Metabolic engineering. Appl. Microbiol. Biot. 55: 263-283.

Nissen, T. L., U. Schulze, J. Nielsen, and J. Villadsen. 1997. Flux distributions in anaerobic, glucose-limited continuous cultures of *Saccharomyces cerevisiae*. Microbiol.-UK 143: 203-218.

Novo, M., M. Quiros, P. Morales, and R. Gonzalez. 2012. Wine technology, pp. 461-488, Handbook of Fruits and Fruit Processing. John Wiley & Sons, Ltd., Oxford, UK.

Novo, M., F. Bigey, E. Beyne, V. Galeote, F. Gavory, S. Mallet, B. Cambon, J. L. Legras, P. Wincker, S. Casaregola, and S. Dequin. 2009. Eukaryote-to-eukaryote gene transfer events revealed by the genome sequence of the wine yeast *Saccharomyces cerevisiae* EC1118. P. Natl. Acad. Sci. USA 106: 16333-16338.

Orth, J. D., I. Thiele, and B. O. Palsson. 2010. What is flux balance analysis? Nat. Biotechnol. 28: 245-248.

Ostergaard, S., L. Olsson, and J. Nielsen. 2000. Metabolic engineering of *Saccharomyces cerevisiae*. Microbiol. Mol. Biol. Rev. 64: 34-50.

Otero, J. M., and J. Nielsen. 2010. Industrial systems biology. Biotechnol. Bioeng. 105: 439-460.

Park, J. M., T. Y. Kim, and S. Y. Lee. 2009. Constraints-based genome-scale metabolic simulation for systems metabolic engineering. Biotechnol. Adv. 27: 979-988.

Pasteur, L. 1857. Mémorie sur la fermentation alcoolique. Ann. Chim. Phys. 58: 323-426.

Petrie, P. R., and V. O. Sadras. 2008. Advancement of grapevine maturity in Australia between 1993 and 2006: putative causes, magnitude of trends and viticultural consequences. Aust. J. Grape Wine Res. 14: 33-45.

Petrik, M., O. Käppeli, and A. Fiechter. 1983. An expanded concept for the glucose effect in the yeast *Saccharomyces uvarum*: Involvement of short- and long-term regulation. J. Gen. Microbiol. 129: 43-49.

Pigeau, G. M., and D. L. Inglis. 2005. Upregulation of ALD3 and GPD1 in *Saccharomyces cerevisiae* during icewine fermentation. J. Appl. Microbiol. 99: 112-125.

Pizarro, F., F. A. Vargas, and E. Agosin. 2007a. A systems biology perspective of wine fermentations. Yeast 24: 977-991.

Pizarro, F., C. Varela, C. Martabit, C. Bruno, J. R. Prez-Correa, and E. Agosin. 2007b. Coupling kinetic expressions and metabolic networks for predicting wine fermentations. Biotechnol. Bioeng. 98: 986-998.

Pretorius, I. S. 2000. Tailoring wine yeast for the new millennium: Novel approaches to the ancient art of winemaking. Yeast 16: 675-729.

Pronk, J. T., H. Y. Steensma, and J. P. vanDijken. 1996. Pyruvate metabolism in *Saccharomyces cerevisiae*. Yeast 12: 1607-1633.

Raghunathan, A. U., J. R. Perez-Correa, E. Agosin, and L. T. Biegler. 2006. Parameter estimation in metabolic flux balance models for batch fermentation - formulation & solution using Differential Variational Inequalities (DVIs). Ann. Oper. Res. 148: 251-270.

Rapp, A., and G. Versini. 1991. Influence of nitrogen compounds in grapes on aroma compounds of wines, pp. 156-164, Proceedings of the International Symposium on Nitrogen in Grapes and Wine, Kos, Grece.

Remize, F., J. M. Sablayrolles, and S. Dequin. 2000. Re-assessment of the influence of yeast strain and environmental factors on glycerol production in wine. J. Appl. Microbiol. 88: 371-378.

Rodrigues, F., P. Ludovico, and C. Leão. 2006. Sugar metabolism in yeasts: An overview of aerobic and anaerobic glucose catabolism, pp. 101-121, Biodiversity and Ecophysiology of Yeasts. Springer Berlin Heidelberg, New York, USA.

Roubos, J. A. 2002. Bioprocess modeling and optimization. Fed-Batch clavulanic acid production by *Streptomyces clavuligerus.* PhD Thesis. Delft University of Technology. Delft, The Nederlands.

Sainz, J., F. Pizarro, J. R. Perez-Correa, and E. Agosin. 2003. Modeling of yeast metabolism and process dynamics in batch fermentation. Biotechnol. Bioeng. 81: 818-828.

Salazar-Parra, C., J. Aguirreolea, M. Sanchez-Diaz, J. J. Irigoyen, and F. Morales. 2010. Effects of climate change scenarios on Tempranillo grapevine (*Vitis vinifera* L.) ripening: Response to a combination of elevated CO2 and temperature, and moderate drought. Plant Soil 337: 179-191.

Sauer, U. 2006. Metabolic networks in motion: C-13-based flux analysis. Mol. Syst. Biol. 2: 62.

Schultz, H. R., and G. V. Jones. 2010. Climate induced historic and future changes in viticulture. J. Wine. Res. 21: 137-145.

Schulze, U., G. Liden, and J. Villadsen. 1996a. Dynamics of ammonia uptake in nitrogen limited anaerobic cultures of *Saccharomyces cerevisiae*. J. Biotechnol. 46: 33-42.

Schulze, U., G. Liden, J. Nielsen, and J. Villadsen. 1996b. Physiological effects of nitrogen starvation in an anaerobic batch culture of *Saccharomyces cerevisiae*. Microbiol.-UK 142: 2299-2310.

Schuster, S., T. Dandekar, and D. A. Fell. 1999. Detection of elementary flux modes in biochemical networks: A promising tool for pathway analysis and metabolic engineering. Trends Biotechnol. 17: 53-60.

Soar, C. J., V. O. Sadras, and P. R. Petrie. 2008. Climate drivers of red wine quality in four contrasting Australian wine regions. Aust. J. Grape Wine Res. 14: 78-90.

Stephanopoulos, G., and J. J. Vallino. 1991. Network rigidity and metabolic engineering in metabolite overproduction. Science 252: 1675-1681.

Stephanopoulos, G. N., A. A. Aristidou, and J. Nielsen. 1998. Comprehensive models for cellular reactions, pp. 81-114, Metab. Eng. Academic Press, San Diego, USA.

Storchmann, K. 2005. English weather and Rhine wine quality: An ordered probit model. J. Wine. Res. 16: 105-120.

Styger, G., B. Prior, and F. F. Bauer. 2011. Wine flavor and aroma. J. Ind. Microbiol. Biotechnol. 38: 1145-1159.

Swanson, W. H., and C. E. Clifton. 1948. Growth and assimilation in cultures of *Saccharomyces cerevisiae*. J. Bacteriol. 56: 115-124.

Swiegers, J. H., E. J. Bartowsky, P. A. Henschke, and I. S. Pretorius. 2005. Yeast and bacterial modulation of wine aroma and flavour. Aust. J. Grape Wine Res. 11: 139-173.

Trnka, M., R. Brazdil, M. Dubrovsky, D. Semeradova, P. Stepanek, P. Dobrovolny, M. Mozny, J. Eitzinger, J. Malek, H. Formayer, J. Balek, and Z. Zalud. 2011. A 200-year climate record in central Europe: Implications for agriculture. Agron. Sustain. Dev. 31: 631-641.

Vallino, J. J., and G. Stephanopoulos. 1993. Metabolic flux distributions in *Corynebacterium glutamicum* during growth and lysine overproduction. Biotechnol. Bioeng. 41: 633-646.

van Gulik, W. M., and J. J. Heijnen. 1995. A metabolic network stoichiometry analysis of mecrobial-growth and product formation. Biotechnol. Bioeng. 48: 681-698.

van Gulik, W. M., W. de Laat, J. L. Vinke, and J. J. Heijnen. 2000. Application of metabolic flux analysis for the identification of metabolic bottlenecks in the biosynthesis of penicillin-G. Biotechnol. Bioeng. 68: 602-618.

Varela, C., F. Pizarro, and E. Agosin. 2004. Biomass content governs fermentation rate in nitrogen-deficient wine musts. Appl. Environ. Microb. 70: 3392-3400.

Vargas, F. A., F. Pizarro, J. R. Perez-Correa, and E. Agosin. 2011. Expanding a dynamic flux balance model of yeast fermentation to genome-scale. BMC Syst. Biol. 5: 50.

Vilanova, M., M. Ugliano, C. Varela, T. Siebert, I. S. Pretorius, and P. A. Henschke. 2007. Assimilable nitrogen utilisation and production of volatile and non-volatile compounds in chemically defined medium by *Saccharomyces cerevisiae* wine yeasts. Appl. Microbiol. Biot. 77: 145-157.

Villadsen, J., J. Nielsen, and G. Lidén. 2011. Chemicals from Metabolic Pathways, pp. 7-62, Bioreaction Engineering Principles. Springer, New York, USA.

Visser, D. 2002. Measuring & modeling *in vivo* kinetics of primary metabolism. PhD Thesis. Delft University of Technology. Delft, The Nederlands.

Wang, N. S., and G. Stephanopoulos. 1983. Application of macroscopic balances to the identification of gross measurement errors. Biotechnol. Bioeng. 25: 2177-2208.

Wiechert, W. 2001. C-13 metabolic flux analysis. Metab. Eng. 3: 195-206.

Wisselink, H. W., C. Cipollina, B. Oud, B. Crimi, J. J. Heijnen, J. T. Pronk, and A. J. A. van Maris. 2010. Metabolome, transcriptome and metabolic flux analysis of arabinose fermentation by engineered *Saccharomyces cerevisiae*. Metab. Eng. 12: 537-551.

Chapter II

♦

Use of chemostat cultures mimicking different phases of wine fermentations as a tool for quantitative physiological analysis

CHAPTER II

Use of chemostat cultures mimicking different phases of wine fermentations as a tool for quantitative physiological analysis

ABSTRACT

Saccharomyces cerevisiae is the most relevant yeast species conducting the alcoholic fermentation that takes place during winemaking. Although the physiology of this model organism has been extensively studied, systematic quantitative physiology studies of this yeast under winemaking conditions are still scarce, thus limiting the understanding of fermentative metabolism of wine yeast strains and the systematic description, modelling and prediction of fermentation processes. In this study, we implemented and validated the use of chemostat cultures as a tool to simulate different stages of a standard wine fermentation, thereby allowing to implement metabolic flux analyses describing the sequence of metabolic states of *S. cerevisae* along the wine fermentation.

Chemostat cultures mimicking the different stages of standard wine fermentations of *S. cerevisiae* EC1118 were performed using a synthetic must and strict anaerobic conditions. The simulated stages corresponded to the onset of the exponential growth phase, late exponential growth phase and cells just entering stationary phase, at dilution rates of 0.27, 0.04, 0.007 h^{-1}, respectively. Notably, measured substrate uptake and product formation rates at each steady state condition were within the range of corresponding conversion rates estimated during the different batch fermentation stages. Moreover, chemostat data were further used for metabolic flux analysis, where biomass composition data for each condition was considered in the stoichiometric model. Metabolic flux distributions were coherent with previous analyses based on batch cultivations data and the pseudo-steady state assumption. Steady state conditions obtained in chemostat cultures reflect the environmental conditions and physiological states of *S. cerevisiae* corresponding to the different growth stages of a typical batch wine fermentation, thereby showing the potential of this experimental approach to systematically study the effect of environmental relevant factors such as temperature, sugar concentration, C/N ratio or (micro) oxygenation on the fermentative metabolism of wine yeast strains.

This chapter has been submitted to *Microbial Cell Factories* as: Felícitas Vázquez-Lima, Paulina Silva, Antonio Barreiro, Rubén Martínez-Moreno, Pilar Morales, Manuel Quirós, Ramon Gonzalez, Joan Albiol and Pau Ferrer. Use of chemostat cultures mimicking different phases of winemaking fermentations as a tool for quantitative physiological analysis

Introduction

During the last decades concern on climate change has increased and it is nowadays well recognised as one of the most important environmental problems faced on Earth. Climate change is already having significant impacts on the world's physicochemical, biological and human systems. Agriculture is one of the main sectors affected by this phenomenon (Lavalle et al. 2009, Olesen et al. 2011, Trnka et al. 2011), with viticulture and viniculture being no exception (Battaglini et al. 2009, Salazar-Parra et al. 2010, Alonso and O'Neill 2011). Climate change alters crop yields and grape quality, and variations in anthocyanin, malic acid or sugar content could ultimately affect wine quality (Jones et al. 2005). This is particularly important in regions of countries such as Spain, France, United States, Chile or Australia, where wine has developed as a key economic sector with broad historical, social, and cultural identity derived from grape growing and production.

Besides, although many of the wine properties and production methods are grape-related, there are numerous features that are dependent on the yeast strain used. These include fermentation performance (e.g. tolerance to stress and the ability to efficiently utilize carbon and nitrogen sources), downstream wine processing (e.g. improved protein and polysaccharide clarification, cell flocculation and sedimentation properties), modulation of alcohol content, levels of both desirable (e.g. resveratrol) and undesirable (e.g. ethyl carbamate) chemical compounds, as well as the modulation of the organoleptic properties resulting from the hundreds of metabolites and flavor compounds that are either produced or liberated from precursors in the grape juice during wine fermentation, including esters, higher alcohols, volatile acids, phenols and thiols (Borneman et al. 2007).

For these reasons, wine producers have launched different initiatives over the last years that aim on one side, to understand and mitigate the impacts of global warming on winemaking and, on the other, to improve their knowledge base on yeast physiology under winemaking conditions for the optimization of production processes.

In the past recent years, systems biology tools have been extensively used to study the physiology of the model yeast *S. cerevisiae*. Nevertheless, the application of such tools to the understanding of yeast physiology under

winemaking conditions is still limited (Rossignol et al. 2003, Pizarro et al. 2007a, Pizarro et al. 2008, Novo et al. 2009, Vargas et al. 2011, Aceituno et al. 2012).

Systematic profiling of yeast metabolism under winemaking conditions is required in order to understand and predict the effect of environmental changes and distinct genetic backgrounds on wine fermentations, as well as to perform a rational optimisation of fermentation processes. Among the strategies for systems-level analysis of cell metabolism, Metabolic Flux Analysis (MFA) has been extensively applied in many physiological studies of yeast, for example to quantify the impact of growth conditions or genetic modifications on metabolic pathway activities (Nissen et al. 1997, Daran-Lapujade et al. 2004, Fredlund et al. 2004, Varela et al. 2004, Frick and Wittmann 2005, Kleijn et al. 2007, Jouhten et al. 2008, Christen and Sauer 2011, Celton et al. 2012, Jorda et al. 2012). Attaining metabolic steady states is crucial to investigate metabolic pathways using MFA methodologies, including MFA based on ^{13}C isotopic labelling. Moreover, characterization of cellular metabolism using isotopic tracers such as ^{13}C-labelled substrates is much more convenient in chemically defined media with one or two carbon sources at a relatively low concentration. Nevertheless, laboratory scale fermentations mimicking wine fermentations may be more complicated due to the higher complexity associated with the medium (composed of several carbon sources including glucose, fructose and amino acids), as well as co-consumption and secretion of substrates and metabolites. To date, several experimental approaches have been proposed for MFA studies of yeast growing under winemaking conditions. Varela and co-workers (2004) reported one of the first examples of the use of MFA to characterize the distribution of carbon fluxes in a wine yeast strain under winemaking conditions. In this study, changes in the wine fermentation process are assumed to be slow in comparison to intracellular metabolite dynamics, that is, intracellular metabolite pools were assumed to be at pseudo-steady state in a given fermentation point. Therefore, metabolic fluxes can be estimated from the measurements of substrate uptake and product formation rates at a given fermentation stage. Recently, this basic approach has been further extended using a genome-scale metabolic model (Vargas et al. 2011). Also, dynamic metabolic flux balance approaches, linking process variables and metabolic fluxes, have been

proposed (Sainz et al. 2003, Pizarro et al. 2007b), allowing for the simulation and prediction of winemaking fermentation kinetic profiles.

Alternatively, chemostat cultures have been extensively used for quantitative physiology analyses of yeast cells. Nevertheless, their application to the study of wine fermentations has been so far very limited. For instance, this approach has been used to investigate the effect of growth parameters such as temperature (Pizarro et al. 2008) or dissolved oxygen concentration (Aceituno et al. 2012) on yeast cells. However, these studies were carried out under environmental conditions not strictly resembling wine fermentations (for instance, they used glucose as a single carbon source). Moreover, conventional continuous cultures were never applied to the study of the different growth stages of a typical wine fermentation. Interestingly, a recent study by Clement and co-workers (Clement et al. 2011) using a continuous multistage bioreactor connecting two or more tanks in series, shows the potential of chemostat cultures for reproducing the different stages of a batch process. However, no MFA studies were performed on such kind of complex experimental set-up.

In this study, we propose the utilization of classic chemostat cultures to obtain metabolic steady states mimicking the different phases of a classical wine-making fermentation process, operated in batch mode. This has allowed for the quantitative physiological analysis of each fermentation phase, as exemplified by the MFA performed with the obtained datasets.

Material and methods

Strain

A commercial yeast strain, *Saccharomyces cerevisiae* EC1118 (Lallemand, Canada) was used in this work. This strain is considered as a model organism in the field and has been used in a wide number of physiological studies related to wine fermentations.

Media composition

Culture medium was a modification of the MS300 medium (Salmon and Barre 1998). It contained per litre: 120 g glucose; 120 g fructose; 6 g citric acid; 6 g

DL-malic acid; 1.7 g YNB w/o amino acids and ammonium sulphate; 60 mg potassium bisulfite; 15 mg ergosterol; 5 mg oleic acid; 0.5 mL Tween 80; 306 mg NH_4Cl; 29 mg L-aspartic acid; 80 mg L-glutamic acid; 52 mg L-serine; 333 mg L-glutamine; 23 mg L-histidine; 12 mg L-glycine; 13 mg L-tyrosine; 50 mg L-threonine; 245 mg L-arginine; 97 mg L-alanine; 14 mg L-cysteine; 29 mg L-valine; 21 mg L-methionine; 116 mg L-tryptophan; 25 mg L-phenylalanine; 22 mg L-isoleucine; 32 mg L-leucine; 11 mg L-lysine and 400 mg L-proline. All the amino acids required for the medium, with the exception of tyrosine, were added in a 50X solution prepared, sterilized by filtration, aliquoted, and then kept at –20 ºC until required. Glucose and fructose were autoclaved separately and added to the rest of medium. Concentration of glucose and fructose into the fresh medium was checked by HPLC in order to have accurate concentrations and taking possible alterations of the glucose-to-fructose ratio due to isomeration. The pH was adjusted to 3.5. Feeding media for continuous experiments had the same composition except that NH_4Cl and the amino acids composition was adjusted to the required experiment. The same medium but with 60 g L^{-1} glucose and fructose and without anaerobic factors (ergosterol, tween 80 and oleic acid) was used for inocula growth.

Culture conditions

All experiments were performed in 2 L bench-top bioreactors (Biostat B and Bplus, Braun Biotech, Melsungen, Germany) with a working volume of 1.5 L for batch experiments and 1 L for continuous processes. Duplicate replicates were performed for each cultivation condition. For inocula development, 0.1 mL cryostock of the Saccharomyces strain were used to inoculate 100 mL of YPD medium. The culture was grown for 48 h at 28 ºC and 150 rpm in a Multitron II incubator (Infors AG, Switzerland). 10 mL of this culture were then used to inoculate 100 mL of inoculum medium and incubated overnight at 28 ºC and 150 rpm. This culture was used to inoculate the bioreactor to an optical density (OD_{600}) of 0.1. Operation parameters in the reactor were temperature 28 ºC, pH 3.5, and 100 rpm stirring rate. No pH control was used during batch processes, while in the continuous culture it was automatically controlled using 2 M NaOH. Data acquisition and control of the different variables was done using an in-house control software. Prior to inoculation, culture medium was sparged with 0.3 L min^{-1} of N_2 to establish

anaerobic conditions. After inoculation, N_2 flow was diverted to the head-space to minimize the stripping of ethanol. With the same purpose, off-gas condenser was kept at 4 ºC throughout the process. N_2 flow throughout the cultivation process (0.3 L min^{-1}) was controlled using a mass flow controller (Bronkhorst High Tech B.V., The Netherlands), and norprene tubing was used to avoid oxygen diffusion. Feed medium was also sparged with N_2 throughout the experiments to maintain anaerobic conditions.

Sampling

When required, samples were taken from the reactor in pre-chilled tubes kept on ice during processing. For elemental and macromolecular biomass composition analyses and extracellular metabolite analysis, samples were centrifuged 10 min at 10,000 rpm and 4 ºC. Supernatants were then filtered through 0.45 µm filters and kept at -20 ºC until analysis, while biomass pellets were washed twice, lyophilized and kept at -80 ºC until analysis. Triplicate samples were taken for all analytical measurements.

Analytical procedures

Biomass dry weight

Cell biomass was monitored by measuring optical density at 600 nm (OD_{600}). For cell dry weight, a known volume of culture broth was filtered through pre-weighted filters that were then washed with 2 volumes of distilled water and dried to constant weight at 105 ºC for 24 h.

Sugars, organic acids, and ethanol

An Ultimate 3000 HPLC system (Dionex Corp) with an IC Sep ICE-Coregel 87H3 column (Transgenomic Inc. USA) equipped with an IR detector was used for the analysis of glucose, fructose, glycerol and ethanol while succinic, lactic, acetic and malic acids were analyzed using the same equipment but with an UV detector. 15 mM sulfuric acid was used as mobile phase. Two process temperatures were used: 70 ºC for the analysis of fructose, and 40 ºC for the analyses of the other metabolites.

CO_2 production

Production of carbon dioxide was monitored on-line in the exhaust gas of the bioreactor using a BCP-CO_2 sensor (BlueSens, Germany). The off-gas was passed through 2 columns containing silica gel to remove the humidity before entering the sensor.

Yeast Assimilable Nitrogen (YAN)

YAN was determined using 2 different commercial kits (Megazyme International, Ireland): K-NOPA which measures the PAN (primary amino acid nitrogen) and K-LARGE which measures the contribution from the side chain of L-arginine and free ammonium ions. Results from these kits were combined to determine the FAN.

Amino acids content of culture and feeding media was determined using a modification of the AccQ·Tag method (Waters Corp., Milford MA, USA). Derivatisation was carried out using the AccQ·Fluor reagent (6-aminoquinolyl-N-hydroxysuccinimidyl carbamate) according to the method specifications; hydrogen peroxide was added to the reaction mixture. Once derivatised, amino acids were separated and analyzed using a Waters Nova-Pak C18 (4 µm, 3.9 x 150 mm) in a HPLC gradient system (Waters 600) equipped with an UV detector (Waters 2487). Detection was performed at 254 nm and α-amino-N-butyric acid (AABA) was used as internal standard.

Biomass composition analysis

Elemental composition of the biomass was analysed using an elemental organic analyzer Thermo EA 1108 (Thermo Scientific, Milan, Italy) following the the conditions recommended by the supplier of the instrument (helium flow at 120 mL min^{-1}, combustion furnace at 1000 ºC, chromatographic column oven at 60 ºC, and 10 mL oxygen loop at 100 kPa).

For amino acid analysis, biomass samples were first hydrolyzed at 105 ºC for 24 h with 6 M HCl in vacuum sealed glass ampoules. After hydrolysis, samples were evaporated under vacuum, re-dissolved in 20 mM HCl, and filtered. Amino acid content of an aliquot of the filtrate is then determined using the AccQ·Tag method (Waters Corp., Milford MA, USA). Derivatisation was carried out using the

AccQ·Fluor reagent (6-aminoquinolyl-N-hydroxysuccinimidyl carbamate) according to the method specifications. Once derivatised, amino acids were separated and analyzed using a Waters Nova-Pak C18 (4 µm, 3.9 x 150 mm) in a HPLC gradient system (Waters 600) provided with an UV detector (Waters 2487). Detection was performed at 254 nm and α-amino-N-butyric acid (AABA) was used as internal standard.

Total protein content of the biomass was determined using the Lowry method as described in Herbert et al. (1971). Biomass suspensions of 0.5 g L^{-1} were used for the analysis. Bovine serum albumin was used as standard.

Total carbohydrate content of the biomass was determined using the phenol-sulfuric method, as described in Herbert et al. (1971). Biomass suspensions of 0.1 g L^{-1} were used for the assays. Glucose was used as standard.

The glycogen content was estimated according to the method described by Smolders et al. (1994), using 20 mg of lyophilized biomass.

The method described by Dragosits et al. (2011) was used to estimate the trehalose content of the biomass. According to the method, 25 mg of lyophilized biomass and a standard solution of 2 g L^{-1} of trehalose were used.

Stoichiometric model and metabolic flux analysis

The stoichiometric model used for metabolic flux analysis (Appendix A) was adapted from the model of Varela and co-workers (2004), as previously described (Quirós et al. 2013). Briefly, the described pathway network includes glycolysis, pentose phosphate pathway, the pyruvate carboxylase reaction, the synthesis of ethanol, glycerol, and acetate, the tricarboxylic acid cycle, synthesis and transport reactions for the amino acids arginine, glutamine, tryptophan, alanine, glutamate, serine, threonine, leucine, aspartate, valine, phenylalanine, and isoleucine, transport reactions for incorporation and secretion of various metabolites, and the synthesis pathways for macromolecular components.

Prior to metabolic flux analysis, consistency analyses for all experimental data based on elemental mass balances was performed using the methodology proposed by Wang and Stephanopoulos (1983). All experimental data passed the consistency test, considering a 95 % significance level for a redundancy of 3. Metabolic fluxes were calculated using the CellNetAnalyzer toolbox for MATLAB

developed by Klamt and co-workers (2007). Consistency index for flux analysis was always below 9.48 (redundancy of 4 at 95 % confidence interval).

Results and discussion

Batch fermentation process

Initially, the fermentation profile for strain EC1118 was studied in a standard batch fermentation at 28 ºC under strict anaerobic conditions with a synthetic must mimicking a typical natural must (i.e. 240 g L^{-1} sugars, with equimolar amounts of glucose and fructose, 200 mg L^{-1} yeast assimilable nitrogen (YAN), pH 3.5, and sulfites) (Quirós et al. 2013), as shown in Figure 1. As it can be observed, fermentation finished after 110-120 h, when carbon sources were completely depleted and CO_2 concentration in the exhaust gas was virtually zero. Fermentation evolution shows that glucose was the preferred carbon source since it was consumed and depleted quicker than fructose, following the behavior already described by other authors (Rossignol et al. 2003, Berthels et al. 2004, Varela et al. 2004, Tronchoni et al. 2009). Ethanol was synthesized throughout the process reaching a maximum concentration close to 12 % (v v^{-1}) at around 106 h, when production stopped because carbon sources became almost depleted. In the case of CO_2 production, it evolved exponentially during the initial stage of the fermentation, followed by a period when started to slow down; this period was coincident with a substantial reduction of the nitrogen content of the medium. Biomass grew exponentially (μ_{max}) during the early stages of the process (8-17 h); after that first stage, growth started to slow down as a result of a substantial reduction of the nitrogen content (both in the form of NH_4^+ and as free α-amino acids (FAN)) of the medium, as shown in Figure 1; at later stages of the process (after 60 h), a stationary growth phase was gradually reached due to the limitation of nitrogen sources and increasing ethanol concentration of the medium. Glycerol, the most abundant product of yeast fermentation after ethanol, was also synthesized during the process, reaching a final concentration of 10 g L^{-1}, which is within the range of concentrations commonly found in these processes (Ribéreau-Gayon et al. 2004). Other products such as acetic, succinic and lactic acid were also produced with final concentrations of 0.7, 0.8 and 0.3 g L^{-1}, respectively. These

results were consistent to those previously reported (Varela et al. 2004) for similar processes. Moreover, profiles determined in this study were also comparable to those described for industrial process (data not shown), thus indicating that our laboratory set-up adequately mimics the standard wine fermentations and the results could then be used as the basis for the modelling and simulation processes.

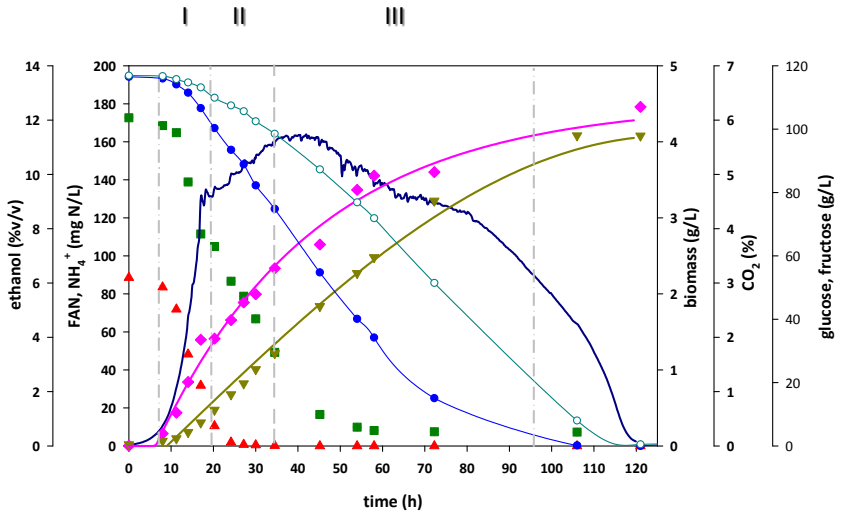

Figure 1. Batch fermentation profile. Vertical discontinued lines indicate the proposed phases. ▲ NH_4^+, ■ FAN, – CO_2, ◆ biomass, ▼ ethanol, ● glucose, ○ fructose.

Next step was defining and choosing the phases from the batch process to be simulated in continuous cultures. As a first approach, the specific growth rates observed during the batch process were the criteria used for the selection of the two first stages to be simulated, corresponding to growing cells. In particular, stage I corresponded to mid-exponential growth phase and stage II to late exponential growth phase. Figure 2 shows an example of how these two stages were defined; in this figure, the first curve represents the interval where the maximum specific growth rate (no nutrient limitations) is achieved and ethanol is produced at a maximum rate, and the second one corresponds to a transition growth phase where CO_2 and ethanol production slow down, NH_4^+ is depleted and growth is sustained solely on free amino nitrogen. For the first phase (8-17 h), a μ_{max} = 0.29 h^{-1} ± 0.01 was calculated as an average from four different batch replicates, while for the transition period –or late exponential growth phase- (20-35 h), a μ_{trans} = 0.04 h^{-1} ±

0.01 was obtained. At the end of the transition phase the CO_2 production rate (CER) peaked, gradually declining thereafter along the following fermentation stage (stationary phase).

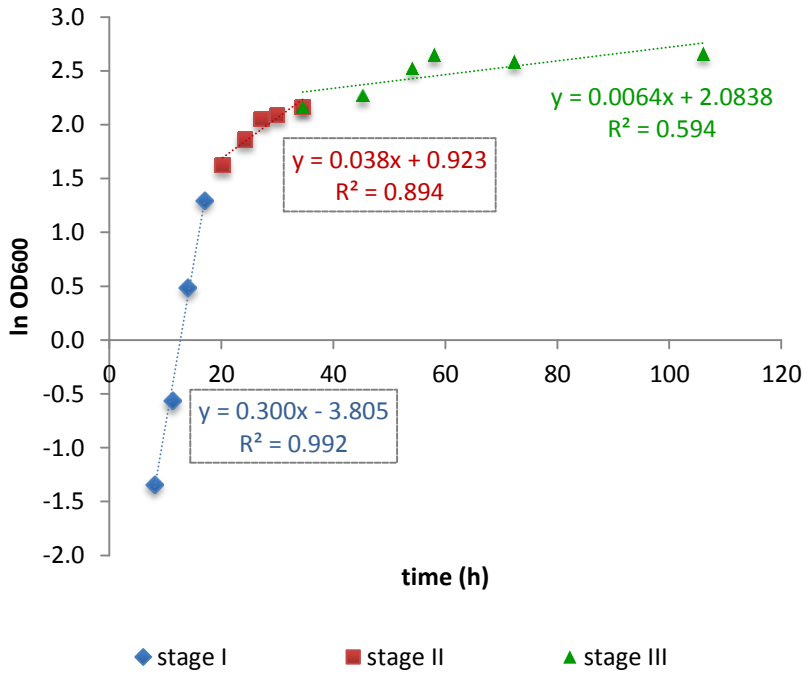

Figure 2. Estimation of the specific growth rates (μ). Calculated growth rates for the three first culture stages of the batch fermentation process. The slope of the regression equations is equivalent to the calculated μ for each phase.

Stage III corresponded to the stationary phase. During this period (35-106 h) growth rate gradually declined from 0.04 to 0 h^{-1}, along with the decline in CO_2 production and accumulation of ethanol. An average μ of 0.007 h^{-1} was estimated for this phase (Figure 2). At the end of this stage, sugar substrates were virtually exhausted and most of the amino acids consumed. At Stage IV (late stationary phase, corresponding to the 106-120 h period), the cells were no longer proliferating (or cell proliferation was equal to cell death), the remaining sugar (fructose) was completely depleted, CO_2 production abruptly fell down and ethanol reached its maximum (11.7 %). This value is slightly lower to that obtained in similar

studies (Varela et al. 2004) and large scale winemaking fermentations with similar initial sugar content (data not shown). This was probably due to limited ethanol stripping as a result of reactor mixing and nitrogen gas sparging. Indeed, this was estimated to be about 0.17 g ethanol L^{-1} h^{-1} in the stage I (A. Barreiro, unpublished results).

With the exception of proline, which is not assimilated in absence of oxygen (Henschke and Jiranek 1993), all the nitrogen sources were utilized. The amino acids and ammonium were assimilated with variable kinetic patterns, following an order of use coherent with those reported in similar recent studies (Crépin et al. 2012) (Figure 3). In particular, amino acids such as Arg, Ala, Trp, Tyr and Gly were consumed at the later stages of the growth phase, after ammonium and some other nitrogen sources had been exhausted, while the rest of amino acids were assimilated earlier, simultaneously to ammonium, or even before (e.g. Leu and Met).

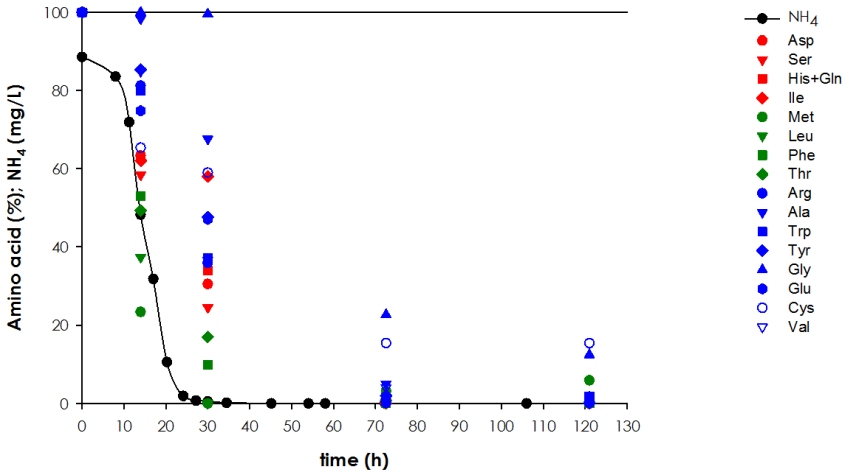

Figure 3. Consumption of ammonium and amino acids during batch fermentation of strain EC1118. The residual NH_4^+ concentration is shown by black solid circles and black line. Early consumption amino acids (Met, Leu, Phe, Thr) are shown in green symbols. Intermediate consumption amino acids (Asp, Ser, His, Gln, Ile) are shown in red symbols. Late consumption amino acids (Arg, Ala, Trp, Tyr, Gly, Glu, Cys, Val) are shown in blue symbols. The residual concentrations of NH_4^+ and amino acids are expressed as percentage of the initial concentration.

Cell viability, cell size and accumulation of reactive oxygen species (ROS) were monitored along the fermentation by flow cytometry. Consistent with previous studies (Landolfo et al. 2008, Mendes-Ferreira et al. 2010), there was a significant ROS accumulation (% of DHE-stained cells) during fermentation, reaching over 70 % of the cell population during the early growth stages (stages I and II). However, these values decreased progressively to about 30 % during stage III, suggesting an adaptation to increased ethanol concentrations. Notably, ROS accumulation did not compromise cell viability, which remained above 90 % during the three growth stages. Nevertheless, the average cell size diminished progressively along stage III, that is, during the onset of the stationary phase. While most of the cells (> 90 %) in stages I and II had a diameter in the range of 10-15 µm, this population fraction progressively decreased to about 50 % along stage III, with a concomitant increase of the cell population in the 7-9 µm (up to about 45 %) and 4-6 µm (up to about 5 %).

Continuous cultures

The two first stages described on the basis of growth rate were subsequently mimicked in continuous cultures carried out at steady state conditions at dilution rates D = 0.27 h^{-1} defined as an approximation to μ_{max}, and D = 0.04 h^{-1}. In these cultures, steady states were verified by on-line monitoring of the off-gas CO_2 concentration and by measuring the concentration of the main metabolites (glucose, fructose, ethanol and glycerol) at 3, 4 and 5 residence times.

Batch and continuous cultures were compared in terms of specific growth, consumption and production specific rates (Table 1). For the calculation of these rates in batch processes, polynomial adjustments were used for the first stage (μ_{max}), where exponential evolutions were observed, while linear adjustments were used for the second stage, since rates were markedly lower than during the first stage and their evolution close to linear.

Table 1 shows that for D = 0.27 and 0.04 h^{-1} almost all the rates estimated for the continuous cultures are within the range of the values obtained for the mimicked batch culture. For cultures at D= 0.27 h^{-1}, feeding medium was the same as the one used for batch cultures. However, for chemostats at D = 0.04 h^{-1}, medium composition had to be modified for a better simulation of the conditions found in the

equivalent batch phase. This was because in the batch process, the FAN was substantially consumed and NH_4^+ depleted during the interval considered, as observed in Figure 1. Several assays were made with best results obtained with a medium containing no NH_4^+ and 70 % of the original amino acids content. It should be mentioned that the concentration of all amino acids was reduced in the same percentage, that is, without taking into account that the different amino acids were consumed at different rates (Nissen et al. 1997). The reason was merely practical, as it would have been cumbersome to adjust the composition of every amino acid individually. Nevertheless, results shown in Table 1 are a clear indication that cell metabolism of the winemaking process during the two first stages is suitably represented by the proposed continuous cultures. For phase I, using a dilution rate close to μ_{max} ($D = 0.27\ h^{-1}$) meant working at conditions with no substrates limitations, since it is known that residual substrate concentration in chemostats is only a function of the dilution rate. In particular, it increases slowly with D at low values but very rapidly as D approaches μ_{max} (Mendes-Ferreira et al. 2010, Zeng and Sun 2010).

Table 1. Comparison between specific rates observed in batch and the equivalent chemostat cultures.

			Specific consumption / production rates (mmols g DCW^{-1} h^{-1})						
		Culture time (h)	Glucose	Fructose	Ethanol	Glycerol	Acetic acid	Succinic acid	Lactic acid
0.27 h^{-1}	Corresponding batch phase	8 – 17	-7.3 – -10.2	-2.2 – -7.7	6.2 – 22.0	1.08 – 3.16	0.07 – 0.19	0.04 – 0.26	0.04 – 0.08
	Chemostat steady state	5.5 RT (1 RT = 3.7 h)	- 14.8 ± 20	- 1.2 ± 28	17.2 ± 3.6	8.3 ± 1.1	n.d.	0.09 ± 0.01	n.d.
0.04 h^{-1}	Corresponding batch phase	20 – 35	-4.4 – -7.2	-2.2 – -3.6	11.2 – 18.6	0.67 – 1.11	0.09 – 0.15	0.03 – 0.05	0.03 – 0.04
	Chemostat steady state	5.5 RT (1 RT = 25 h)	-5.0 ± 1.4	-2.3 ± 1.5	12.7 ± 1.0	0.97 ± 0.3	n.d	0.07 ± 0.01	n.d.
0.02 h^{-1}	Corresponding batch phase	30 – 58	-2.7 – -4.8	-2.31– -3.1	7.2 – 12.8	0.4 – 0.7	0.02 – 0.1	0.02 – 0.03	0.02 – 0.06
	Chemostat steady state	3 RT (1 RT = 50 h)	-3.0 ± 0.6	-1.52 ± 0.6	7.9 ± 0.6	0.70 ± 0.26	0.03 ± 0.003	0.06 ± 0.01	n.d.
0.007 h^{-1}	Corresponding batch phase	60 – 106	0 – -2.52	-1.79 – -2.07	0.78 – 8.11	0.03 – 0.36	0 – 0.04	0.02	0.003
	Chemostat steady state	3 RT (1 RT = 5.9 d)	-2.0 ± 0.3	-1.34 ± 0.3	5.92 ± 0.6	0.58 ± 0.35	n.d.	0.04 ± 0.004	n.d.

n.d., not determined (product concentration below detection limits).

For mimicking and modelling of later stages of the process, the same rationale was used as a first approach for the selection of the interval corresponding to the onset of the stationary phase. The mean growth rate calculated for this phase was $\mu = 0.007\ h^{-1}$. Therefore, as a first approach, an equivalent continuous culture was performed at a dilution rate $D = 0.007\ h^{-1}$ using the same feeding medium as for experiments at $D = 0.04\ h^{-1}$. Comparison between specific rates obtained at these conditions and the equivalent batch stage (III) corresponding from 35 – 100 h approximately, showed a good correspondence (Table 1). However, the chosen interval for this batch stage was very long, and thereby comprised a series of different physiological states, as reflected by the wide intervals of specific conversion rates. For this reason, in a second approach, phase III was further divided into two sub-stages, an early one starting immediately after stage II with a mean specific growth rate $\mu = 0.02\ h^{-1}$, followed by another with a mean specific growth rate $\mu = 0.007\ h^{-1}$, starting at around 60 h of fermentation. Corresponding chemostats were then ran at a $D = 0.02\ h^{-1}$ with the same medium as for $D = 0.04\ h^{-1}$, while for experiments at $D = 0.007\ h^{-1}$, medium was redefined containing no NH_4^+ and 40 % of the original amino acids content. This reformulation was calculated on the basis of biomass yields on nitrogen estimated from preliminary chemostats at $D = 0.007\ h^{-1}$ with the original medium with no NH_4^+ (data not shown). This further readjustment of the composition was done to improve matching with the corresponding batch conditions. Table 1 shows the comparisons between the rates obtained for these two batch sub-stages and their corresponding chemostats. As it can be observed, for both cases rate values are within the same ranges with one significant exception: the fructose consumption rate during the later stage, which falls below the lower bound of the corresponding specific conversion rates observed in the stage III of the batch fermentation. This observation could be related to the fact that equimolar glucose:fructose amounts are used in the chemostat feed, whereas in the onset of the stationary phase fructose concentration is higher than glucose.

Metabolic Flux Analysis (MFA)

The changes in metabolic fluxes in the central carbon metabolism of *S. cerevisiae* over a series of conditions, resembling different growth stages of wine fermentation with decreasing growth rate, were calculated using the stoichiometric model described in Appendix A. Biomass composition (particularly the C/N ratio) was strongly affected by growth conditions, as indicated by the differences in elemental composition and major macromolecular components (protein and carbohydrates) relative abundance. Therefore, elemental and macromolecular biomass composition for each fermentation stage (Additional Files) was incorporated in the mathematical model, allowing for a significant improvement in the adjustment of C and N balances compared to the bibliographical values. Carbon and nitrogen balances in chemostat cultures had between 2 % to 11 %, and 0.1 to 5 % error, respectively, before the data reconciliation step. Consistency index was below 7.8 (for a redundancy of 3 and 95 % significance level), indicating that no gross measurement errors of substrates and products conversion rates.

Overall, the metabolic flux distributions (Figure 4; see also Additional files for fluxes normalised with respect to the glucose uptake flux) were coherent with previous MFA based on batch cultivations datasets (Varela et al. 2004). As stated above, the carbon source assimilation depends on the fermentation stage: At a D of 0.27 h^{-1} (stage I), about 90 % of the C consumption corresponds to glucose, while at the lower dilution rates of 0.04 and 0.007 h^{-1} (stages II and III) this fraction is reduced to about 70 % and 60 %, respectively. As expected, most of the carbon was used for energy production using the ethanol fermentative pathway; the fraction of assimilated C source used for ethanol production increased from stage I to stages II and III, from about 60 % to 90 %, with a concomitant decrease in the carbon source to glycerol as the D was reduced (from about 30 % to 10 %). That is, flux ratio between the ethanol and glycerol pathways increases when shifting from stage I to later stages. Notably, this effect was clearly observed despite the relative amino acid composition of the feed medium was the same for all chemostat cultures, in contrast to batch cultures where amino acids are consumed sequentially. It is well known that the nitrogen source profile influences product (i.e., ethanol, glycerol, succinate, etc) yields (Camarasa et al. 2003). Conversely,

less than 1 % carbon was directed to the production of other metabolites (succinate, lactate, acetate).

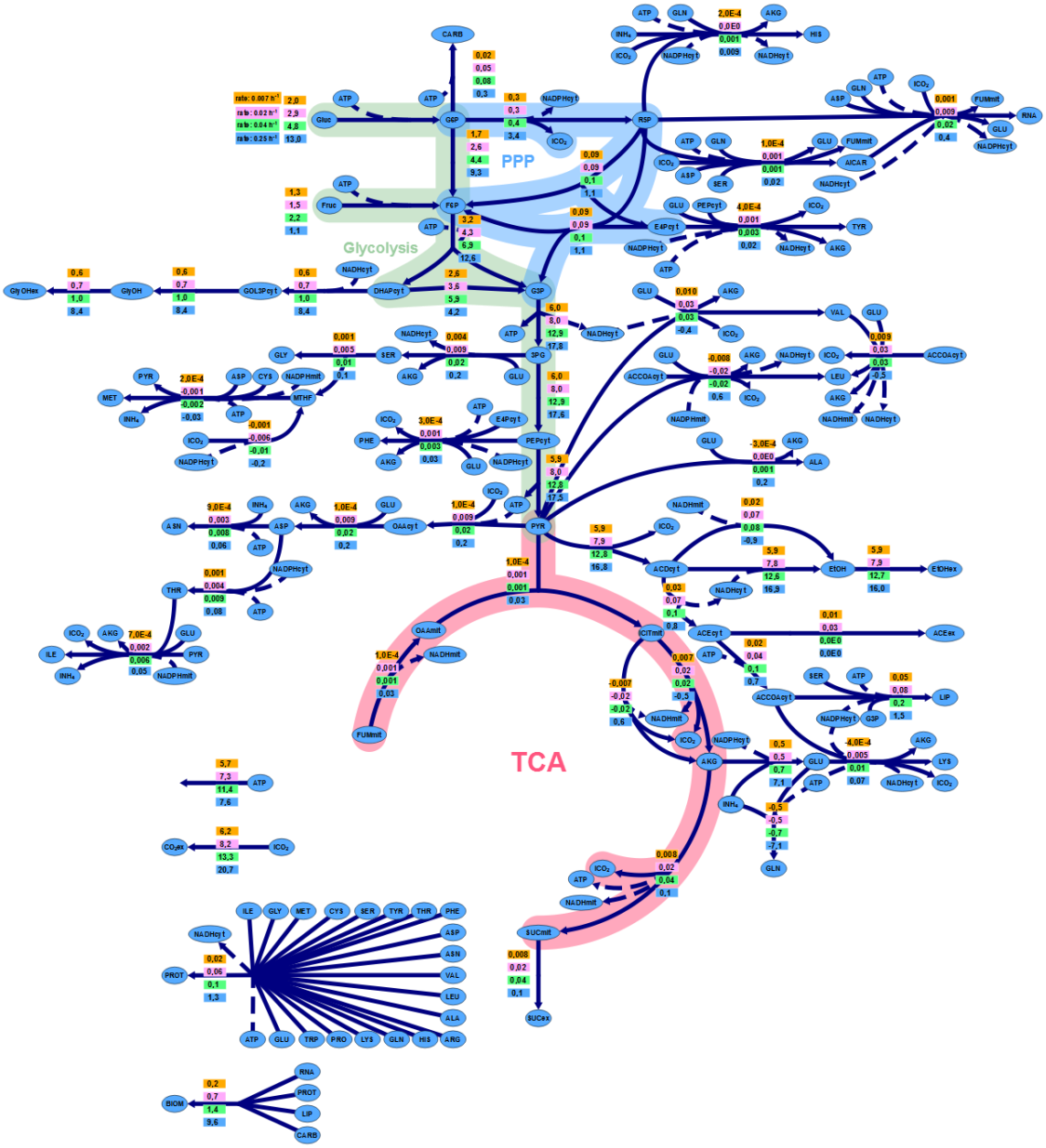

Figure 4. Metabolic flux distributions in the EC1118 strain during growth in chemostat cultures at different dilution rates. The values in the boxes correspond, from top to bottom, to fluxes (mmol h^{-1} $gDCW^{-1}$) at D = 0.27, 0.04, 0.02 and 0.007 h^{-1}, respectively.

The calculated glycolytic and oxidative PPP branch split flux was also in agreement with previous MFA and ^{13}C-MFA studies of *S. cerevisiae* under anaerobic conditions, i.e. most of carbon flux from glucose+fructose (75-95 %) was channelled to glycolysis (Varela et al. 2004, Jouhten et al. 2008). Specifically, the fraction of carbon directed to this pathway, the major source of NADPH required for biosynthetic pathways, diminished as the growth rate decreased.

As already described in several MFA studies (Nissen et al. 1997, Camarasa et al. 2003, Varela et al. 2004, Jouhten et al. 2008), the TCA cycle operated as a two separated -oxidative and reductive- branched pathway due to the fact that in the model used the activity of Succinyl CoA synthetase was considered negligible under anaerobic conditions (Costenoble et al. 2011, Vargas et al. 2011) and correspondingly set to zero. Also, consistent with previous studies, the anaplerotic flux was the major source of mitochondrial oxaloacetate.

Conclusion

Our first series of results, obtained from experiments simulating the three phases of wine-growing fermentations under standard conditions, suggest that steady states obtained in chemostat cultures at defined growth rates actually reflect the yeast physiological state observed in the corresponding growth phase of the batch fermentation. The experimental data obtained from these cultures has been integrated into a metabolic model, allowing for the quantitative description of the metabolic state of cells (metabolic fingerprint) under each growth condition. Moreover, these results proved that it is possible to define different wine-growing fermentation phases through chemostat cultures and, consequently, they have been further used to characterise metabolic changes due to temperature and increased sugar content (Quirós et al. 2013), providing the basis for the future construction of a predictive physiological model aiming to mimic the global process. Conventional chemostat cultures may offer a simpler and robust alternative to continuous multistage bioreactor systems (Clement et al. 2011) for quantitative physiology studies of wine making fermentations.

Current efforts are geared towards the establishment of cultivation strategies achieving metabolic states resembling non-proliferating cells, that is,

conditions mimicking late fermentation phases with zero growth rates and increasingly higher ethanol concentration (e.g. up to 13-15 %), the influence of nitrogen sources on cell growth and product formation, as well as the use of ^{13}C isotopic labelling techniques for further refinement of the metabolic models. Importantly, beyond identifying and characterising strain- and environmental-dependent physiological differences, our approach seeks to correlate physiological responses with transcriptional and metabolic changes in the future. As a first proof-of-concept of our approach, we have recently used chemostat cultures to investigate the effect of sugar concentration and temperature on exponentially growing yeast in wine fermentations (Quirós et al. 2013).

The final aim is to integrate all experimental data in a framework metabolic model that can be effectively used to describe and predict a wine fermentation, as well as facilitating the rational design of reliable fermentation processes. The model could additionally be used as a tool for characterizing the metabolic behavior of different wine yeast strains (metabolic fingerprint or phenotype), as well as for the selection of the most appropriate yeast strain as a function of the grape must composition or, in the optimal design and usage of enological additives.

Aknowledgements

This work is part of the Deméter Project, funded by the CDTI (Spanish Centre for Technological Industrial Development) through the Ingenio 2010-CENIT program. We thank Elena Cámara (Department of Chemical Engineering, UAB) for technical assistance and guidance in the flow cytometry analyses, as well as the personnel at the SCT-UB for trouble shutting support in the amino acid analyses.

Appendix A: Stoichiometric model

Glycolysis

r1 Glc + ATP ==> G6P

r2 Fruc + ATP ==> F6P

r3 G6P <==> F6P

r4 F6P + ATP <==> DHAP + GLA3P

r5 DHAP <==> GLA3P

r6 GLA3P <==> 3PG + NADH + ATP

r7 3PG <==> PEP

r8 PEP <==> PYR + ATP

Glycerol metabolism

r9 DHAP + NADH <==> GL3P

r10 GL3P <==> GL

Pyruvate metabolism

r11 PYR <==> iCO_2 + ACAL

r12 NADH + ACAL <==> EtOH

r13 ACAL + NADHmit <==> EtOH

r14 ACAL <==> NADPH + AC

r15 AC + ATP <==> ACCOA

Pentose phosphate pathway

r16 G6P <==> 2 NADPH + iCO_2 + R5P

r17 2 R5P <==> F6P + E4P

r18 R5P + E4P <==> F6P + GAL3P

Tricarboxylic acid cycle

r19 PYR + OAAmit <==> iCO_2 + ICITmit + NADHmit

r20 ICITmit <==> iCO_2 + AKG + NADHmit

r21 ICITmit <==> iCO_2 + AKG + NADPHmit

r22 AKG <==> iCO_2 + SUCCmit + ATP + NADHmit

r23 FUMmit <==> OAAmit + NADHmit

Anaplerotic reaction

r24 PYR + iCO_2 + ATP <==> OAA

Amino acid metabolism

r25 NADPH + AKG + iNH_4 <==> GLU

r26 ATP + iNH_4 + GLU <==> GLN

r27 OAA + GLU <==> AKG + ASP

r28 3PG + GLU <==> NADH + AKG + SER

r29 PYR + GLU <==> AKG + ALA

r30 2 NADPH + 2 ATP + ASP <==> THR

r31 THR + NADH <==> iCO_2 + PROPex

r32 2 PYR + ACCOA + GLU <==> 2 iCO_2 + 2 NADH + AKG + LEU

r33 ACCOA + NADHmit + GLU + VAL <==> iCO_2 + NADH + AKG + LEU

r34 AKG + LEU <==> iCO_2 + GLU + IAMI-OH

r35 2 PYR + NADPH + GLU <==> iCO_2 + AKG + VAL

r36 AKG + VAL <==> iCO_2 + GLU + IBUT-OH

r37 2 PEP + NADPH + E4P + ATP + GLU <==> iCO_2 + AKG + PHE

r38 AKG + PHE <==> iCO_2 + GLU + PHEEtOH

r39 PYR + NADPHmit + GLU + THR <==> iCO_2 + AKG + iNH_4 + ILE

r40 AKG + ILE <==> iCO_2 + GLU + AMI-OH

r41 2 NADPH + ACCOA + 3 ATP + 2 GLU <==> iCO_2 + 2 NADH + AKG + LYS

r42 2 ATP + iNH_4 + ASP <==> ASN

r43 2 NADPH + iCO_2 <==> MTHF

r44 SER <==> MTHF + GLY

r45 3 NADPHmit + 3 ATP + ASP + MTHF + CYS <==> PYR + iNH_4 + MET

r46 2 PEP + NADPH + E4P + 3 ATP + GLU <==> iCO_2 + NADH + AKG + TYR

r47 NADPH + iCO_2 + R5P + 5 ATP + iNH_4 + GLN <==> 2 NADH + AKG + HIS

r48 AKG + TRP <==> iCO_2 + GLU + I3-EtOH

r49 NADPH + AKG + ARG <==> iCO_2 + 2 iNH_4 + GLU + PRO

r50 NADH + AC + CYS ==> 5 NADPH + ACCOA + ATP + SER

Nitrogen uptake

r51 ATP + NH_4ex ==> iNH_4

r52 ATP + ALAex ==> ALA

r53 ATP + ARGex ==> ARG

r54 ATP + ASPex ==> ASP

r55 ATP + CYSex ==> CYS

r56 ATP + GLNex ==> GLN

r57 ATP + GLUex ==> GLU

r58 ATP + GLYex ==> GLY

r59 ATP + HISex ==> HIS

r60 ATP + ILEex ==> ILE

r61 ATP + LEUex ==> LEU

r62 ATP + LYSex ==> LYS

r63 ATP + METex ==> MET

r64 ATP + PHEex ==> PHE

r65 ATP + SERex ==> SER

r66 ATP + THRex ==> THR

r67 ATP + TRPex ==> TRP

r68 ATP + TYRex ==> TYR

r69 ATP + VALex ==> VAL

Product release

r70 AC ==> ACex

r71 EtOH <==> EtOHex

r72 GL <==> GLex

r73 SUCCmit ==> SUCCex

r74 iCO_2 ==> CO_2ex

r75 DHAP ==> LACex

Synthesis of AICAR

r76 iCO_2 + R5P + 6 ATP + 2 GLN + ASP + SER ==> NADPH + FUMmit + 2 GLU + 9 AICAR

Maintenance

r77 ATP ==>

Macromolecules biosynthesis

Synthesis of nucleic acid

r78 0.057 iCO_2 + 0.048 R5P + 0.132 NADH + 0.489 ATP + 0.105 GLN + 0.075 ASP + 0.511 AICAR ==> 0.135 NADPH + 0.027 FUMmit + 0.105 GLU + NA

Synthesis of carbohydrates

r79 G6P + ATP ==> 6 CARB

Synthesis of lipids

r80 0.022 GAL3P + 0.831 NADPH + 0.416 ACCOA + 0.400 ATP + 0.034 SER ==> LIP

Synthesis of proteins (r81)

0.27 h^{-1}

4 ATP + 0.052344 GLU + 0.052344 GLN + 0.048496 ASP + 0.066138 SER + 0.070466 ARG + 0.094046 ALA + 0.055908 THR + 0.075811 LEU + 0.067013 VAL + 0.033301 PHE + 0.049971 ILE + 0.046925 PRO + 0.076823 LYS + 0.10019 GLY + 0.003752 CYS + 0.048496 ASN + 0.006474 MET + 0.020285 TYR + 0.009742 TRP + 0.02147 HIS= 4.786 PROT

0.04 h^{-1}

4 ATP + 0.052732 GLU + 0.052732 GLN + 0.052443 ASP + 0.073552 SER + 0.0484 ARG + 0.094517 ALA + 0.061251 THR + 0.075916 LEU + 0.065404 VAL + 0.033467 PHE + 0.050062 ILE + 0.060942 PRO + 0.072938 LYS + 0.092748 GLY + 0.002989 CYS + 0.052443 ASN + 0.00345 MET + 0.025046 TYR + 0.008607 TRP + 0.02036 HIS + 3.6e-005 NADHcyt = 4.7669 PROT

0.02 h^{-1}

4 ATP + 0.053808 GLU + 0.053808 GLN + 0.054029 ASP + 0.073792 SER + 0.046254 ARG + 0.09815 ALA + 0.061934 THR + 0.075751 LEU + 0.064016 VAL +

0.033968 PHE + 0.049044 ILE + 0.045537 PRO + 0.07309 LYS + 0.091933 GLY + 0.004528 CYS + 0.054029 ASN + 0.008273 MET + 0.025584 TYR + 0.012445 TRP + 0.020026 HIS = 0.00035 NADHcyt + 4.7783 PROT

0.007 h^{-1}

4 ATP + 0.053808 GLU + 0.053808 GLN + 0.054029 ASP + 0.073792 SER + 0.046254 ARG + 0.09815 ALA + 0.061934 THR + 0.075751 LEU + 0.064016 VAL + 0.033968 PHE + 0.049044 ILE + 0.045537 PRO + 0.07309 LYS + 0.091933 GLY + 0.004528 CYS + 0.054029 ASN + 0.008273 MET + 0.025584 TYR + 0.012445 TRP + 0.020026 HIS = 0.00035 NADHcyt + 4.7783 PROT

Synthesis of biomass (r82)

0.27 h^{-1}

0.16798 CARB + 0.040493 RNA + 0.63291 PROT + 0.15862 LIP ==> BIOM

0.04 h^{-1}

0.3504 CARB + 0.012122 RNA + 0.49628 PROT + 0.14119 LIP ==> BIOM

0.02 h^{-1}

0.42961 CARB + 0.012487 RNA + 0.44784 PROT + 0.11007 LIP ==> BIOM

0.007 h^{-1}

0.46243 CARB + 0.004016 RNA + 0.34184 PROT + 0.19172 ==> BIOM

Appendix B: Abbreviations

3PG	3-Phospho-D-glycerate
ACCOA	Acetyl-CoA
ACAL	Acetaldehyde
AC	Acetate
ACex	Extracellular Acetate
AICAR	1-(5'-Phosphoribosyl)-5-amino-4-imidazolecarboxamide
AKG	2-Oxoglutarate
ALA	L-Alanine
ALAex	Extracellular L-Alanine
AMI-OH	Amylalcohol
ARG	L-Arginine
ARGex	Extracellular L-Arginine
ASN	L-Asparragine
ASP	L-Aspartate
ASPex	Extracellular L-Aspartate
ATP	Adenosin Triphosphate
BIOM	Biomass
CARB	Carbohydrate
CO_2ex	Extracellular CO_2
CYS	L-Cysteine
CYSex	Extracellular L-Cysteine
DHAP	Di-hydroxyAcetona Phosphate
E4P	D-Erythrose 4-phosphate
EtOH	Ethanol
EtOHex	Extracellular Ethanol
Fruc	D-Fructose
F6P	D-Fructose 6-phosphate
FUMmit	Mitochondrial Fumarate
GLA3P	Glyceraldehyde 3-Phosphate
G6P	D-Glucose 6-Phosphate
GLN	L-Glutamine

GLNex	Extracellular L-Glutamine
GLU	L-Glutamate
Glc	D-Glucose
GLUex	Extracellular L-Glutamate
GLY	Glycine
GLYex	Extracellular Glycine
GL	Glycerol
GLex	Extracellular Glycerol
GL3P	Cytosolic Glycerol 3-Phosphate
HIS	L-Histidine
HISex	Extracellular L-Histidine
I3-EtOH	Indole-3-ethanol
IAMI-OH	Isoamyl alcohol
IBUT-OH	Isobutanol
ICITmit	Mitochondrial isocitrate
iCO_2	Intracellular CO_2
ILE	L-Isoleucine
ILEex	Extracellular L-Isoleucine
iNH_4	Intracellular NH_4
LACex	Extracellular Lactate
LEU	L-Leucine
LEUex	Extracellular L-Leucine
LIP	Lipid
LYS	L-Lysine
LYSex	Extracellular L-Lysine
MET	L-Methionine
METex	Extracellular L-Methionine
MTHF	5,10-Methyltetrahydrofolate
NADH	Cytosolic NADH
NADHmit	Mitochondrial NADH
NADPH	Cytosolic NADPH
NADPHmit	Mitochondrial NADPH
NH_4ex	Extracellular NH_4

OAA	Cytosolic Oxaloacetate
OAAmit	Mitochondrial Oxaloacetate
PEP	Cytosolic Phosphoenolpyruvate
PHE	L-Phenylalanine
PHEEtOH	2-Phenyl ethanol
PHEex	Extracellular L-Phenylalanine
PRO	L-Proline
PROPex	Extracellular n-Propanol
PROT	Protein
PYR	Pyruvate
R5P	D-Ribose 5-Phosphate
NA	Nucleic acid
SER	L-Serine
SERex	Extracellular L-Serine
SUCCex	Extracellular Succinate
SUCCmit	Mitochondrial Succinate
THR	L-Threonine
THRex	Extracellular L-Threonine
TRP	L-Triptophan
TRPex	Extracellular L-Triptophan
TYR	L_Tyrosine
TYRex	Extracellular L-Tyrosine
VAL	L-Valine
VALex	Extracellular L-Valine

References

Aceituno, F. F., M. Orellana, J. Torres, S. Mendoza, A. W. Slater, F. Melo, and E. Agosin. 2012. Oxygen response of the wine yeast *Saccharomyces cerevisiae* EC1118 grown under carbon-sufficient, nitrogen-limited enological conditions. Appl. Environ. Microb. 78: 8340-8352.

Alonso, A. D., and M. A. O'Neill. 2011. Climate change from the perspective of Spanish wine growers: A three-region study. Brit. Food J. 113: 205-221.

Battaglini, A., G. Barbeau, M. Bindi, and F. W. Badeck. 2009. European winegrowers' perceptions of climate change impact and options for adaptation. Reg. Environ. Change. 9: 61-73.

Berthels, N. J., R. R. Cordero Otero, F. F. Bauer, J. M. Thevelein, and I. S. Pretorius. 2004. Discrepancy in glucose and fructose utilisation during fermentation by Saccharomyces cerevisiae wine yeast strains. FEMS Yeast Res. 4: 683-689.

Borneman, A. R., P. J. Chambers, and I. S. Pretorius. 2007. Yeast systems biology: Modelling the winemaker's art. Trends Biotechnol. 25: 349-355.

Camarasa, C., J. P. Grivet, and S. Dequin. 2003. Investigation by 13C-NMR and tricarboxylic acid (TCA) deletion mutant analysis of pathways for succinate formation in *Saccharomyces cerevisiae* during anaerobic fermentation. Microbiology 149: 2669-2678.

Celton, M., I. Sanchez, A. Goelzer, V. Fromion, C. Camarasa, and S. Dequin. 2012. A comparative transcriptomic, fluxomic and metabolomic analysis of the response of Saccharomyces cerevisiae to increases in NADPH oxidation. BMC Genomics 13: 317.

Clement, T., M. Perez, J. R. Mouret, J. M. Sablayrolles, and C. Camarasa. 2011. Use of a continuous multistage bioreactor to mimic winemaking fermentation. Int. J. Food Microbiol. 150: 42-49.

Costenoble, R., P. Picotti, L. Reiter, R. Stallmach, M. Heinemann, U. Sauer, and R. Aebersold. 2011. Comprehensive quantitative analysis of central carbon and amino-acid metabolism in *Saccharomyces cerevisiae* under multiple conditions by targeted proteomics. Mol. Syst. Biol. 7.

Crépin, L., T. Nidelet, I. Sanchez, S. Dequin, and C. Camarasa. 2012. Sequential use of nitrogen compounds by *Saccharomyces cerevisiae* during wine fermentation: a model based on kinetic and regulation characteristics of nitrogen permeases. Appl. Environ. Microb. 78: 8102-8111.

Christen, S., and U. Sauer. 2011. Intracellular characterization of aerobic glucose metabolism in seven yeast species by 13C flux analysis and metabolomics. FEMS Yeast Res. 11: 263-272.

Daran-Lapujade, P., M. L. A. Jansen, J.-M. Daran, W. van Gulik, J. H. de Winde, and J. T. Pronk. 2004. Role of transcriptional regulation in controlling fluxes in central carbon metabolism of *Saccharomyces cerevisiae*: A chemostat culture study. J. Biol. Chem. 279: 9125-9138.

Dragosits, M., D. Mattanovich, and B. Gasser. 2011. Introduction and measurement of UPR and osmotic stress in the yeast *Pichia pastoris*, pp. 165-188. In P. M. Conn (ed.), Methods in Enzymology, vol. 489.

Fredlund, E., L. M. Blank, J. Schnürer, U. Sauer, and V. Passoth. 2004. Oxygen- and glucose-dependent regulation of central carbon metabolism in *Pichia anomala*. Appl. Environ. Microb. 70: 5905-5911.

Frick, O., and C. Wittmann. 2005. Characterization of the metabolic shift between oxidative and fermentative growth in *Saccharomyces cerevisiae* by comparative C-13 flux analysis. Microb. Cell Fact. 4: 30.

Henschke, P. A., and V. Jiranek. 1993. Yeast - Metabolism of nitrogen compounds, pp. 77-164. In G. H. Fleet (ed.), Wine microbiology and biotechnology. Harwood Academic Press., Chur, Switzerland.

Herbert, B. N., H. J. Gould, and E. B. Chain. 1971. Crystal protein of *Bacillus thuringiensis var. tolworthi*. Eur. J. Biochem. 24: 366-375.

Jones, G., M. White, O. Cooper, and K. Storchmann. 2005. Climate change and global wine quality. Climatic Change 73: 319-343.

Jorda, J., P. Jouhten, E. Camara, H. Maaheimo, J. Albiol, and P. Ferrer. 2012. Metabolic flux profiling of recombinant protein secreting *Pichia pastoris* growing on glucose:methanol mixtures. Microb. Cell Fact. 11: 57.

Jouhten, P., E. Rintala, A. Huuskonen, A. Tamminen, M. Toivari, M. Wiebe, L. Ruohonen, M. Penttila, and H. Maaheimo. 2008. Oxygen dependence of metabolic fluxes and energy generation of *Saccharomyces cerevisiae* CEN.PK113-1A. BMC Syst. Biol. 2: 60.

Klamt, S., J. Saez-Rodriguez, and E. D. Gilles. 2007. Structural and functional analysis of cellular networks with CellNetAnalyzer. BMC Syst. Biol. 1: 2.

Kleijn, R. J., J.-M. A. Geertman, B. K. Nfor, C. Ras, D. Schipper, J. T. Pronk, J. J. Heijnen, A. J. A. Van Maris, and W. A. Van Winden. 2007. Metabolic flux analysis of a glycerol-overproducing *Saccharomyces cerevisiae* strain based on GC-MS, LC-MS and NMR-derived 13C-labelling data. FEMS Yeast Res. 7: 216-231.

Landolfo, S., H. Politi, D. Angeozzi, and I. Mannazzu. 2008. ROS accumulation and oxidative damage to cell structures in *Saccharomyces cerevisiae* wine strains during fermentation of high-sugar-containing medium. BBA-Gen. Subjects 1780: 892-898.

Lavalle, C., F. Micale, T. D. Houston, A. Camia, R. Hiederer, C. Lazar, C. Conte, G. Amatulli, and G. Genovese. 2009. Climate change in Europe. 3. Impact on agriculture and forestry. A review (Reprinted). Agron. Sustain. Dev. 29: 433-446.

Mendes-Ferreira, A., B. Sampaio-Marques, C. Barbosa, F. Rodrigues, V. Costa, A. Mendes-Faia, P. Ludovico, and C. Leao. 2010. Accumulation of non-superoxide anion reactive oxygen species mediates nitrogen-limited alcoholic fermentation by *Saccharomyces cerevisiae*. Appl. Environ. Microb. 76: 7918-7924.

Nissen, T. L., U. Schulze, J. Nielsen, and J. Villadsen. 1997. Flux distributions in anaerobic, glucose-limited continuous cultures of *Saccharomyces cerevisiae*. Microbiol.-UK 143: 203-218.

Novo, M., F. Bigey, E. Beyne, V. Galeote, F. Gavory, S. Mallet, B. Cambon, J. L. Legras, P. Wincker, S. Casaregola, and S. Dequin. 2009. Eukaryote-to-eukaryote gene transfer events revealed by the genome sequence of the wine yeast *Saccharomyces cerevisiae* EC1118. P. Natl. Acad. Sci. USA 106: 16333-16338.

Olesen, J. E., M. Trnka, K. C. Kersebaum, A. O. Skjelvåg, B. Seguin, P. Peltonen-Sainio, F. Rossi, J. Kozyra, and F. Micale. 2011. Impacts and adaptation of European crop production systems to climate change. European Journal of Agronomy 34: 96-112.

Pizarro, F., F. A. Vargas, and E. Agosin. 2007a. A systems biology perspective of wine fermentations. Yeast 24: 977-991.

Pizarro, F., C. Varela, C. Martabit, C. Bruno, J. R. Prez-Correa, and E. Agosin. 2007b. Coupling kinetic expressions and metabolic networks for predicting wine fermentations. Biotechnol. Bioeng. 98: 986-998.

Pizarro, F. J., M. C. Jewett, J. Nielsen, and E. Agosin. 2008. Growth temperature exerts differential physiological and transcriptional responses in laboratory and wine strains of *Saccharomyces cerevisiae*. Appl. Environ. Microb. 74: 6358-6368.

Quirós, M., R. Martínez-Moreno, J. Albiol, P. Morales, F. Vázquez-Lima, A. Barreiro-Vázquez, P. Ferrer, and R. Gonzalez. 2013. Metabolic flux analysis during the exponential growth phase of *Saccharomyces cerevisiae* in wine fermentations. PLOS ONE 8: e71909.

Ribéreau-Gayon, P., D. Dubourdieu, B. Donèche, and A. Lanvaud. 2004. Traité d'oenologie. Micobiologia du vin., 5e édition ed. La vigne, Paris.

Rossignol, T., L. Dulau, A. Julien, and B. Blondin. 2003. Genome-wide monitoring of wine yeast gene expression during alcoholic fermentation. Yeast 20: 1369-1385.

Sainz, J., F. Pizarro, J. R. Perez-Correa, and E. Agosin. 2003. Modeling of yeast metabolism and process dynamics in batch fermentation. Biotechnol. Bioeng. 81: 818-828.

Salazar-Parra, C., J. Aguirreolea, M. Sanchez-Diaz, J. J. Irigoyen, and F. Morales. 2010. Effects of climate change scenarios on Tempranillo grapevine (*Vitis vinifera* L.) ripening: Response to a combination of elevated CO2 and temperature, and moderate drought. Plant Soil 337: 179-191.

Salmon, J.-M., and P. Barre. 1998. Improvement of nitrogen assimilation and fermentation kinetics under enological conditions by derepression of alternative nitrogen-assimilatory pathways in an industrial *Saccharomyces cerevisiae* strain. Appl. Environ. Microb. 64: 3831-3837.

Smolders, G. J. F., J. Vandermeij, M. C. M. Vanloosdrecht, and J. J. Heijnen. 1994. Stoichiometric model of the aerobic metabolism of the biological phosphorus removal process. Biotechnol. Bioeng. 44: 837-848.

Trnka, M., R. Brazdil, M. Dubrovsky, D. Semeradova, P. Stepanek, P. Dobrovolny, M. Mozny, J. Eitzinger, J. Malek, H. Formayer, J. Balek, and Z. Zalud. 2011. A 200-year climate record in central Europe: Implications for agriculture. Agron. Sustain. Dev. 31: 631-641.

Tronchoni, J., A. Gamero, F. N. Arroyo-Lopez, E. Barrio, and A. Querol. 2009. Differences in the glucose and fructose consumption profiles in diverse *Saccharomyces* wine species and their hybrids during grape juice fermentation. Int. J. Food Microbiol. 134: 237-243.

Varela, C., F. Pizarro, and E. Agosin. 2004. Biomass content governs fermentation rate in nitrogen-deficient wine musts. Appl. Environ. Microb. 70: 3392-3400.

Vargas, F. A., F. Pizarro, J. R. Perez-Correa, and E. Agosin. 2011. Expanding a dynamic flux balance model of yeast fermentation to genome-scale. BMC Syst. Biol. 5: 50.

Wang, N. S., and G. Stephanopoulos. 1983. Application of macroscopic balances to the identification of gross measurement errors. Biotechnol. Bioeng. 25: 2177-2208.

Zeng, A.-P., and J. Sun. 2010. Continuous Culture, Manual of Industrial Microbiology and Biotechnology, Third Edition.

Additional files

Table A1. Overview of the macroscopic growth parameters of the EC1118 strain growing in cultures.

	D (h^{-1})							
	0.27		0.04		0.02		0.007	
mmol $(h \cdot gDCW)^{-1}$	Bal	sd	Bal	sd	Bal	sd	Bal	sd
Glucose	-15	28	-4.9	1.4	-3.0	0.6	-2.0	0.3
Fructose	-1	28	-2.3	1.5	-1.5	0.6	-1.3	0.3
Glycerol	8.1	1.1	0.97	0.29	0.69	0.26	0.58	0.35
Etanol	17.2	3.6	12.7	1.0	7.9	0.6	5.9	0.6
Succinate	0.09	0.01	0.07	0.01	0.06	0.01	0.039	0.004
Acetate	0.000	0.000	0.000	0.000	0.027	0.003	0.012	0.001
Lactate	0.000	0.000	0.000	0.000	0.000	0.000	0.000	0.000
Asp	-0.048	0.009	-0.0031	0.0003	-0.0014	0.0001	0.0032	0.0004
Glu	-0.01	0.03	-0.008	0.001	-0.0035	0.0004	-0.0012	0.0001
Ser	-0.042	0.024	-0.007	0.001	-0.0032	0.0003	-0.0010	0.0001
Gln	-0.54	0.09	-0.032	0.003	-0.0151	0.0015	-0.0043	0.0004
Hys	-0.030	0.006	-0.0019	0.0002	-0.0009	0.0001	-0.00021	0.00003
Gly	0.014	0.010	-0.0016	0.0002	-0.0007	0.0001	-0.00016	0.00004
Thr	-0.054	0.019	-0.006	0.001	-0.0028	0.0003	-0.0008	0.0001
Arg	-0.059	0.067	-0.020	0.002	-0.0093	0.0009	-0.0028	0.0003
Ala	-0.006	0.059	-0.014	0.002	-0.0062	0.0007	-0.0019	0.0003
Tyr	-0.013	0.003	-0.0009	0.0001	-0.0004	0.00005	-0.0001	0.00002
Val	-0.004	0.013	-0.0034	0.0003	-0.0016	0.0002	-0.00052	0.00005
Met	-0.033	0.006	-0.0020	0.0002	-0.0009	0.0001	-0.00018	0.00002
Cys	-0.042	0.004	-0.0016	0.0002	-0.0008	0.0001	-0.0002	0.0000
Ile	-0.013	0.008	-0.0018	0.0002	-0.0008	0.0001	-0.0002	0.0001
Trp	-0.076	0.025	-0.008	0.001	-0.0038	0.0004	-0.0007	0.0001
Leu	-0.021	0.012	-0.0034	0.0003	-0.0016	0.0002	-0.0005	0.0001
Phe	-0.022	0.007	-0.0020	0.0002	-0.0010	0.0001	-0.00026	0.00003
Lys	-0.027	0.003	0.0034	0.0005	0.0021	0.0003	0.0010	0.0001
NH_4	-0.5	0.2	-	-	-	-	-	-
Biomass	9.5	0.9	1.4	0.1	0.69	0.04	0.25	0.02
CO_2	19.0	1.8	13.2	1.0	8.2	0.6	6.3	0.5

Reconciled measured substrates and products consumption or production rates at steady state conditions in each experiment. Substrate consumption, biomass and metabolites production rates for each strain. n.d., not detectable. Consistency index h was below 7.81 for a redundancy of 3 (95 % significance level) in all cases.

Table A2. Biomass C-molecular and macromolecular composition for S. cerevisiae EC1118.

D (h^{-1})	Elemental composition	Protein (mg g^{-1})	Carbohydrates (mg g^{-1})	Trehalose (mg g^{-1})	Glycogen (mg g^{-1})
0.27	$CH_{1.91}O_{0.54}N_{0.21}$	473	161	95	11
0.04	$CH_{1.80}O_{0.57}N_{0.14}$	453	235	99	40
0.02	$CH_{1.85}O_{0.64}N_{0.13}$	382	470	96	58
0.007	$^{*}CH_{1.75}O_{0.56}N_{0.098}$	262	474	n.d.	121

Macromolecular components abundance is expressed as mg of component per gram of cell dry weight.
n.d., not determined.
* Calculated from biomass macromolecular composition.

Table A3. Amino acid (mg $gDCW^{-1}$) composition of *S. cerevisiae* EC1118.

	D (h^{-1})			
Amino acid	0.27	0.04	0.02	0.007
Asp+Asn	51.5	45.7	44.9	32.8
Ser	26.8	23.2	23.4	18.8
Glu+Gln	62.9	55.1	50.6	32.9
Gly	26.6	20.1	19.1	13.6
His	13.7	10.6	10	7.4
Arg	51.2	25.6	26.3	18.5
Thr	26.3	22.7	22.8	18.1
Ala	31.1	25.9	25.4	17.6
Pro	21.2	22.2	16.1	13.7
Cys	n.d.	2.1	1.7	0
Tyr	15.4	16.8	15.2	11.2
Val	30.9	25.9	23.1	16.9
Met	n.d.	4.8	0	0
Lys	45.8	35.2	34.1	24.8
Ileu	26.3	22.6	20.2	15.1
Leu	39.9	33.5	31.2	23.1
Phe	22.8	19.1	18.2	13.3
Total	492.4	411.1	382.3	277.8

Amino acid composition of the whole cell extract of EC1118 strain. Amino acid composition measured for each of the growth condition tested in chemostat cultures.

Table A4. Metabolic fluxes. Fluxes are given in mmol h^{-1} $gDCW^{-1}$ (Continued on next pages)

	D (h^{-1})							
	0.27		0.04		0.02		0.007	
Reaction	Bal	sd	Bal	sd	Bal	sd	Bal	sd
r1	13	28	4.8	1.4	2.93	0.59	2.00	0.32
r2	1	28	2.2	1.5	1.49	0.61	1.35	0.34
r3	9.3	0.8	4.36	0.88	2.61	0.59	1.70	0.52
r4	13	1	6.86	0.38	4.28	0.29	3.23	0.32
r5	4.2	1.0	5.89	0.52	3.59	0.44	2.63	0.51
r6	17.8	1.2	12.87	0.71	7.97	0.54	5.95	0.58
r7	17.6	1.2	12.85	0.71	7.96	0.54	5.95	0.58
r8	17.5	1.2	12.84	0.71	7.95	0.54	5.95	0.58
r9	8.36	0.98	0.97	0.52	0.69	0.49	0.60	0.55
r10	8.36	0.98	0.97	0.52	0.69	0.49	0.60	0.55
r11	16.8	1.1	12.8	0.7	7.9	0.5	5.9	0.6
r12	15.9	2.3	12.6	0.8	7.8	0.6	5.9	0.6
r13	0.1	2.0	0.1	0.4	0.1	0.3	0.0	0.2
r14	0.79	0.15	0.103	0.035	0.066	0.051	0.03	0.22
r15	0.72	0.18	0.101	0.040	0.038	0.029	0.021	0.019
r16	3.39	0.69	0.40	0.28	0.28	0.26	0.28	0.36
r17	1.13	0.23	0.13	0.09	0.09	0.09	0.09	0.12
r18	1.08	0.24	0.13	0.09	0.09	0.09	0.09	0.12
r19	0.033	0.003	0.001	0.000	0.001	0.000	0.000	0.000
r20	-0.037	1.057	0.018	0.197	0.023	0.145	0.007	0.073
r21	0.069	1.058	-0.017	0.197	-0.022	0.146	-0.007	0.073
r22	0.110	0.093	0.035	0.052	0.020	0.040	0.008	0.023
r23	0.033	0.003	0.001	0.000	0.001	0.000	0.000	0.000
r24	0.19	0.21	0.02	0.04	0.01	0.03	0.00	0.03
r25	6.62	1.56	0.69	0.59	0.52	0.53	0.54	0.60
r26	-6.10	2.00	-0.67	0.62	-0.51	0.55	-0.54	0.61
r27	0.19	0.21	0.02	0.04	0.01	0.03	0.00	0.03
r28	0.22	0.20	0.02	0.04	0.01	0.02	0.00	0.01
r29	0.15	0.24	0.00	0.04	0.00	0.03	0.00	0.02

	D (h^{-1})							
	0.27		0.04		0.02		0.007	
Reaction	Bal	sd	Bal	sd	Bal	sd	Bal	sd
r30	0.08	0.17	0.01	0.03	0.00	0.02	0.00	0.02
r31	-	-	-	-	-	-	-	-
r32	0.11	1.00	-0.02	0.19	-0.02	0.14	-0.01	0.07
r33	-0.03	0.98	0.03	0.18	0.03	0.14	0.01	0.07
r34	-	-	-	-	-	-	-	-
r35	0.05	0.97	0.03	0.18	0.03	0.14	0.01	0.07
r36	-	-	-	-	-	-	-	-
r37	0.03	0.08	0.00	0.02	0.00	0.01	0.00	0.01
r38	-	-	-	-	-	-	-	-
r39	0.05	0.10	0.01	0.02	0.00	0.01	0.00	0.01
r40	-	-	-	-	-	-	-	-
r41	0.074	0.055	0.012	0.022	0.005	0.017	-0.0004	0.0099
r42	0.062	0.006	0.008	0.002	0.0034	0.0011	0.0009	0.0006
r43	-0.179	0.127	-0.014	0.020	-0.0055	0.0142	-0.0012	0.0078
r44	0.149	0.101	0.012	0.014	0.0052	0.0102	0.0014	0.0064
r45	-0.030	0.077	-0.002	0.014	-0.0004	0.0100	0.0002	0.0045
r46	0.017	0.055	0.003	0.010	0.0012	0.0071	0.0004	0.0045
r47	0.009	0.077	0.001	0.014	0.0004	0.0100	0.0002	0.0055
r48	0.046	0.173	0.007	0.028	0.003	0.020	0.0004	0.0084
r49	0.034	0.224	0.012	0.039	0.0070	0.0269	0.0003	0.0011
r50	0.069	0.100	0.003	0.020	0.0009	0.0141	-0.0003	0.0065
r51	0.5	0.21	-	-	-	-	-	-
r52	-0.03	0.06	0.014	0.002	0.006	0.001	0.0019	0.0003
r53	0.12	0.07	0.020	0.002	0.010	0.001	0.0011	0.0003
r54	0.034	0.009	0.0031	0.0003	0.0014	0.000145	0.0032	0.000356
r55	0.044	0.004	0.0016	0.0002	0.0008	7.69E-05	0	2.21E-05
r56	0.36	0.09	0.049	0.003	0.025	0.001	0.0072	0.0004
r57	-0.07	0.03	0.012	0.001	0.0061	0.0004	0.0019	0.0001

Continued on nex page

	D (h^{-1})							
	0.27		0.04		0.02		0.007	
Reaction	Bal	sd	Bal	sd	Bal	sd	Bal	sd
r58	-0.02	0.01	0.0016	0.0002	0.0007	0.0001	0.00020	0.00004
r59	0.018	0.006	0.0019	0.0002	0.0009	0.0001	0.00020	0.00003
r60	0.012	0.008	0.0018	0.0002	0.0008	0.0001	0.00020	0.00006
r61	0.020	0.012	0.0034	0.0003	0.0016	0.0002	0.00050	0.00005
r62	0.024	0.003	-0.0007	0.0005	-0.0001	0.0003	0.0017	0.0001
r63	0.038	0.006	0.0020	0.0002	0.00090	0.00009	0.00000	0.00002
r64	0.014	0.007	0.002	0.000214	0.0010	0.0001	0.00030	0.00003
r65	0.022	0.024	0.007	0.001	0.0032	0.0003	0.0010	0.0001
r66	0.04	0.02	0.006	0.001	0.0028	0.0003	0.0008	0.0001
r67	0.06	0.03	0.008	0.001	0.0038	0.000377	0.00070	0.00007
r68	0.009	0.003	0.0009	0.0001	0.00040	0.00005	0.00010	0.00002
r69	0.0004	0.0133	0.0034	0.000349	0.0016	0.000165	0.0005	5.33E-05
r70	0.000	0.000	0.000	0.000	0.027	0.003	0.011	0.001
r71	16.0	3.6	12.7	1.0	7.9	0.6	5.9	0.6
r72	8.4	1.1	1.0	0.3	0.7	0.3	0.6	0.4
r73	0.110	0.009	0.035	0.007	0.020	0.006	0.008	0.004
r74	20.7	1.8	13.3	1.0	8.3	0.6	6.2	0.5
r75	0.0000	0.0000	0.0000	0.0000	0.0000	0.0000	0.0000	0.0000
r76	0.022	0.002	0.0010	0.0002	0.00050	0.00014	0.00010	0.00003
r77	6.1	2.7	11.4	0.8	7.3	0.6	5.7	0.6
r78	0.39	0.04	0.017	0.003	0.009	0.003	0.0010	0.0006
r79	0.27	0.03	0.083	0.016	0.049	0.014	0.019	0.011
r80	1.52	0.15	0.202	0.040	0.075	0.022	0.048	0.027
r81	1.27	0.12	0.149	0.029	0.064	0.019	0.018	0.010
r82	9.61	0.88	1.429	0.079	0.681	0.041	0.249	0.017

Bal: Balanced rate of the reaction.

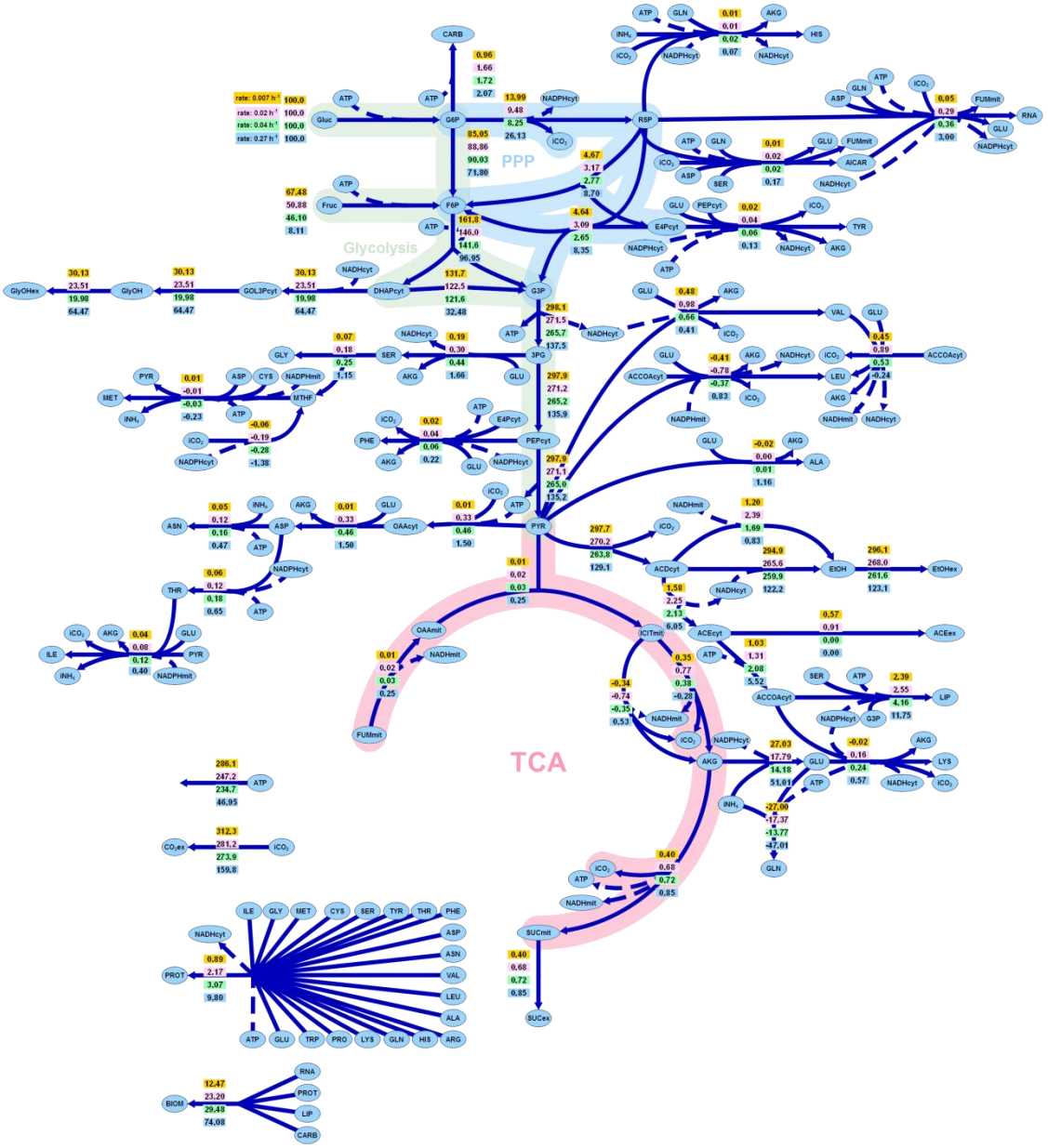

Figure A1. Metabolic fluxes. Metabolic flux distributions in the EC1118 strain during growth in chemostat cultures at different dilution rates. The values in the boxes correspond, from top to bottom, to fluxes at D = 0.27, 0.04, 0.02 and 0.007 h^{-1}, respectively. Fluxes are normalized with respect glucose uptake flux % C-mol (C-mol glucose)$^{-1}$.

Chapter III

♦

Metabolic flux analysis during the exponential growth phase of Saccharomyces cerevisiae in wine fermentation

CHAPTER III

Metabolic flux analysis during the exponential growth phase of *Saccharomyces cerevisiae* in wine fermentation

Abstract

As a consequence of the increase in global average temperature, grapes with the adequate phenolic and aromatic maturity tend to be overripe by the time of harvest, resulting in increased sugar concentrations and imbalanced C/N ratios in fermenting musts. This fact sets obvious additional hurdles in the challenge of obtaining wines with reduced alcohols levels, a new trend in consumer demands. It would therefore be interesting to understand *Saccharomyces cerevisiae* physiology during the fermentation of must with these altered characteristics. The present study aims to determine the distribution of metabolic fluxes during the yeast exponential growth phase, when both carbon and nitrogen sources are in excess, using continuous cultures. Two different sugar concentrations were studied under two different winemaking temperature conditions. Although consumption and production rates for key metabolites were severely affected by the different experimental conditions studied, the general distribution of fluxes in central carbon metabolism was basically conserved in all cases. It was also observed that temperature and sugar concentration exerted a higher effect on the pentose phosphate pathway and glycerol formation than on glycolysis and ethanol production. Additionally, nitrogen uptake, both quantitatively and qualitatively, was strongly influenced by environmental conditions. This work provides the most complete stoichiometric model used for Metabolic Flux Analysis of *S. cerevisiae* in wine fermentations employed so far, including the synthesis and release of relevant aroma compounds and could be used in the design of optimal nitrogen supplementation of wine fermentations.

This chapter has been published in PLOS ONE as: Manuel Quirós, Rubén Martínez-Moreno, Joan Albiol, Pilar Morales, Felícitas Vázquez-Lima, Antonio Barreiro-Vázquez, Pau Ferrer and Ramon Gonzalez Metabolic flux analysis during the exponential growth phase of *Saccharomyces cerevisiae* in wine fermentation. doi:10.1371/journal.pone.0071909

Introduction

Over the past few decades, the intensified emissions of greenhouse gases and aerosol particles mainly derived from industrial activity and transport have led to one of the major challenges in the history of mankind: global warming (Grassl 2011). Apart from known consequences such as the melting of the polar ice caps, this phenomenon is also affecting agriculture. In fact, the increase in temperature has already had a noteworthy effect on, among others, the grape and wine industry (Mira de Orduña 2010).

Global warming has been shown to cause lower yields in *Vitis vinifera*, changes in plagues and microbiological diseases and drastic modifications in grape physiology. With respect to the latter, changes in acidity, phenolic maturation, tannin content and sugar concentration have been proven to occur, especially in warm climates (Jones et al. 2005). Among these parameters, increased sugar concentrations may cause important changes in the physiology of *Saccharomyces cerevisiae*, the yeast species mainly responsible for the alcoholic fermentation that takes place during winemaking. High sugar concentrations induce an osmotic stress response in yeast, which can result in stuck or sluggish fermentations and lead to increased formation of fermentation by-products such as glycerol and acetic acid (Erasmus et al. 2004, Pigeau and Inglis 2005).

Although the physiology of *S. cerevisiae* has been thoroughly studied and characterized over the last century due to the status of this yeast as model organism, the distribution of metabolic fluxes occurring during wine fermentations has not been tackled in depth. Due to the intrinsic dynamic nature of this process, yeast metabolism undergoes a series of physiological adaptive changes in response to the continuous environmental variations that take place, clearly hampering its understanding.

During the last decade, several laboratories have aimed to study yeast physiology under winemaking conditions. Varela et al. (2004) described the metabolic flux distribution of yeast during sluggish and normal fermentations using batch cultures. This group has further extended this approach by developing a genome-scale dynamic flux balance model that allows prediction of metabolite

production in batch cultures (Vargas et al. 2011). In this context, Clement et al. (2011) studied the fermentation process in a “multistage bioreactor system”, where two or four fermenters, operating in continuous mode, were connected in tandem mimicking sequential stages of standard batch wine fermentations. This allowed the achievement of a series of metabolic steady states resembling those found in each stage of wine fermentation. Nevertheless, this cultivation strategy was not used for further Metabolic Flux Analysis (MFA) studies. As an alternative, we have recently developed a simple approach for metabolic phenotyping of yeast during wine fermentations. In short, batch fermentations are first systematically characterized, including measurements of growth and consumption/production rates of the main metabolites along the whole process. Based on the evolution of physiological parameters, the fermentation is divided into three defined phases: phase I, corresponding to the yeast exponential growth phase; phase II, when nitrogen becomes a limiting nutrient; and phase III, where most of the ethanol is produced at near zero growth rate. Finally, based on the batch parameters, specific feeds are defined in order to independently mimic each of these phases using continuous cultures (Barreiro-Vázquez et al. 2010). This strategy allows for an easy and reliable calculation of the distribution of metabolic fluxes (Hoskisson and Hobbs 2005).

In the present study, we investigated the impact of growth temperature and sugar content on the distribution of metabolic fluxes of *S. cerevisiae* EC1118 growing under phase I conditions at fermentation temperatures typical for red (28 °C) and white (16 °C) wines. Emulating an extreme increase in sugar concentration motivated by global warming, we have used a synthetic must with 280 g L^{-1} glucose and compared the obtained results with a control must containing 240 g L^{-1} glucose. A control must with 240 g L^{-1} glucose and another, emulating an extreme increase in sugar concentration motivated by global warming with 280 g L^{-1} glucose, have been used. In all cases, media were supplemented with potassium metabisulphite in order to mimic cellar conditions. During this first phase, yeast reaches its maximum growth rate (μ_{max}) that depends on fermentation temperature, organic and inorganic nitrogen sources are available and not growth-limiting, and high sugar and low ethanol concentrations are present in the fermenting must.

The proposed and validated model includes reactions from central carbon and nitrogen metabolism. With regard to previously used models, the latter has been expanded to incorporate transport reactions for ammonium and 19 different amino acids, their anabolism and/or catabolism and, for the first time, pathways involved in the synthesis of aroma precursors. Moreover, the present work combines the application of a stoichiometric model for analyzing the metabolic flux distribution of *S. cerevisiae* under winemaking conditions using continuous cultures in bioreactors.

Material and methods

Strains and culture conditions

Saccharomyces cerevisiae LALVIN EC1118, the strain used in this study, is a commercial wine yeast strain isolated from the Champagne region (France) produced and commercialized by Lallemand Inc. (Ontario, Canada). The strain was grown at 28 °C and routinely maintained at 4 °C on YPD plates containing 2% glucose (w v^{-1}), 2% peptone, 1% yeast extract and 2% agar, and in glycerol stocks at -80 ºC.

Batch and continuous cultivations

A modification of a chemically defined synthetic must previously described (Bely et al. 1990) was used both for the batch and the continuous cultures. The medium contained the following components (expressed per litre): glucose, 240 or 280 g; malic acid, 6 g; citric acid, 6 g; DifcoTM Yeast Nitrogen Base w/o amino acids and ammonium sulphate (BD, Sparks, USA), 1,7 g; ammonium chloride, 306 mg; alanine, 97 mg; arginine, 245 mg; aspartic acid, 29 mg; cysteine, 14 mg; glutamic acid, 80 mg; glutamine, 333 mg; glycine, 12 mg; histidine, 23 mg; isoleucine, 22 mg; leucine, 32 mg; lysine, 11 mg; methionine, 21 mg; phenylalanine, 25 mg; proline, 400 mg; serine, 52 mg; threonine, 50 mg; tryptophan, 116 mg; tyrosine, 13 mg; valine, 29 mg; ergosterol, 15 mg; sodium oleate, 5 mg; Tween 80, 0.5 mL and potassium metabisulphite, 60 mg. All cultures were run in a DASGIP parallel fermentation platform (DASGIP AG, Jülich, Germany) equipped with four SR0400SS vessels. Batch cultures were performed in duplicate using 300 mL as

the initial working volume and were used to establish the specific production and consumption rates of the main metabolites (e.g. glucose, glycerol, ethanol, CO2, biomass, acetic acid, lactic acid and succinic acid) throughout the whole fermentative process. Continuous cultures were performed in duplicate at a constant volume of 200 mL at near μmax dilution rate (D): 0.25 h^{-1} for those fermentations performed at 28 ºC and 0.1 h^{-1} for those performed at 16 °C. These D values had been experimentally determined previously in the aforementioned batch cultures. Agitation was maintained at 250 rpm and the temperature kept at 28 or 16 ºC using a water bath and a 1:1 water/ethylenglycol-cooled chiller. During batch and continuous cultures, the pH of the medium was kept at 3.5 by the automated addition of 2N NaOH. Anaerobic conditions were maintained by gassing the headspace of the bioreactors with pure nitrogen gas (3.5 sL h^{-1}). The use of spargers was avoided in order to reduce ethanol stripping. The effluent fermentation gas measured every 30 s for determination of CO_2 concentration with a GA4 gas analyzer (DASGIP AG). For the inoculation of both batch and continuous cultures, EC1118 was grown in Falcon tubes containing 25 mL YPD and incubated at 28 °C and 150 rpm orbital shaking for 48h in order to reach stationary phase. Cells were then washed twice in sterile deionized water, resuspended in 5 mL of the synthetic must and inoculated to an initial OD600 0.2. Steady states were sampled only after all continuous cultures had been running for at least five residence times and the CO_2 production rate, the biomass values and the concentration of the main metabolites were constant.

Analytical methods

HPLC quantification of main metabolites

The concentration of glucose, glycerol, ethanol and lactic, acetic and succinic acid was determined following the protocol described by Quirós et al. (2010) using a Surveyor Plus chromatograph (Thermo Fisher Scientific, Waltham, MA) equipped with a refraction index and a photodiode array detector (Surveyor RI Plus and Surveyor PDA Plus, respectively) on a 300 × 7.7 mm HyperREZTM XP Carbohydrate H+ (8 μm particle size) column and guard (Thermo Fisher Scientific). The column was maintained at 50 °C and 1.5 mM H_2SO_4 was used as the mobile phase at a flow rate of 0.6 mL min^{-1}. Prior to injection in duplicate, samples were

filtered through 0.22 µm pore size nylon filters (Symta, Madrid, Spain) and diluted when necessary 10 or 20-fold.

The concentration of each amino acid was analyzed in duplicate according to the method of Gomez-Alonso et al. (2007) using an Accela 600 chromatograph (Thermo Fisher Scientific) equipped with a PDA detector and a 250 × 4.6 mm ACE C18-HL ID (5 µm particle size) column and guard (ACE, Aberdeen, Scotland).

The concentration of ammonium was determined enzymatically using the R-Biopharm assay kit Cat. No. 11 112 732 035 (Darmstadt, Germany).

GC-MS determination

The volatile fraction of steady states was analyzed using headspace solid-phase micro extraction coupled with gas chromatography-mass spectrometry (HS-SPME/GCMS) by a modification of the protocol described by Pozo-Bayon et al. (2001). A Thermo Scientific Trace GC Ultra gas chromatograph equipped with a Thermo Scientific Triplus Autosampler and coupled to a Thermo Scientific ISQ mass detector was used for gas chromatography-mass-spectrometry.

Five fusel alcohols (propanol, isoamyl alcohol, amyl alcohol, isobutanol and 2-phenylethanol) were quantified using 2 ml of fermentation broth. One gram of sodium chloride was added to the sample placed in a 20 mL headspace vial, followed by 10 µL of 2000 ppm internal standard solution (4-methyl-2-pentanol and 1-nonanol in 0.5 % ethanol). Briefly, the vial was tightly capped with a PTFE/Silicone cap and then heated for 10 min at 70 °C. Then, a Supelco 100 µm PDMS fiber was exposed to the headspace of the sample vials for 30 min and desorbed in the GC inlet for 4 min. The instrument was fitted with a 30 m × 0.25 mm TG-WAXMS A fused-silica capillary column, 0.25 mm film thickness (Thermo Fisher Scientific). The GC temperature program was as follows: 40 °C (5 min hold), 3 °C min^{-1} up to 200 ºC and 15 ºC min^{-1} up to 240 ºC (10 min hold), while the 0.75 mm I.D. SPME liner was held at 180 ºC. Helium was used as the carrier gas at a flow rate of 1 mL min^{-1}, operating in split mode (ratio 30). For the MS detector, the temperatures of transfer line and ion source were both 250 °C, ionization mode was electron impact at a voltage of 70 eV and acquisitions were performed in SIM mode (dwell time 50 ms). Instrument control, data analysis and quantification results were carried out with Xcalibur 2.1 software. Volatile compounds were identified and

quantified by comparison with standards, and analyses were carried out in duplicate.

Biomass analyses

Determination of cell growth and biomass dry weight

To determine cell growth during the course of batch fermentations, the optical density (OD) was monitored using a Shimadzu UV-1800 Spectrophotometer (Shimadzu Europe GmbH, Duisberg, Germany). When necessary, samples were diluted with deionized water to obtain OD600 measurements in the linear range of 0.1-0.4 units. OD data were then transformed to dry cell weight values using a calibration curve for *S. cerevisiae* EC1118 in the synthetic must described above. When steady states were reached, biomass dry weight was determined in triplicate by filtering 5 ml (for fermentations run at 28 °C) or 15 mL (for fermentations run at 16 °C) of the cultures followed by 10 mL distilled water through a 25 mm, 0.45 µm pore size pre-dried and pre-weighed nitrocellulose filter (Millipore, Billerica, USA). Filters were then heat dried in an oven at 70 °C until weight was constant (12-24 h).

Biomass lyophilization

Samples of cultivation broth from all steady states were centrifuged at 10,000 rpm for 5 min and the cell pellet was washed three times in sterile distilled water. The recovered pellet was immediately frozen by immersion in liquid nitrogen and lyophilized during 72 h. Once lyophilized, cell pellets were additionally dried in an oven at 65 °C for 24 h.

Biomass total carbohydrates content

To determine the biomass total carbohydrates content, an aqueous solution of lyophilized biomass was prepared at a concentration of 0.1 g L^{-1} and subjected in triplicate to the phenol-sulphuric acid method as described by Segarra et al. (1995) using a standard curve of glucose (Sigma-Aldrich).

Biomass total protein content and amino acid composition

Total protein content and amino acid composition of the biomass was determined following the protocol described by Carnicer et al. (2009). This allowed us to estimate the molar fraction of each amino acid in the average protein.

Biomass elementary composition

Biomass recovered from 50 mL of each steady state was washed three times with deionized water, dried in an oven at 70 °C for 72 hours and crushed thoroughly using a porcelain mortar and pestle. The fine powdered biomass was dried again in the same conditions for 24 h and 1 mg analyzed in an EA 1110 CHNS-O elemental analyzer (CE-Instruments/Thermo Fisher Scientific) coupled to an E3200 autosampler and a thermoconductivity detector.

In order to determine the biomass ash content, the powdered biomass was placed in a pre-weighted crucible and calcinated in a muffle furnace at 800 °C for 24 h. The difference in weight was measured with an AB204-S electronic precision scale (Mettler Toledo, Columbus, USA).

Consistency check, data reconciliation and statistical analysis

Data obtained during continuous cultures were checked for consistency and reconciled based on a χ^2-test ($p \leq 0.05$) as proposed by Wang and Stephanopoulos (1983). The test proposed by Lange and Heijnen (2001) was used for verification of consistency and reconciliation of macromolecular and elementary biomass compositional data. This test allowed for the estimation of the non-measured biomass lipid and nucleic acid content.

The physiological parameters and metabolic flux values obtained in all conditions were compared by means of Student's t-test at 95 % confidence level. Principal Components Analysis (PCA) was performed in order to identify relevant experimental condition effects using IBM SPSS win 19.0 software (IBM Corp., Armonk, USA).

Stoichiometric model

The stoichiometric model used to represent the metabolic network of *S. cerevisiae* EC1118 was adapted from the model of Varela et al. (2004) (See Appendix A). While the reactions involved in central carbon metabolism have been used with minor modifications, nitrogen metabolism has been thoroughly revised and expanded. Therefore, the uptake reactions for ammonium and the 19 amino acids present in the medium have been included in the model (proline transport was not included as it is not degraded under anaerobic conditions according to Ingledew et al. (1987)). On the other hand, reactions involved in either synthesis or catabolism of amino acids have been included according to the following criteria. When the ratio "incorporation rate into the biomass/uptake rate" (mol gDW^{-1} h^{-1}/mol gDW^{-1} h^{-1}) of a specific amino acid was ≥ 1, the biosynthetic pathway for that amino acid was included. In contrast, when this ratio was < 1, it has been assumed that there is an excess of such compound in the cell and, therefore, the corresponding degradation pathway was included. The total cell content of each amino acid residue was estimated from the molar fraction of each amino acid in the total protein.

Additionally, some alternative amino acid degradation routes, such as the Ehrlich pathway, which involves the synthesis of isoamyl alcohol, active amyl alcohol and isobutanol, among others, have also been included in the proposed stoichiometric model.

The final metabolic network consists of m=87 metabolites and n=81 reactions (Appendix A). The existence and stoichiometry of each reaction was verified using the Saccharomyces Genome Database (SGD, www.yeastgenome.org) and the Kyoto Encyclopedia of Genes and Genomes (KEGG, www.genome.jp/kegg/).

Software

All numerical calculations were performed using Matlab 2010b (MathWorks Inc., Natick, MA, USA). CellDesigner 4.2 (Systems Biology Institute, Tokio, Japan) was used for metabolic network design and Cell-Net-Analyzer 9.4 (Klamt et al. 2007) for MFA.

Results and discussion

Quantitative physiology of S. cerevisiae EC1118 during anaerobic continuous cultures at near μ_{max} dilution rate

General physiology

Although the metabolism of *S. cerevisiae* has extensively been extensively described and studied under different laboratory growth conditions, data regarding key physiological parameters in the different stages of wine fermentation are not easily found in the literature. One of the main objectives of the present work is to contribute to the understanding of yeast physiology by providing accurate production and consumption rates of the main metabolites during the initial stages of wine fermentation in different enological conditions. Since there are important physiological and transcriptional differences between laboratory and industrial wine yeast strains (Pizarro et al. 2008), the broadly used wine yeast strain EC1118 was chosen as a model in this work.

Results for consumption/production rates (Table S1) were experimentally obtained from two independent replicates for each condition of glucose concentration, temperature and dilution rate (see Material and methods) and represent the basis for all the calculations performed in this work. Due to the essential need for rates accuracy in order to achieve correct calculated fluxes, special attention was paid in their determination following the recommendations proposed by Heijnen and Verheijen (2011). All balances (carbon, nitrogen and redox) closed with >95% recovery in all cases.

From a general point of view, a strong effect of temperature and dilution rate on the consumption or production rates of the different metabolites could be observed, with higher rates at 28 °C. As an example, glucose uptake rates, representing the main entrance of carbon into the system (carbon skeletons of amino acids also contribute to C uptake) were approximately three times higher at 28 °C and D = 0.25 h^{-1} at both sugar concentrations than at 16 °C and D = 0.1 h^{-1} (87.1 vs. 29.2 C-mmol gDW^{-1} h^{-1} at 240 g L^{-1} and 76.3 vs. 23.3 C-mmol gDW^{-1} h^{-1} at 280 g L^{-1}, Figures 1 and 2). These differences must be mainly due to the difference in growth rate and not to the effect of temperature, as exactly the same relationship had been previously observed between *S. cerevisiae* growing at 30 °C in glucose

limited chemostats operated at D = 0.3 h^{-1} and D = 0.1 h^{-1} (Nissen et al. 1997). On the other hand, an impact of sugar concentration was also observed, although this effect was less pronounced (Table S1). Several authors have described that both temperature and growth rate affect physiology of *S. cerevisiae* (Tai et al. 2007, Pizarro et al. 2008, Yu et al. 2012). Our results showed that the combination of a decreased temperature and dilution rate always caused the same effect, reducing the consumption or production rate of the different metabolites. However, the maximum specific growth rate (μ) is strongly affected by temperature, which hampers the dissection of the effect due to temperature from that caused by the specific growth rate (Tai et al. 2007). In fact, a large overlap between genes reported to be regulated by temperature and genes controlled by growth rate has also been demonstrated (Regenberg et al. 2006, Tai et al. 2007, Pizarro et al. 2008). However, other relevant studies have also shown that the effect of dilution rate on parameters such as glucose consumption, glycerol (Nissen et al. 1997, Boender et al. 2009), ethanol (Nissen et al. 1997), or biomass production (Tai et al. 2007) was stronger than the effect of temperature. In our opinion, it would be very interesting to look deeper into the temperature effect since Tai et al. (2007) described the slight overlap existing between transcriptomic databases of *S. cerevisiae* wine strain from previous low-temperature adaptation studies (Beltran et al. 2006) and lab strains (Sahara et al. 2002, Schade et al. 2004, Murata et al. 2006). This fact would be due to the many peculiarities characterizing a grape must such as low pH, high sugar concentration or mixed nitrogen sources present at low concentration.

In all cases of this study, between 81.3 and 84.9% of carbon uptake was used in energy production (measured as ethanol and CO_2). Sugar concentration exerted a slight (not significant) effect on ethanol and CO_2 yields on glucose, with yields always being higher at 240 g L^{-1} glucose. On the other hand, the highest acetic acid yields were found at 280 g L^{-1} glucose (Table 1). In contrast, temperature and dilution rate affected biomass and glycerol yields. Higher biomass yields were observed at 16 °C (μ=0.1 h^{-1}) while higher glycerol yields were calculated at 28 °C (μ=0.25 h^{-1}) (Table 1).

Table 1. Yields on glucose (C-mol C-mol^{-1} glucose) for the main metabolites resulting from anaerobic continuous cultures.

	240 g L^{-1} Glucose		280 g L^{-1} Glucose	
	16 °C	28 °C	16 °C	28 °C
Ethanol	0.555 ± 0.005 ^{a}	0.557 ± 0.002 ^{a}	0.532 ± 0.007 ^{a}	0.541 ± 0.009 ^{a}
CO_2	0.291 ± 0.001 ^{a}	0.292 ± 0.001 ^{a}	0.281 ± 0.005 ^{a}	0.287 ± 0.008 ^{a}
Glycerol	0.044 ± 0.001 ^{a}	0.053 ± 0.001 ^{ab}	0.047 ± 0.001 ^{a}	0.064 ± 0.001 ^{b}
Acetic acid	0.007 ± 0.000 ^{ab}	0.006 ± 0.000 ^{a}	0.009 ± 0.000 ^{b}	0.009 ± 0.000 ^{b}
Biomass	0.100 ± 0.004 ^{ab}	0.086 ± 0.003 ^{a}	0.129 ± 0.002 ^{b}	0.095 ± 0.001 ^{a}
Carbon rec	0.998 ± 0.006	0.994 ± 0.004	0.998 ± 0.009	0.997 ± 0.012

Different superscripts indicate statistically significant differences between values.
Carbon rec: carbon recovery

Pathways involved in energy production are strongly regulated, regardless of culture conditions (Pronk et al. 1996, Rodrigues et al. 2006). As a result, and as indicated above, not significant differences in ethanol and CO_2 yields were observed between different growth conditions as previously reported by other authors (Nissen et al. 1997). On the other hand, glycerol, acetic acid and biomass yields are more related to the internal redox balance (Overkamp 2002, Jain et al. 2012) and therefore presented higher variability depending on growth conditions (Table 1). The distribution of carbon to different metabolites (and throughout the different metabolic pathways) will be more extensively discussed in the following sections.

Biomass composition

Although the elemental and macromolecular composition for *S. cerevisiae* biomass has been determined in multiple studies, none of the culture conditions employed resembled the composition of a grape must. We were therefore motivated to perform these analyses in the four conditions studied. Furthermore, the precise knowledge of these values is essential for energetic and metabolic calculations (Lange and Heijnen 2001). If the cellular composition changes with

culture conditions, it is important to consider the differences in fluxes to the different macromolecular pools (Nissen et al. 1997).

The biomass unit C formulae determined were very similar in the four conditions studied (Table 2) and are consistent with those reported by Albers and co-workers (1996). Nevertheless, significant differences in the N content were found when the formulae obtained were compared to that calculated by Lange and Heijnen (2001) for *S. cerevisiae* grown at 0.1 h^{-1} using measurements of dried molecular biomass composition. This finding could be due to differences in the nitrogen sources and concentrations employed in both studies. Albers and co-workers (1996) had previously described that growth on different nitrogen sources (ammonium, glutamate and a mixture of twenty aminoacids) can alter the amino acidic composition of yeast protein and cause differences in the nitrogen content of the biomass.

The molar fraction of each amino acid did not significantly vary between the four conditions studied (Table S3), resulting in almost identical protein unit C formulae in all cases (Table 2). Values for this formulae were within ± 10% of those obtained by Lange and Heijnen (2001), although significant differences were observed for the sulfur content. Following the aforementioned argument for the biomass unit C formula, these differences could be due to the presence of sulfur amino acids (methionine and cysteine) as part of the nitrogen sources present in the medium employed in the present work.

Table 2. Elemental and macromolecular composition of the biomass in the four conditions used in the present study

	240 g L^{-1} Glucose		280 g L^{-1} Glucose	
	16 °C	28 °C	16 °C	28 °C
Total proteins (g gDW^{-1})	0.52 ± 0.07	0.49 ± 0.06	0.51 ± 0.07	0.41 ± 0.06
Total carbohydrates (g gDW^{-1})	0.30 ± 0.04	0.28 ± 0.03	0.35 ± 0.04	0.26 ± 0.03
Carbohydrates/Proteins (g g^{-1})	0.58 ± 0.1	0.57 ± 0.1	0.69 ± 0.12	0.62 ± 0.12
Ash (g gDW^{-1})	0.060 ± 0.003	0.060 ± 0.003	0.080 ± 0.004	0.097 ± 0.005
Unit C Formulae[a]	$CH_{1.604}N_{0.209}O_{0.488}$	$CH_{1.600}N_{0.207}O_{0.488}$	$CH_{1.612}N_{0.203}O_{0.503}$	$CH_{1.612}N_{0.201}O_{0.471}$
Protein C Formulae[b]	$CH_{1.612}N_{0.297}O_{0.303}S_{0.005}$	$CH_{1.618}N_{0.308}O_{0.297}S_{0.005}$	$CH_{1.614}N_{0.307}O_{0.296}S_{0.005}$	$CH_{1.615}N_{0.309}O_{0.296}S_{0.005}$

[a] Calculated from biomass elemental analysis; [b] Calculated from the amino acidic analysis of cell protein. The Unit C Formulae used for lipids, carbohydrate and nucleic acids were taken from Kovarova-Kovar and Egli (1998). Significant differences were not found between conditions ($p < 0.05$).

Proteins were the main constituent of the biomass, normally representing around 50 % of the cell dry weight and not showing significant differences between growth conditions. The same trend was also observed for the carbohydrate content, in all conditions close to 30% (Table 2). These two main constituents have been described as growth rate dependent and, while higher amounts of proteins have been quantified at higher growth rates, higher amounts of carbohydrates have been measured at lower growth rates (Schulze et al. 1996, Nissen et al. 1997). The effect of temperature on these two macromolecular biomass components has also been described. While an increase in total protein content has been measured at the low temperature, increased content in carbohydrates has been determined at the high temperature (Tai et al. 2007, Pizarro et al. 2008). The absence of statistical differences between conditions could be due to the opposite effect that both parameters (temperature and dilution rate) exert on these macromolecular components. Independently of the conditions, proteins and carbohydrates represent between 67 to 86% of the biomass dry weight. In all cases, higher metabolic fluxes derived towards biomass production resulted in an increase of the metabolic fluxes destined to protein and carbohydrate biosynthesis. Consequently, the nucleic acid and lipid content presented the opposite dynamic (Table 3).

Table 3. Fluxes directed towards the synthesis of the main macromolecular components of the biomass expressed as C-mmol per 100 C-mmol glucose.

	240 g L^{-1} Glucose		280 g L^{-1} Glucose	
	16 °C	28 °C	16 °C	28 °C
Carbohydrates	3.06 ± 0.11 ^{b}	2.38 ± 0.07 ^{a}	4.67 ± 0.06 ^{c}	2.45 ± 0.03 ^{a}
Nucleic acids	0.91 ± 0.03 ^{a}	1.28 ± 0.04 ^{b}	0.84 ± 0.01 ^{a}	1.29 ± 0.02 ^{b}
Proteins	1.27 ± 0.04 ^{bc}	0.89 ± 0.03 ^{a}	1.65 ± 0.02 ^{c}	0.96 ± 0.01 ^{ab}
Lipids	0.32 ± 0.01 ^{a}	0.88 ± 0.03 ^{b}	0.14 ± 0.002 ^{a}	1.28 ± 0.02 ^{c}
Biomass	10.5 ± 0.4 ^{a}	8.8 ± 0.3 ^{a}	13.7 ± 0.2 ^{b}	9.8 ± 0.1 ^{a}

Different superscripts indicate statistically significant differences between values ($p < 0.05$).

Metabolic flux balancing

General metabolic flux analysis

The stoichiometric model used in this work is described in the Materials and methods section. Besides the given details, additional particularities should be noted. Although a grape must is being mimicked, glucose has been used as the only carbon source. A previous characterization of batch cultures using equimolar amounts of glucose and fructose showed that fructose uptake was much lower than glucose consumption during yeast exponential growth phase (data not shown). For this reason, and to improve the accuracy in the determination of sugar uptake, we decided to use glucose as the sole carbon source.

On the other hand, regarding nitrogen metabolism, the ratio “incorporation rate into the biomass/uptake rate” (mol gDW^{-1} h^{-1}/mol gDW^{-1} h^{-1}) for each amino acid, allowed us to define whether anabolic or catabolic reactions had to be included in each case (see Materials and methods). As shown in Table 4, the ratios for serine, glutamine, threonine and arginine were below 1 in all conditions. Moreover, values for glutamate and tryptophan were below 1 only at 28 °C.

Table 4. Ratio “incorporation rate into the biomass/uptake rate” for each amino acid.

	240 g L^{-1} Glucose		280 g L^{-1} Glucose	
	16 °C	28 °C	16 °C	28 °C
Alanine	1.13	0.91	2.15	1.07
Arginine	0.51	0.57	0.70	0.53
Aspartate	1.79	1.36	1.55	1.33
Cysteine	ND	0.90	ND	1.12
Glutamine	0.27	0.23	0.38	0.28
Glutamate	1.29	0.85	2.57	0.96
Glycine	24.12	15.27	47.45	21.44
Histidine	6.57	25.28	17.61	34.99
Isoleucine	1.89	1.68	2.22	1.73
Leucine	1.92	1.73	2.06	1.78
Lysine	3.92	4.23	2.81	3.63
Methionine	1.02	1.08	1.16	1.04
Phenylalanine	2.42	1.50	3.08	1.62
Serine	0.73	0.79	0.85	0.84
Threonine	0.82	0.83	0.89	0.89
Tryptophan	1.11	0.63	2.28	0.73
Tyrosine	42.69	4.24	19.40	8.02
Valine	2.42	2.39	3.06	2.08

ND: Not determined (cysteine consumption was not detected at low temperature).

In order to deepen our knowledge and understanding of yeast amino acid metabolism under winemaking conditions, the model used to represent the metabolic network of *S. cerevisiae* was expanded from that of Varela and co-workers (2004) including the transport reactions for 19 amino acids and ammonium and anabolic or catabolic pathways according to the criteria mentioned above. Moreover, according to the current trend in oenological research (Charnomordic et al. 2010), the metabolism of fusel alcohols (directly related to amino acid breakdown) has also been included.

Under the anaerobic conditions imposed to mimic the environment predominating in wine fermentations, carbon flux was mainly directed to energy production (measured as ethanol and CO_2) in all cases. The flux towards the tri-carboxylic acid cycle (TCA) remained at levels below 1%, which should be enough to maintain the intracellular levels of key metabolic intermediates (Villadsen et al. 2011). This carbon distribution under anaerobic conditions in a Crabtree positive strain has been previously described (Pronk et al. 1996, Rodrigues et al. 2006) also under winemaking conditions (Varela et al. 2004, Cadiere et al. 2011). Figures 1 and 2 show the general flux distribution obtained for each condition expressed as C-mmol gDW^{-1} h^{-1} and normalized to the specific glucose uptake. The reproducibility of the experimental set-up was tested and confirmed using PCA (Figure S1). Metabolic flux distribution will be described and discussed in the following subsections in order to provide an exhaustive analysis of our results.

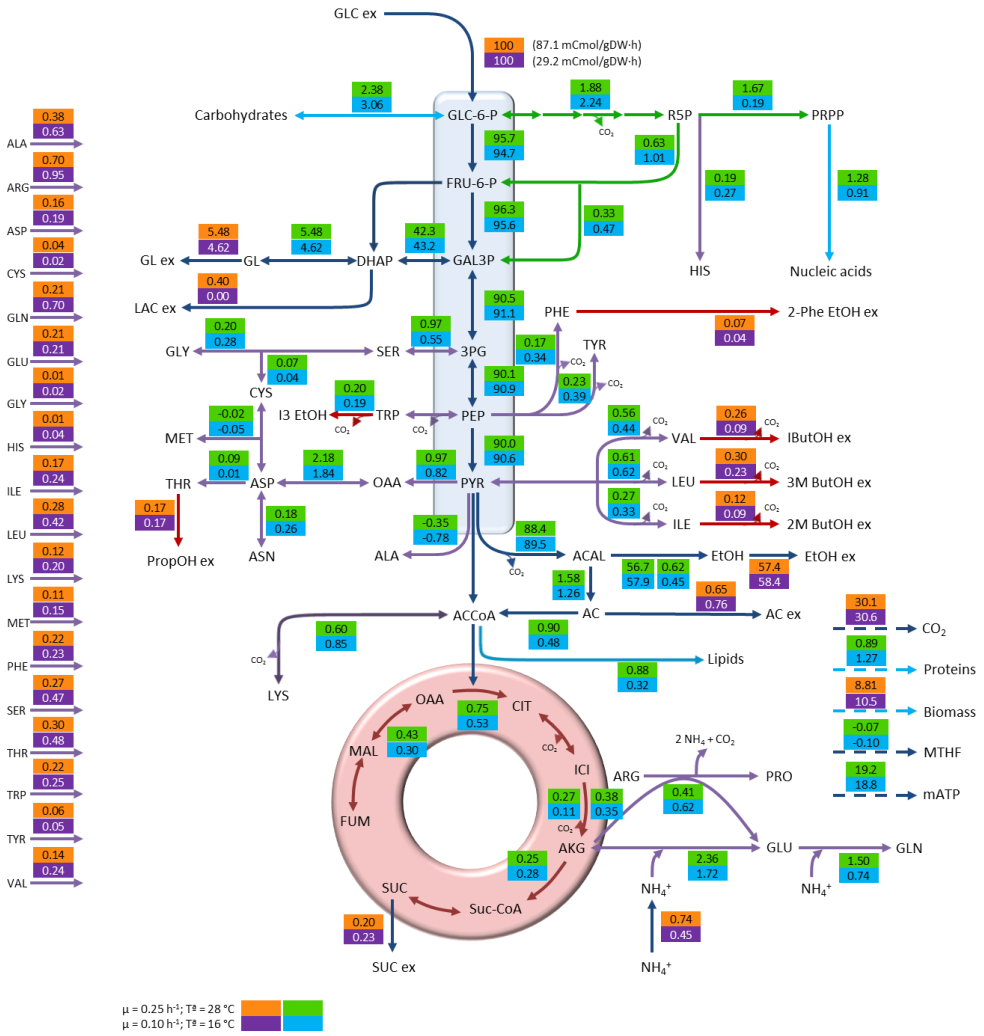

Figure 1. Distribution of metabolic fluxes at 240 g L^{-1} glucose expressed as C-mmol per 100 C-mmol glucose. The measured specific glucose uptake is shown next to the normalized value. Orange/purple boxes: measured and reconciled values; Green/blue boxes: calculated values.

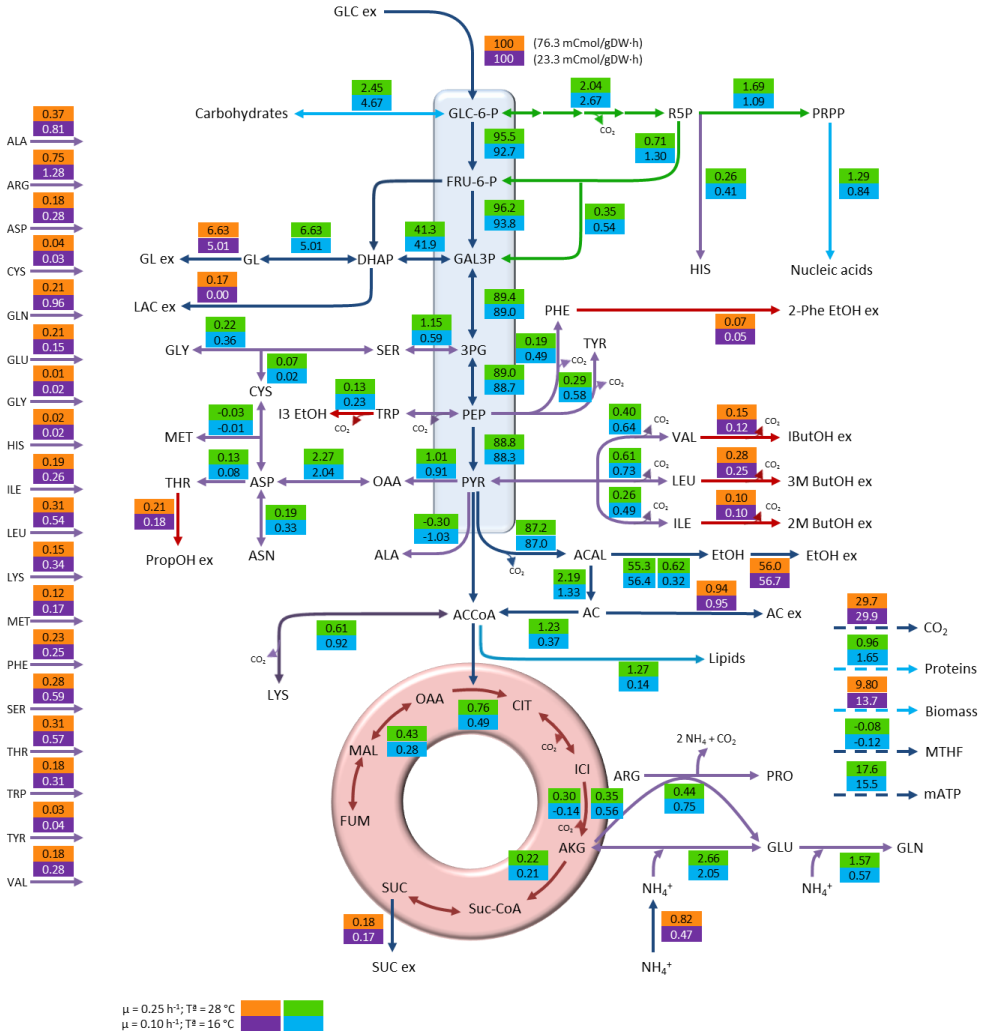

Figure 2. Distribution of metabolic fluxes at 280 g L^{-1} glucose expressed as C-mmol per 100 C-mmol glucose. The measured specific glucose uptake is shown next to the normalized value. Orange/purple boxes: measured and reconciled values; Green/blue boxes: calculated values.

Central carbon metabolism

The analysis of the effect of the studied variables on central carbon metabolism has been focused on the glucose 6-phosphate branch point and the trioses phosphate and pyruvate nodes.

- Glucose 6-phosphate branch point

The C flux directed to glycolysis was higher at 28 °C than at 16 °C. This resulted in a lower C flux to the two minor branches, i.e., pentose phosphate pathway (PPP) and carbohydrate biosynthesis. On the other hand, the flux directed towards glycolysis at 240 g L^{-1} glucose was higher than at 280 g L^{-1} while those directed to carbohydrate biosynthesis and PPP were higher at 280 g L^{-1}; these results are illustrated in Figure 3, panel A. The PPP provides substrates for the synthesis of key products in cellular metabolism. This pathway is involved in the synthesis of nucleic acids (RNA and DNA), some amino acids and the redox carrier NADPH (Villadsen et al. 2011), and has been described as growth rate-dependent by different authors (Nissen et al. 1997, Varela et al. 2004). Our results showed higher fluxes at the lowest dilution rate used but this fact must be explained by the effect of temperature. Unfortunately, to our knowledge, the effect of temperature on the flux diverted to PPP has not been studied in detail. Nevertheless, as NADPH is mainly consumed in biomass synthesis, higher biomass yields on glucose would demand an increased flux towards the PPP, which, in our study occurs at 16 °C at both sugar concentrations. When the carbon fluxes towards PPP in our culture conditions were analyzed together with those reported by Cadiere et al. (2011), Nissen et al. (1997) and (2004), a wide range of values could be observed. This fact could indicate that the glucose 6-phosphate node is flexible and the flux could be easily modulated depending on cell requirements, at least under anaerobic conditions.

The flux in the remaining branch of this node is directed towards carbohydrate biosynthesis. Following the same trend observed for the PPP, higher fluxes were calculated at 16 °C compared to 28 °C and at 280 g L^{-1} glucose compared to 240 g L^{-1}.

As our work focuses on exponentially growing cells and despite the osmotic pressure imposed by high sugar concentrations, the carbon flux directed towards

this branch is expected to be destined to structural (mainly glucans and mannoproteins) rather than to reserve carbohydrates (glycogen and trehalose) (Albers et al. 1998, Varela et al. 2004, Pizarro et al. 2008), as recently observed for *Pichia pastoris* (Carnicer et al. 2009) and *S. cerevisiae* (Lange and Heijnen 2001). Higher fluxes directed towards biomass synthesis were also observed at 16 °C compared to 28 °C and at 280 g L^{-1} of glucose compared to 240 g L^{-1}, which would therefore require a higher demand for structural components.

- Trioses phosphate node

Carbon fate at this branch point was mainly glycolysis in all conditions. However, slight differences were observed depending on the conditions studied. In this way, the glycolytic flux (always accounting for more than 93%) was higher at 16 °C than at 28 °C while the flux towards glycerol was higher at 28 °C. Regarding the sugar concentration effect, the glycolytic flux was higher at 240 g L^{-1} glucose while that directed to glycerol biosynthesis was higher at 280 g L^{-1} (Figure 3, panel B).

Glycerol has been often referred to as a "secondary metabolite" in wine fermentation due to its lower concentration in wine when compared to ethanol. However, glycerol is not "secondary" from a metabolic point of view. Synthesis of this compound plays a major role during anaerobic growth, providing precursors for the synthesis of phospholipids, protecting yeast from high osmotic pressure (caused by high sugar concentrations found in winemaking) and maintaining cell redox balance (Reijenga 2002, Swiegers et al. 2005). However, the analysis of the effect of redox balance in the fluxes towards glycerol was troublesome, mainly due to the interconnection of redox balance and nitrogen metabolism (Albers et al. 1996, Bakker et al. 2001, Jain et al. 2012). We can still hypothesize that the lower flux towards glycerol production at 16 °C could be partly explained by the higher uptake of amino acids at this temperature as described below. The uptake and metabolism of amino acids present in the medium involved a higher consumption of NADH, and thereby, lower fluxes towards glycerol formation are needed to compensate redox balance. As the glycerol present in wine is mainly produced during the first stages of fermentation, when yeast growth takes place, this lower carbon flux towards glycerol formation at 16 °C could be partly responsible for the lower concentrations of this metabolite found by the end of wine batch fermentations carried out in our

laboratory when compared to 28 °C (data not shown). Supporting this finding, Gamero et al. (2013) have also recently reported lower glycerol concentrations by the end of batch fermentations performed using several *S. cerevisiae* strains at 12 °C compared to 28 °C.

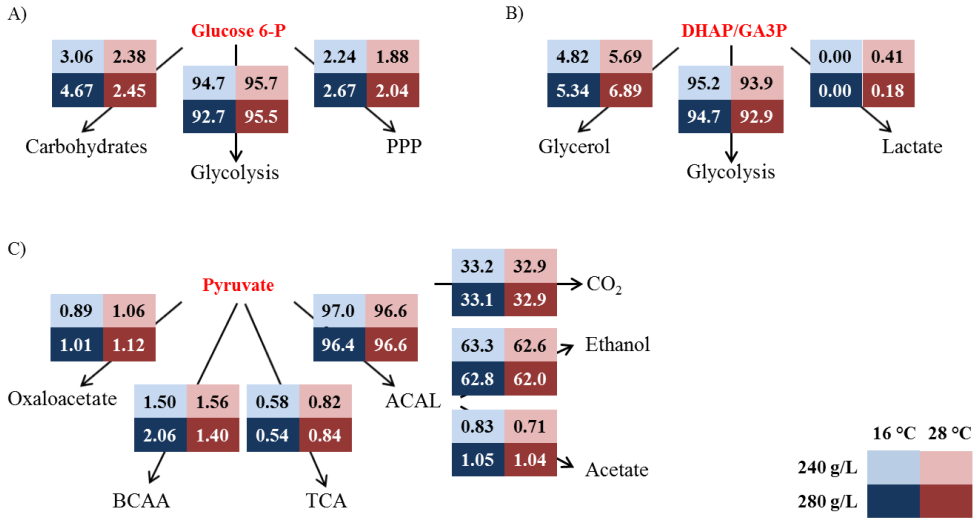

Figure 3. Flux distribution at different nodes. A) Glucose 6-P branch point; B) Trioses phosphate node; C) Pyruvate branch point. PPP: Pentose phosphate pathway; DHAP: Di-hydroxy-acetone phosphate; GA3P: Glyceraldehyde 3-phosphate; BCAA: Brain-chain amino acids; TCA: Tri-carboxylic acid cycle; ACAL: Acetaldehyde. Boxes in light colours indicate 240 g of g L^{-1} glucose. Boxes in dark colours indicate 280 g L^{-1} glucose. Blue indicates 16 °C. Red indicates 28 °C.

The C flux towards acetic acid production was also higher at 280 g L^{-1} glucose and was always accompanied by higher fluxes towards glycerol. This fact could be explained through redox balance, as the excretion of 1 mol of acetate involves the synthesis of 2 moles of NADH (Schulze et al. 1996). Additionally, higher C flux towards glycerol biosynthesis at 280 g L^{-1} glucose, irrespective of temperature, could be due to the increase in osmotic pressure.

The synthesis of lactic acid represents the remaining pathway at this node. Under anaerobic conditions, lactic acid is synthesized from dihydroxyacetone phosphate by the methylglyoxal by-pass. This pathway has always been described as functional at very low rates and under 'overflow metabolism' conditions (Pronk et

al. 1996). Our results showed small amounts of lactic acid at 28 °C (45 and 15 mg L^{-1}, for 240 and 280 g L^{-1} of glucose, respectively) and concentrations below the detection limit (5 mg L^{-1}) in the cultures performed at 16 °C. Low levels of lactic acid are still likely to be produced at 16 °C as all the conditions studied implied overflow metabolism through glycolysis (Figure 3, panel B).

- Pyruvate branch point

The pyruvate node represents one of the most important regulation points in carbon metabolism and the key to energy production (Pronk et al. 1996). In this way, carbon can either follow catabolic reactions (acetaldehyde production and TCA cycle) or anabolic pathways (oxaloacetic acid production (OAA) and amino acid biosynthesis). The fate of pyruvate to branched chain amino acid (BCAA) will be thoroughly described in a following subsection.

In all cases, the C flux from pyruvate was mainly derived towards the formation of acetaldehyde, oscillating in a very narrow range from 96.4 to 97.0%. Notably, the carbon flux to TCA was reduced in about 30% at 16 °C compared to 28 °C, regardless of sugar concentration. On the other hand, the flux towards OAA was not severely affected by the variables studied (Figure 3, panel C).

Around 99% of the C flux diverted to acetaldehyde was used in the concomitant production of energy, CO_2 and ethanol. The rest of the flux was directed to the production of acetic acid. A clear effect of sugar concentration was observed in its production, being higher at 280 g L^{-1} glucose. The increase in the flux oscillated between 20% and 30% at 16 and 28 °C, respectively (Figure 3, panel C).

In general, the metabolic flux distribution calculated at this branch point in our work agrees with that proposed by other authors under anaerobic conditions (Nissen et al. 1997, Varela et al. 2004, Cadiere et al. 2011, Yu et al. 2012). These similarities could indicate the tight regulation of this node under anaerobic conditions, contrary to that observed at the glucose 6-phosphate node. The slight differences found in the split acetaldehyde/TCA cycle could be related to growth rate as cells were growing faster at 28 °C and, in consequence, demanding higher amounts of building-blocks from the TCA cycle.

- Nitrogen metabolism

Simultaneous uptake of ammonium and amino acids was observed in all of the conditions studied. Analyzing data obtained in the control condition (240 g L^{-1} glucose at 28 °C), amino acids could be differentially grouped according to the percentage of consumption in the steady states (Table S2). Thus, while the consumption of lysine accounted for 98.2% of its original amount in the feed, the consumption of several amino acids such as alanine, tryptophan or tyrosine, and ammonium was below 40%. Other amino acids such as arginine, aspartic and glutamic acid, serine, glutamine, threonine, methionine, leucine, isoleucine and phenylalanine presented intermediate consumption percentages, ranging from 40 to 80%. Our results provide additional information to previously reported data obtained using both winemaking conditions (Beltran et al. 2004, Beltran et al. 2005) and synthetic media with a complex mixture of nitrogen sources (Albers et al. 1996, Godard et al. 2007). A recent study (Crépin et al. 2012) has furthered the understanding of the co-consumption of organic and inorganic nitrogen sources and explained it based on the kinetic characteristics of transporters as well as nitrogen catabolite repression (NCR) and Ssy1p-Ptr3p-Ssy5 (SPS)-mediated control, and allowed the classification of the different nitrogen sources according to their order of consumption (Table S2).

When the consumption of amino acids was analyzed in the three remaining conditions, it was observed to be strongly affected both by sugar concentration, with all cases higher at 240 g L^{-1} glucose than at 280 g L^{-1} at both temperatures studied (except for tyrosine at 16 °C), and by temperature and dilution rate, with all cases higher at 28 °C than at 16 °C (Table S2). However, it is interesting to point out that the intensity of the effect exerted by these parameters clearly differed among amino acids (their consumption did not increase or decrease to the same extent). Interestingly, these differences did not seem to affect the amino acid composition of the cellular protein (Table S3) and, consequently, the C formulae of the protein determined for each condition (Table 2). The similarity in the amino acidic composition of cell proteins grown in different conditions is consistent with data reported in literature and has even been observed for *S. cerevisiae* cells grown on three different nitrogen sources (Albers et al. 1996).

Temperature and dilution rate exerted a clear effect on nitrogen metabolism while that of sugar concentration was negligible. Table 5 (panel A) shows the uptake of organic and inorganic nitrogen sources, expressed as N-mmol gDW^{-1} h^{-1}. Regardless of sugar concentration, an approximate 2.4 fold increase in the total nitrogen uptake was observed at 28 °C (D = 0.25 h^{-1}) compared to 16 °C (D = 0.1 h^{-1}). This data is in accordance with a previous study performed in nitrogen limited anaerobic cultures of *S. cerevisiae*, which demonstrated the existence of a linear relationship between dilution rate and ammonium uptake rate (Schulze et al. 1996). However, due to the differential glucose uptake observed between conditions, the amount of nitrogen incorporated per C unit was higher at 16 °C (D = 0.1 h^{-1}) than at 28 °C (Table 5, panel B) although not significantly different. In all cases, nitrogen was mostly incorporated in the form of amino acids. However, the organic/inorganic nitrogen ratio changed with growth temperature. While ammonium represented 37-38% of the total N incorporated at 28 °C and D = 0.25 h^{-1}, this percentage significantly dropped to approximately 15.5-18.5% at 16 °C and D = 0.1 h^{-1} (Table 5, panel C). This result could be explained by an alleviation of NCR observed at low temperatures and deduced from the expression of genes coding for ammonium and amino acid permeases (MEP2 and GAP1) observed by other authors (Beltran et al. 2007).

Considering amino acids individually, it is worth mentioning that arginine, alanine and glutamine account for approximately 60% of the total organic nitrogen incorporated (approx. 40, 10 and 10%, respectively). Aspartic acid, serine and threonine represented approximately 19%, individually accounting for around 6-7%. Another group formed by glutamic acid, isoleucine, leucine, lysine, methionine, phenylalanine, tryptophan and valine accounted for around 19% of the total organic nitrogen incorporated, each of them never representing more than 4%. The individual contribution of the remaining amino acids never exceeded 1%. Detailed data are shown in Table 5, panel D.

Table 5. A) Uptake rate of organic and inorganic nitrogen sources; B) Incorporation of total, organic and inorganic nitrogen normalized by glucose uptake; C) Percentage of organic and inorganic nitrogen incorporated; D) Contribution of each amino acid (in percentage) to the incorporation of organic nitrogen. (Continued on next page)

	240 g L^{-1} Glucose		280 g L^{-1} Glucose	
N-mmol gDW^{-1} h^{-1}	16 °C	28 °C	16 °C	28 °C
Total	0.70 ± 0.01 [a]	1.74 ± 0.05 [b]	0.70 ± 0.01 [a]	1.58 ± 0.04 [b]
Organic	0.57 ± 0.01 [a]	1.09 ± 0.02 [b]	0.59 ± 0.01 [a]	0.98 ± 0.02 [b]
Inorganic	0.13 ± 0.01 [a]	0.64 ± 0.02 [b]	0.11 ± 0.01 [a]	0.60 ± 0.03 [b]
N-mmol $C\text{-}mol^{-1}$ Glucose				
Total	24.0 ± 0.6	19.9 ± 2.1	30.2 ± 1.5	21.5 ± 1.6
Organic	19.5 ± 0.5	12.6 ± 1.4	25.5 ± 1.3	13.3 ± 1.0
Inorganic	4.5 ± 0.3	7.4 ± 0.8	4.7 ± 0.5	8.2 ± 0.7
% of N incorporated				
Organic	81.3 ± 1.84 [a]	63.0 ± 1.87 [b]	84.4 ± 2.13 [a]	61.9 ± 2.02 [b]
Inorganic	18.7 ± 1.45 [a]	37.0 ± 1.44 [b]	15.6 ± 1.56 [a]	38.1 ± 2.13 [b]
Amino acid contribution to organic N uptake (%)				
Alanine	10.7	10.0	10.6	9.2
Arginine	36.7	41.9	37.8	42.2
Aspartate	4.9	6.2	5.5	6.7
Cysteine	0.4	1.2	0.3	1.0
Glutamine	14.3	6.6	15.1	6.3
Glutamate	2.2	3.3	1.1	3.2
Glycine	0.5	0.5	0.5	0.4
Histidine	0.3	0.1	0.1	0.2

Continued on next page

	240 g L^{-1} Glucose		280 g L^{-1} Glucose	
	16 °C	28 °C	16 °C	28 °C
Amino acid contribution to organic N uptake (%)				
Isoleucine	2.0	2.3	1.7	2.3
Leucine	3.6	3.7	3.5	3.8
Lysine	3.4	3.1	4.4	3.8
Methionine	1.6	1.7	1.3	1.7
Phenylalanine	1.3	1.9	1.1	1.9
Serine	8.1	7.1	7.7	7.0
Threonine	6.2	6.0	5.6	5.9
Tryptophan	1.2	1.6	1.1	1.2
Tyrosine	0.3	0.5	0.2	0.3
Valine	2.5	2.3	2.2	2.7

Different superscripts indicate statistically significant differences between values ($p < 0.05$).

It should be highlighted that the individual contribution of amino acids to the total nitrogen uptake differed between conditions. While the contribution of glutamine increased at low temperature, that of glutamic acid decreased (for more details, see Table 5, panel D). Overall, when the total amount of nitrogen incorporated per gram of biomass (N-mmol gDW^{-1}) was analyzed, significantly higher values were obtained for the continuous cultures performed at 16 °C at both sugar concentrations. This implies that the biomass yield on nitrogen (gDW N-$mmol^{-1}$) in a synthetic medium mimicking grape must decreases at low temperatures as had previously been reported for the industrial strain CEN.PK 113-7D and EC1118 in a medium that only presented inorganic nitrogen sources (Pizarro et al. 2008). As commented in a previous section, it is important to point out that this differential consumption of organic and inorganic nitrogen sources exerts an effect on the cell redox balance and, consequently, on the production of glycerol.

These results support the data presented by other authors (Beltran et al. 2007) and indicate that the quantity and quality of yeast nitrogen requirements during the exponential growth phase are not the same at optimum and low temperatures. Improved nitrogen supplementations (for, for example, white wine fermentations) could be formulated on the basis of these findings. Indeed, Martinez-Moreno et al. (2012) have already demonstrated the differential effect of organic nitrogen sources on biomass formation, yeast vitality and fermentation kinetics.

Metabolism of fusel alcohols and their amino acidic precursors

Fusel alcohols produced by yeast during wine fermentation have a strong impact on the sensorial properties of the final product (Charnomordic et al. 2010). For this reason and for the first time, five of the most relevant fusel alcohols (i.e., isoamyl alcohol, active amyl alcohol, phenyl 2-ethanol, n-propanol and isobutanol) have been analyzed and included in a stoichiometric model. These compounds derive both from the catabolism of different amino acids (leucine, isoleucine, phenylalanine, threonine and valine, respectively) and/or anabolic pathways from pyruvate (Swiegers et al. 2005). As discussed above, the total amount of nitrogen supplied by these five amino acids accounts for 15.6% in the conditions studied, with threonine the most prevalent (Table 5, panel D). It should be noted that the relative contribution of these amino acids to the organic fraction of nitrogen incorporated, except for phenylalanine, was very stable between all conditions studied.

The production of each of these fusel alcohols normalized to their amino acidic precursor is shown in Table 6. In general, the amount of fusel alcohol produced could be explained based on the catabolism of each of its amino acidic precursors. However, it is interesting to point out the cases of isoamyl alcohol and isobutanol production. Regardless of the condition studied, both fusel alcohols demand a higher amount of amino acidic precursors for their synthesis than that provided by the uptake from the medium. In fact, coefficients higher than 1.0 (Table 6) indicate that their synthesis could not be supported exclusively from the amino acids present in the medium (leucine and valine, respectively) at 240 g L^{-1} glucose and 28 °C. Taking into account the data obtained for the rest of the fusel alcohols included in this study and the fate of exogenous amino acids inside the cells

observed by Crépin (2012), we could hypothesize that the anabolic pathways involved in the synthesis of fusel alcohols are also active during the yeast exponential growth phase in all conditions studied. Additionally, this fact is supported by the results provided by our stoichiometric model.

Table 6. Production of fusel alcohols expressed as C-mmol per C-mmol of amino acid precursor transported into the cell.

	240 g L^{-1} Glucose		280 g L^{-1} Glucose	
	16 °C	28 °C	16 °C	28 °C
Amyl alcohol / Isoleucine	0.37	0.70	0.38	0.54
Propanol / Threonine	0.35	0.57	0.31	0.67
Isoamyl alcohol / Leucine	0.55	1.08	0.47	0.92
Isobutanol / Valine	0.37	1.86	0.42	0.83
Phenyl ethanol / Phenylalanine	0.19	0.34	0.20	0.30

The production of fusel alcohols normalized per gram of biomass (C-mmol gDW^{-1}) was significantly higher in all continuous cultures performed at 28 °C (D = 0.25 h^{-1}) compared to those performed at 16 °C. An effect of sugar concentration was also observed, with higher effects at 240 g L^{-1} glucose than at 280 g L^{-1} at the two temperatures assayed. These findings could also be partly explained as a result of the redox balance in the cell. As in the case of glycerol, the biosynthesis of these compounds could contribute to the regeneration of the NAD^+.

Conclusions

In this work, metabolic flux analysis has been applied to study the physiology of *S. cerevisiae* during the exponential growth phase in a winemaking process using two different sugar concentrations at two different fermentation temperatures. The stoichiometric model proposed in the present paper represents an extension of that described by Varela and co-workers (2004) incorporating the synthesis and release of aroma compounds and represents the most complete

stoichiometric model used to study yeast metabolism in winemaking thus far. Clear differences have been found in consumption and production rates of the main metabolites analyzed in the study depending mainly on temperature and dilution rate (Table S1). Despite these differences, the distribution of carbon fluxes did not change drastically when the four conditions were compared, likely due to the similarities in the stress factors employed in all cases (high sugar and low nitrogen content). However, results obtained have shown that the variables studied (temperature and sugar concentration) exerted a higher effect on the pentose phosphate pathway and glycerol formation than on glycolysis and ethanol production. On the other hand, nitrogen metabolism was strongly affected by the growth conditions studied. Specifically, clear differences in the uptake of organic and inorganic nitrogen sources were observed. These findings could be employed in the design of optimal supplementation strategies of musts containing low initial nitrogen content in order to avoid stuck of sluggish fermentations. Furthermore, the reported data support the simultaneous operation of anabolic and catabolic pathways involved in the synthesis of fusel alcohols. Additional studies are being carried out in the remaining phases of fermentation in order to contribute to the understanding of the impact of nitrogen additions on fermentation kinetics and the improvement of the aroma profile of the resulting wines.

Acknowledgements

The authors would like to thank Cristina Juez Ojeda for the analytical work using HPLC, Miguel Ángel Fernández Recio for the determination of volatile compounds using GC-MS and Tara Negrave for kindly revising the English grammar and style on this manuscript.

Appendix A: Stoichiometric model

Glycolisys

Glc + ATP ==> G6P

G6P <==> F6P

F6P + ATP <==> DHAP + GLA3P

DHAP <==> GLA3P

GLA3P <==> 3PG + NADH + ATP

3PG <==> PEP

PEP <==> PYR + ATP

Glycerol metabolism

DHAP + NADH <==> GL3P

GL3P <==> GL

Pyruvate metabolism

PYR <==> iCO_2 + ACAL

NADH + ACAL <==> EtOH

ACAL + NADHmit <==> EtOH

ACAL <==> NADPH + AC

AC + ATP <==> ACCOA

Pentose phosphate pathway

G6P <==> 2 NADPH + iCO_2 + R5P

2 R5P <==> F6P + E4P

R5P + E4P <==> F6P + GAL3P

Tricarboxylic acid cycle

PYR + OAAmit <==> iCO_2 + ICITmit + NADHmit

ICITmit <==> iCO_2 + AKG + NADHmit

ICITmit <==> iCO_2 + AKG + NADPHmit

AKG <==> iCO_2 + SUCCmit + ATP + NADHmit

FUMmit <==> OAAmit + NADHmit

Anaplerotic reaction

PYR + iCO_2 + ATP <==> OAA

Amino acid metabolism

NADPH + AKG + iNH_4 <==> GLU

ATP + iNH_4 + GLU <==> GLN

OAA + GLU <==> AKG + ASP

3PG + GLU <==> NADH + AKG + SER

PYR + GLU <==> AKG + ALA

2 NADPH + 2 ATP + ASP <==> THR

THR + NADH <==> iCO_2 + PROPex

2 PYR + ACCOA + GLU <==> 2 iCO_2 + 2 NADH + AKG + LEU

ACCOA + NADHmit + GLU + VAL <==> iCO_2 + NADH + AKG + LEU

AKG + LEU <==> iCO_2 + GLU + IAMI-OH

2 PYR + NADPH + GLU <==> iCO_2 + AKG + VAL

AKG + VAL <==> iCO_2 + GLU + IBUT-OH

2 PEP + NADPH + E4P + ATP + GLU <==> iCO_2 + AKG + PHE

AKG + PHE <==> iCO_2 + GLU + PHEEtOH

PYR + NADPHmit + GLU + THR <==> iCO_2 + AKG + iNH_4 + ILE

AKG + ILE <==> iCO_2 + GLU + AMI-OH

2 NADPH + ACCOA + 3 ATP + 2 GLU <==> iCO_2 + 2 NADH + AKG + LYS

2 ATP + iNH_4 + ASP <==> ASN

2 NADPH + iCO_2 <==> MTHF

SER <==> MTHF + GLY

3 NADPHmit + 3 ATP + ASP + MTHF + CYS <==> PYR + iNH_4 + MET

2 PEP + NADPH + E4P + 3 ATP + GLU <==> iCO_2 + NADH + AKG + TYR

NADPH + iCO_2 + R5P + 5 ATP + iNH_4 + GLN <==> 2 NADH + AKG + HIS

AKG + TRP <==> iCO_2 + GLU + I3-EtOH

NADPH + AKG + ARG <==> iCO_2 + 2 iNH_4 + GLU + PRO

NADH + AC + CYS ==> 5 NADPH + ACCOA + ATP + SER

Nitrogen uptake

ATP + NH_4ex ==> iNH_4

ATP + ALAex ==> ALA

ATP + ARGex ==> ARG

ATP + ASPex ==> ASP

ATP + CYSex ==> CYS

ATP + GLNex ==> GLN

ATP + GLUex ==> GLU

ATP + GLYex ==> GLY

ATP + HISex ==> HIS

ATP + ILEex ==> ILE

ATP + LEUex ==> LEU

ATP + LYSex ==> LYS

ATP + METex ==> MET

ATP + PHEex ==> PHE

ATP + SERex ==> SER

ATP + THRex ==> THR

ATP + TRPex ==> TRP

ATP + TYRex ==> TYR

ATP + VALex ==> VAL

Products release

AC ==> ACex

EtOH <==> EtOHex

GL <==> GLex

SUCCmit ==> SUCCex

iCO_2 ==> CO_2ex

DHAP ==> LACex

Synthesis of AICAR

iCO_2 + R5P + 6 ATP + 2 GLN + ASP + SER ==> NADPH + FUMmit + 2 GLU + 9 AICAR

Maintenance

ATP ==>

Macromolecular biosynthesis

Synthesis of nucleic acid

0.057 iCO2 + 0.048 R5P + 0.132 NADH + 0.489 ATP + 0.105 GLN + 0.075 ASP + 0.511 AICAR ==> 0.135 NADPH + 0.027 FUMmit + 0.105 GLU + NA

Synthesis of carbohydrates

G6P + ATP ==> 6 CARB

Synthesis of lipids

0.022 GAL3P + 0.831 NADPH + 0.416 ACCOA + 0.400 ATP + 0.034 SER ==> LIP

Synthesis of proteins

240 g L^{-1} glucose and 16 °C

0.015 NADPHcyt + 4 ATP + 0.087 ALA + 0.080 ARG + 0.051 ASN + 0.051 ASP + 0.004 CYS + 0.051 GLU + 0.051 GLN + 0.081 GLY + 0.024 HIS + 0.046 ILE + 0.076 LEU + 0.082 LYS + 0.020 MET + 0.035 PHE + 0.044 PRO + 0.062 SER + 0.058 THR + 0.008 TRP + 0.025 TYR + 0.063 VAL = 4.887 PROT

240 g L^{-1} glucose and 28 °C

0.032 NADPHcyt + 4 ATP + 0.092 ALA + 0.090 ARG + 0.050 ASN + 0.050 ASP + 0.004 CYS + 0.050 GLU + 0.050 GLN + 0.081 GLY + 0.022 HIS + 0.045 ILE + 0.074 LEU + 0.079 LYS + 0.021 MET + 0.034 PHE + 0.042 PRO + 0.064 SER + 0.058 THR + 0.009 TRP + 0.024 TYR + 0.062 VAL = 4.871 PROT

280 g L^{-1} glucose and 16 °C

0.0001 NADPHcyt + 4 ATP + 0.085 ALA + 0.088 ARG + 0.051 ASN + 0.051 ASP + 0.004 CYS + 0.052 GLU + 0.052 GLN + 0.080 GLY + 0.024 HIS + 0.046 ILE + 0.075 LEU + 0.080 LYS + 0.020 MET + 0.034 PHE + 0.041 PRO + 0.061 SER + 0.057 THR + 0.008 TRP + 0.026 TYR + 0.0623 VAL = 4.905 PROT

280 g L^{-1} glucose and 28 °C

0.001 NADPHcyt + 4 ATP + 0.088 ALA + 0.088 ARG + 0.050 ASN + 0.050 ASP + 0.0041 CYS + 0.051 GLU + 0.051 GLN + 0.083 GLY + 0.027 HIS + 0.045 ILE + 0.075 LEU + 0.079 LYS + 0.020 MET + 0.034 PHE + 0.041 PRO + 0.062 SER + 0.058 THR + 0.008 TRP + 0.024 TYR + 0.061 VAL = 4.883 PROT

Synthesis of biomass

240 g L^{-1} glucose and 16 °C

0.080 NADPHcyt + 0.290 CARB + 0.086 RNA + 0.590 PROT + 0.030 LIP = 1 BIOM

240 g L^{-1} glucose and 28 °C

0.039 NADPHcyt + 0.270 CARB + 0.145 RNA + 0.490 PROT + 0.100 LIP = 1 BIOM

280 g L^{-1} glucose and 16 °C

0.075 NADPHcyt + 0.340 CARB + 0.061 RNA + 0.590 PROT + 0.010 LIP = 1 BIOM

280 g L^{-1} glucose and 28 °C

0.036 NADPHcyt + 0.250 CARB + 0.132 RNA + 0.480 PROT + 0.130 LIP = 1 BIOM

Appendix B: Abbreviations

3PG	3-Phospho-D-glycerate
ACCOA	Acetyl-CoA
ACAL	Acetaldehyde
AC	Acetate
ACex	Extracellular Acetate
AICAR	1-(5'-Phosphoribosyl)-5-amino-4-imidazolecarboxamide
AKG	2-Oxoglutarate
ALA	L-Alanine
ALAex	Extracellular L-Alanine
AMI-OH	Amylalcohol
ARG	L-Arginine
ARGex	Extracellular L-Arginine
ASN	L-Asparragine
ASP	L-Aspartate
ASPex	Extracellular L-Aspartate
ATP	Adenosin Triphosphate
BIOM	Biomass
CARB	Carbohydrate
CO_2ex	Extracellular CO_2
CYS	L-Cysteine
CYSex	Extracellular L-Cysteine
DHAP	Di-hydroxyAcetona Phosphate
E4P	D-Erythrose 4-phosphate
EtOH	Ethanol
EtOHex	Extracellular Ethanol
F6P	D-Fructose 6-phosphate
FUMmit	Mitochondrial Fumarate
GLA3P	Glyceraldehyde 3-Phosphate
G6P	D-Glucose 6-Phosphate
GLN	L-Glutamine
GLNex	Extracellular L-Glutamine

GLU	L-Glutamate
Glc	D-Glucose
GLUex	Extracellular L-Glutamate
GLY	Glycine
GLYex	Extracellular Glycine
GL	Glycerol
GLex	Extracellular Glycerol
GL3P	Glycerol 3-Phosphate cytosolic
HIS	L-Histidine
HISex	Extracellular L-Histidine
I3-EtOH	Indole-3-ethanol
IAMI-OH	Isoamyl alcohol
IBUT-OH	Isobutanol
ICITmit	Mitochondrial isocitrate
iCO_2	Intracellular CO_2
ILE	L-Isoleucine
ILEex	Extracellular L-Isoleucine
iNH_4	Intracellular NH_4
LACex	Extracellular Lactate
LEU	L-Leucine
LEUex	Extracellular L-Leucine
LIP	Lipid
LYS	L-Lysine
LYSex	Extracellular L-Lysine
MET	L-Methinine
METex	Extracellular L-Methionine
MTHF	5,10-Methyltetrahydrofolate
NADH	Cytosolic NADH
NADHmit	Mitochondrial NADH
NADPH	Cytosolic NADPH
NADPHmit	Mitochondrial NADPH
NH_4ex	Extracellular NH_4
OAA	Cytosolic Oxaloacetate

OAAmit	Mitochondrial Oxaloacetate
PEP	Cytosolic Phosphoenolpyruvate
PHE	L-Phenylalanine
PHEEtOH	2-Phenyl ethanol
PHEex	Extracellular L-Phenylalanine
PRO	L-Proline
PROPex	Extracellular n-Propanol
PROT	Protein
PYR	Pyruvate
R5P	D-Ribose 5-Phosphate
NA	Nucleic acid
SER	L-Serine
SERex	Extracellular L-Serine
SUCCex	Extracellular Succinate
SUCCmit	Mitochondrial Succinate
THR	L-Threonine
THRex	Extracellular L-Threonine
TRP	L-Triptophan
TRPex	Extracellular L-Triptophan
TYR	L_Tyrosine
TYRex	Extracellular L-Tyrosine
VAL	L-Valine
VALex	Extracellular L-Valine

References

Albers, E., L. Gustafsson, C. Niklasson, and G. Liden. 1998. Distribution of C-14-labelled carbon from glucose and glutamate during anaerobic growth of *Saccharomyces cerevisiae*. Microbiol.-UK 144: 1683-1690.

Albers, E., C. Larsson, G. Liden, C. Niklasson, and L. Gustafsson. 1996. Influence of the nitrogen source on *Saccharomyces cerevisiae* anaerobic growth and product formation. Appl. Environ. Microb. 62: 3187-3195.

Bakker, B. M., K. M. Overkamp, A. J. A. van Maris, P. Kotter, M. A. H. Luttik, J. P. van Dijken, and J. T. Pronk. 2001. Stoichiometry and compartmentation of NADH metabolism in *Saccharomyces cerevisiae*. FEMS Microbiol. Rev. 25: 15-37.

Barreiro-Vázquez, A., N. Adelantado, F. Vázquez-Lima, R. Gonzalez, J. Albiol, M. Quirós, R. Martinez-Moreno, P. Morales, and P. Ferrer. Year. Published. Investigating the use of chemostat cultures mimicking different phases of winemaking fermentations as a tool for physiological analysis and modeling. *In*, 4th Conference on Physiology of Yeast and Filamentous Fungi, 2010, Rotterdam, Netherlands.

Beltran, G., N. Rozes, A. Mas, and J. M. Guillamon. 2007. Effect of low-temperature fermentation on yeast nitrogen metabolism. World J. Microb. Biot. 23: 809-815.

Beltran, G., M. Novo, N. Rozes, A. Mas, and J. M. Guillamon. 2004. Nitrogen catabolite repression in *Saccharomyces cerevisiae* during wine fermentations. FEMS Yeast Res. 4: 625-632.

Beltran, G., B. Esteve-Zarzoso, N. Rozes, A. Mas, and J. M. Guillamon. 2005. Influence of the timing of nitrogen additions during synthetic grape must fermentations on fermentation kinetics and nitrogen consumption. J. Agric. Food Chem. 53: 996-1002.

Beltran, G., M. Novo, V. Leberre, S. Sokol, D. Labourdette, J. M. Guillamon, A. Mas, J. Francois, and N. Rozes. 2006. Integration of transcriptomic and metabolic analyses for understanding the global responses of low-temperature winemaking fermentations. FEMS Yeast Res. 6: 1167-1183.

Bely, M., J. M. Sablayrolles, and P. Barre. 1990. Automatic detection of assimilable nitrogen deficiencies during alcoholic fermentation in oenological conditions. J. Ferment. Bioeng. 70: 246-252.

Boender, L. G. M., E. A. F. de Hulster, A. J. A. van Maris, P. A. S. Daran-Lapujade, and J. T. Pronk. 2009. Quantitative physiology of *Saccharomyces cerevisiae* at near-zero specific growth rates. Appl. Environ. Microb. 75: 5607-5614.

Cadiere, A., A. Ortiz-Julien, C. Camarasa, and S. Dequin. 2011. Evolutionary engineered *Saccharomyces cerevisiae* wine yeast strains with increased in vivo flux through the pentose phosphate pathway. Metab. Eng. 13: 263-271.

Carnicer, M., K. Baumann, I. Toplitz, F. Sanchez-Ferrando, D. Mattanovich, P. Ferrer, and J. Albiol. 2009. Macromolecular and elemental composition analysis and extracellular metabolite balances of *Pichia pastoris* growing at different oxygen levels. Microb. Cell Fact. 8: 65.

Clement, T., M. Perez, J. R. Mouret, J. M. Sablayrolles, and C. Camarasa. 2011. Use of a continuous multistage bioreactor to mimic winemaking fermentation. Int. J. Food Microbiol. 150: 42-49.

Crépin, L. 2012. Variabilité dans l'utilixation de l'azote chez *Saccharomices cerevisae* et cónsequences sur la production de biomasse en fermentation oenologique. PhD Thesis. Université Montpellier II. Montpellier.

Crépin, L., T. Nidelet, I. Sanchez, S. Dequin, and C. Camarasa. 2012. Sequential use of nitrogen compounds by *Saccharomyces cerevisiae* during wine fermentation: a model based on kinetic and regulation characteristics of nitrogen permeases. Appl. Environ. Microb. 78: 8102-8111.

Charnomordic, B., R. David, D. Dochain, N. Hilgert, J. R. Mouret, J. M. Sablayrolles, and A. Vande Wouwer. 2010. Two modelling approaches of winemaking: First principle and metabolic engineering. Math. Comp. Model Dyn. 16: 535-553.

Erasmus, D. J., M. Cliff, and H. J. J. van Vuuren. 2004. Impact of yeast strain on the production of acetic acid, glycerol, and the sensory attributes of icewine. Am. J. Enol. Vitic. 55: 371-378.

Gamero, A., J. Tronchoni, A. Querol, and C. Belloch. 2013. Production of aroma compounds by cryotolerant *Saccharomyces* species and hybrids at low and moderate fermentation temperatures. J. Appl. Microbiol. 114: 1405-1414.

Godard, P., A. Urrestarazu, S. Vissers, K. Kontos, G. Bontempi, J. van Helden, and B. Andre. 2007. Effect of 21 different nitrogen sources on global gene expression in the yeast *Saccharomyces cerevisiae*. Mol. Cell Biol. 27: 3065-3086.

Gomez-Alonso, S., I. Hermosin-Gutierrez, and E. Garcia-Romero. 2007. Simultaneous HPLC analysis of biogenic amines, amino acids, and ammonium ion as aminoenone derivatives in wine and beer samples. J. Agric. Food Chem. 55: 608-613.

Grassl, H. 2011. Climate change challenges. Surv. Geophys. 32: 319-328.

Heijnen, S. J., and P. J. T. Verheijen. 2011. Chapter 23 - How to obtain true and accurate rate-values, pp. 457-508. In M. V. Daniel Jameson and V. W. Hans (eds.), Methods in Enzymology, vol. Volume 500. Academic Press.

Hoskisson, P. A., and G. Hobbs. 2005. Continuous culture - making a comeback? Microbiol.-Sgm 151: 3153-3159.

Ingledew, W. M., C. A. Magnus, and F. W. Sosulski. 1987. Influence of oxygen on proline utilization during the wine fermentation. Am. J. Enol. Vitic. 38: 246-248.

Jain, V. K., B. Divol, B. A. Prior, and F. F. Bauer. 2012. Effect of alternative NAD(+)-regenerating pathways on the formation of primary and secondary aroma compounds in a *Saccharomyces cerevisiae* glycerol-defective mutant. Appl. Microbiol. Biot. 93: 131-141.

Jones, G., M. White, O. Cooper, and K. Storchmann. 2005. Climate change and global wine quality. Climatic Change 73: 319-343.

Klamt, S., J. Saez-Rodriguez, and E. D. Gilles. 2007. Structural and functional analysis of cellular networks with CellNetAnalyzer. BMC Syst. Biol. 1: 2.

Kovarova-Kovar, K., and T. Egli. 1998. Growth kinetics of suspended microbial cells: From single-substrate-controlled growth to mixed-substrate kinetics. Microbiol. Mol. Biol. Rev. 62: 646-666.

Lange, H. C., and J. J. Heijnen. 2001. Statistical reconciliation of the elemental and molecular biomass composition of *Saccharomyces cerevisiae*. Biotechnol. Bioeng. 75: 334-344.

Martinez-Moreno, R., P. Morales, R. Gonzalez, A. Mas, and G. Beltran. 2012. Biomass production and alcoholic fermentation performance of

Saccharomyces cerevisiae as a function of nitrogen source. FEMS Yeast Res. 12: 477-485.

Mira de Orduña, R. 2010. Climate change associated effects on grape and wine quality and production. Food Res. Int. 43: 1844-1855.

Murata, Y., T. Homma, E. Kitagawa, Y. Momose, M. S. Sato, M. Odani, H. Shimizu, M. Hasegawa-Mizusawa, R. Matsumoto, S. Mizukami, K. Fujita, M. Parveen, Y. Komatsu, and H. Iwahashi. 2006. Genome-wide expression analysis of yeast response during exposure to 4 degrees C. Extremophiles 10: 117-128.

Nissen, T. L., U. Schulze, J. Nielsen, and J. Villadsen. 1997. Flux distributions in anaerobic, glucose-limited continuous cultures of *Saccharomyces cerevisiae*. Microbiol.-UK 143: 203-218.

Overkamp, K. 2002. Mitochondrial oxidation of cytosolic NADH in yeast: physiological analysis and metabolic engineering. PhD Thesis., Delft University of Technology Delft, The Nederlands.

Pigeau, G. M., and D. L. Inglis. 2005. Upregulation of ALD3 and GPD1 in *Saccharomyces cerevisiae* during icewine fermentation. J. Appl. Microbiol. 99: 112-125.

Pizarro, F. J., M. C. Jewett, J. Nielsen, and E. Agosin. 2008. Growth temperature exerts differential physiological and transcriptional responses in laboratory and wine strains of *Saccharomyces cerevisiae*. Appl. Environ. Microb. 74: 6358-6368.

Pozo-Bayon, M. A., E. Pueyo, P. J. Martin-Alvarez, and M. C. Polo. 2001. Polydimethylsiloxane solid-phase microextraction-gas chromatography method for the analysis of volatile compounds in wines - Its application to the characterization of varietal wines. J. Chromatogr. A 922: 267-275.

Pronk, J. T., H. Y. Steensma, and J. P. vanDijken. 1996. Pyruvate metabolism in *Saccharomyces cerevisiae*. Yeast 12: 1607-1633.

Quirós, M., D. Gonzalez-Ramos, L. Tabera, and R. Gonzalez. 2010. A new methodology to obtain wine yeast strains overproducing mannoproteins. Int. J. Food Microbiol. 139: 9-14.

Regenberg, B., T. Grotkjaer, O. Winther, A. Fausboll, M. Akesson, C. Bro, L. K. Hansen, S. Brunak, and J. Nielsen. 2006. Growth-rate regulated genes have profound impact on interpretation of transcriptome profiling in *Saccharomyces cerevisiae*. Genome Biol. 7: R107.

Reijenga, K. 2002. Dynamic control of yeast glycolysis. PhD Thesis., Vrije Universiteit Amsterdam Amsterdam, The Nederlands.

Rodrigues, F., P. Ludovico, and C. Leão. 2006. Sugar metabolism in yeasts: An overview of aerobic and anaerobic glucose catabolism, pp. 101-121, Biodiversity and Ecophysiology of Yeasts. Springer Berlin Heidelberg, New York, USA.

Sahara, T., T. Goda, and S. Ohgiya. 2002. Comprehensive expression analysis of time-dependent genetic responses in yeast cells to low temperature. J. Biol. Chem. 277: 50015-50021.

Schade, B., G. Jansen, M. Whiteway, K. D. Entian, and D. Y. Thomas. 2004. Cold adaptation in budding yeast. Mol. Biol. Cell. 15: 5492-5502.

Schulze, U., G. Liden, J. Nielsen, and J. Villadsen. 1996. Physiological effects of nitrogen starvation in an anaerobic batch culture of *Saccharomyces cerevisiae*. Microbiol.-UK 142: 2299-2310.

Segarra, I., C. Lao, E. Lopez-Tamames, and M. C. De La Torre-Boronat. 1995. Spectrophotometric methods for the analysis of polysaccharide levels in winemaking products. Am. J. Enol. Vitic. 46: 564-570.

Swiegers, J. H., E. J. Bartowsky, P. A. Henschke, and I. S. Pretorius. 2005. Yeast and bacterial modulation of wine aroma and flavour. Aust. J. Grape Wine Res. 11: 139-173.

Tai, S. L., P. Daran-Lapujade, M. C. Walsh, J. T. Pronk, and J. M. Daran. 2007. Acclimation of *Saccharomyces cerevisiae* to low temperature: A chemostat-based transcriptome analysis. Mol. Biol. Cell. 18: 5100-5112.

Varela, C., F. Pizarro, and E. Agosin. 2004. Biomass content governs fermentation rate in nitrogen-deficient wine musts. Appl. Environ. Microb. 70: 3392-3400.

Vargas, F. A., F. Pizarro, J. R. Perez-Correa, and E. Agosin. 2011. Expanding a dynamic flux balance model of yeast fermentation to genome-scale. BMC Syst. Biol. 5: 50.

Villadsen, J., J. Nielsen, and G. Lidén. 2011. Chemicals from Metabolic Pathways, pp. 7-62, Bioreaction Engineering Principles. Springer, New York, USA.

Wang, N. S., and G. Stephanopoulos. 1983. Application of macroscopic balances to the identification of gross measurement errors. Biotechnol. Bioeng. 25: 2177-2208.

Yu, Z., H. Zhao, M. Zhao, H. Lei, and H. Li. 2012. Metabolic flux and nodes control analysis of brewer's yeasts under different fermentation temperature during beer brewing. Appl. Biochem. Biotech. 168: 1938-1952.

Suplementary matherial

Table S 1. Measured consumption/production rates of the different metabolites analyzed in the study. (Continued on next pages).

	240 g L^{-1} Glucose				280 g L^{-1} Glucose			
	16 °C		28 °C		16 °C		28 °C	
	mmol gDW^{-1} h^{-1}	Sd	mmol gDW^{-1} h^{-1}	sd	mmol gDW^{-1} h^{-1}	sd	mmol gDW^{-1} h^{-1}	sd
Glucose	-4.76	0.56	-20.51	0.98	-4.19	0.61	-16.31	1.36
Glycerol	0.38	0.01	1.37	0.15	0.34	0.02	1.39	0.12
Ethanol	8.29	0.24	25.7	2.00	6.79	0.30	21.47	1.82
Succinic acid	0.02	0.00	0.04	0.01	0.01	0.00	0.03	0.00
Acetic acid	0.12	0.00	0.29	0.05	0.12	0.01	0.36	0.03
Lactic acid	ND	-	0.1157	0.0139	ND	-	0.0424	0.0008
Ala	-0.0353	0.0007	-0.0925	0.0101	-0.0178	0.0006	-0.0705	0.0037
Arg	-0.0724	0.0013	-0.1427	0.0153	-0.0568	0.0025	-0.1426	0.0128
Asp	-0.013	0.0006	-0.0335	0.0021	-0.0148	0.0005	-0.0322	0.0034
Cys	ND	-	-0.0045	0.0015	ND	-	-0.0032	0.0001

Continued on next page

	240 g L^{-1} Glucose				280 g L^{-1} Glucose			
	16 °C		28 °C		16 °C		28 °C	
	mmol gDW^{-1} h^{-1}	Sd	mmol gDW^{-1} h^{-1}	sd	mmol gDW^{-1} h^{-1}	sd	mmol gDW^{-1} h^{-1}	sd
Gln	-0.0852	0.0038	-0.2004	0.0254	-0.0614	0.0027	-0.1552	0.0067
Glu	-0.0181	0.0006	-0.053	0.0037	-0.0092	0.0001	-0.0449	0.0029
Gly	-0.0015	0.0004	-0.0049	0.0005	-0.0008	0.0001	-0.0033	0.0007
His	0.0017	0.0001	0.0007	0.0021	0.0006	0.0000	0.0007	0.0028
Ile	-0.0112	0.0002	-0.0244	0.0031	-0.0093	0.0003	-0.0223	0.001
Leu	-0.0182	0.0005	-0.0392	0.0047	-0.0164	0.0004	-0.0359	0.0014
Lys	-0.0095	0.0004	-0.017	0.0022	-0.0129	0.0003	-0.0187	0.0004
Met	-0.0087	0.0002	-0.018	0.0017	-0.0077	0.0003	-0.0168	0.0001
NH_4	-0.0657	0.0008	-0.5219	0.0331	-0.0555	0.0014	-0.494	0.036
Phe	-0.0066	0.0002	-0.0206	0.0021	-0.005	0.0001	-0.0181	0.0005
Ser	-0.0389	0.0012	-0.0733	0.0077	-0.0327	0.0013	-0.0625	0.0028
Thr	-0.0324	0.0009	-0.0635	0.0076	-0.0285	0.0011	-0.0552	0.0022

Continued on next page

	240 g L^{-1} Glucose				280 g L^{-1} Glucose			
	16 °C		28 °C		16 °C		28 °C	
	mmol gDW^{-1} h^{-1}	Sd	mmol gDW^{-1} h^{-1}	sd	mmol gDW^{-1} h^{-1}	sd	mmol gDW^{-1} h^{-1}	sd
Trp	-0.0033	0.0012	-0.0129	0.0031	-0.0016	0.0001	-0.0099	0.0007
Tyr	-0.0003	0.0004	-0.0051	0.0007	-0.0006	0.0001	-0.0025	0.0002
Val	-0.0119	0.0009	-0.0234	0.0008	-0.0092	0.0003	-0.0253	0.0016
Amyl alcohol	0.0024	0.0002	0.0095	0.001	0.0021	0.0002	0.0067	0.0005
Isoamyl alcohol	0.0062	0.0004	0.0242	0.0026	0.0053	0.0004	0.019	0.0015
Propanol	0.0081	0.0031	0.0248	0.0001	0.0069	0.0006	0.0253	0.0064
Isobutanol	0.0024	0.0002	0.0183	0.0016	0.0025	0.0001	0.0101	0.0003
Phenyl ethanol	0.0009	0.0001	0.0046	0.0002	0.0009	0.0001	0.0035	0.0002
Biomass	3.72	0.00	9.02	0.00	3.75	0.00	8.68	0.00
CO_2	9.04	0.16	25.78	3.11	6.88	0.33	21.31	1.23

sd values correspond to the standard deviation of the average value measured in two independent biological replicates.
Consumption rates are indicated with a minus sign.
ND: Not detected in the analysis.

Table S 2. Percentage of consumption of each amino acid in the steady states of each condition ((mg L-1 in the steady state/ mg L-1 in the feed)•100).

	240 g L^{-1} Glucose		280 g L^{-1} Glucose		
	16 °C	28 °C	16 °C	28 °C	Code
Alanine	25.2	37.5	9.4	25.9	
Arginine	39.8	44.2	23.1	40.3	
Aspartate	47.3	61.6	36.4	52.2	
Cysteine	n.d.	18.8	n.d.	14.6	
Glutamine	37.8	47.3	20.1	33.4	
Glutamate	24.8	41.1	9.1	30.9	
Glycine	7.7	13.5	2.8	8.5	
Histidine	n.d.	n.d.	n.d.	n.d.	
Isoleucine	53.9	66.5	32.8	55.3	
Leucine	59.4	72.9	39.7	61.1	
Lysine	97.1	98.2	96.6	97.7	
Methionine	71.6	79.5	47.8	70.0	
NH_4	8.3	37.3	5.1	31.2	
Phenylalanine	35.6	62.7	19.3	50.3	
Proline	0	0	0	0	
Serine	61.8	65.8	38.4	50.7	
Threonine	60.8	67	39.2	52.8	
Triptophan	7.4	15	2.7	11.5	
Tyrosine	3.0	31.0	5.1	14.2	
Valine	38.3	46.3	22	41.6	

Code: colour values given according to the classification proposed by Crépin et al. (2012). Pink: prematurely consumed; Green: early consumed; Blue: late consumed. Those amino acids left in white were not classified by the authors; n.d.: not determined.

Table S 3. Molar fraction of amino acids present in proteins.

	240 g L^{-1} Glucose		280 g L^{-1} Glucose	
	16 °C	28 °C	16 °C	28 °C
Ala	0.087	0.092	0.085	0.088
Arg	0.080	0.090	0.088	0.088
Asx	0.102	0.100	0.102	0.100
Cys[a]	0.004	0.004	0.004	0.004
Glx	0.102	0.100	0.105	0.101
Gly	0.081	0.081	0.080	0.083
His	0.024	0.022	0.024	0.027
Ile	0.046	0.045	0.046	0.045
Leu	0.076	0.074	0.075	0.075
Lys	0.082	0.079	0.080	0.079
Met[a]	0.020	0.021	0.020	0.020
Phe	0.035	0.034	0.034	0.034
Pro	0.044	0.042	0.041	0.041
Ser	0.062	0.064	0.061	0.062
Thr	0.058	0.058	0.057	0.058
Trp[a]	0.008	0.008	0.008	0.008
Tyr	0.025	0.024	0.026	0.024
Val	0.063	0.062	0.063	0.061
Sum	0.999	1.000	0.999	0.998

[a]Not properly quantified in the analysis. Data from taken from Lange and Heijnen (2001). Asx: Asn + Asp; Glx: Gln + Glu.

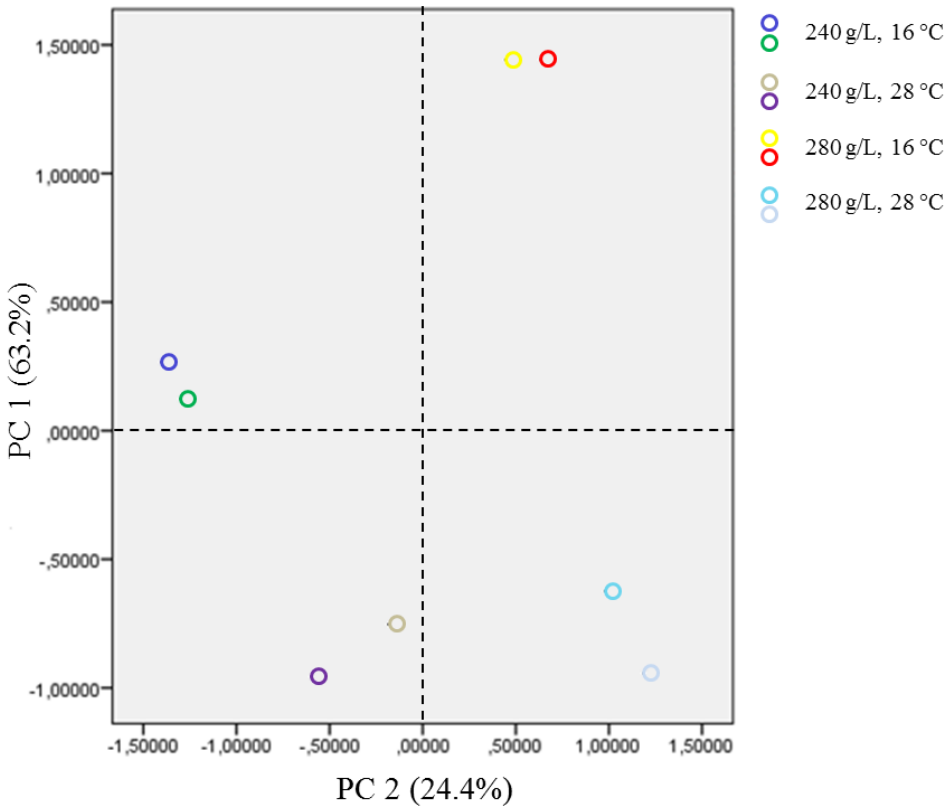

Figure S 1. PCA performed to verify the reproducibility of the steady states obtained for each condition. These two components explained 87.6% of the variance.

Chapter IV

♦

New insights into the advantages of ammonium as winemaking nutrient

CHAPTER IV

New insights into the advantages of ammonium as winemaking nutrient

Abstract

Nitrogen limitation is the most common cause for stuck or sluggish fermentation in winemaking, and it is usually dealt with by supplementing grape juice with either ammonium salts or organic nutrients. These practices have a direct impact on both fermentation kinetics and the sensorial features of the final product. The aim of this work is to provide a detailed analysis and characterization of yeast physiology in response to ammonium supplementation during alcoholic fermentation. Our results indicate that the choice of supplementation strategy has an impact on several enological parameters like fermentation length, volatile acidity, final glycerol content, and aroma profile. We also conclude that a rational use of ammonium for the correction of nitrogen deficiencies might be advantageous over the use of complex nitrogen sources, at least in terms of volatile acidity and glycerol levels. However, ammonium over-supplementation has a negative impact on quality related parameters, notably on volatile acidity. Production of several volatile compounds relevant for wine aroma perception is also differentially influenced by standard or excess ammonium supplementation. Propanol production seems to be specifically stimulated when growth is sustained by ammonium as the only nitrogen source. New knowledge generated in this work might help winemakers anticipate the impact of different nitrogen nutrition strategies on the sensory properties of wines.

This chapter has been submitted to International Journal of Food Microbiology as: Rubén Martínez-Moreno, Manuel Quirós, Pilar Morales, Ramon Gonzalez New insights into the advantages of ammonium as winemaking nutrient

Rubén Martínez-Moreno, Manuel Quirós, Pilar Morales, Ramon Gonzalez, New insights into the advantages of ammonium as a winemaking nutrient, International Journal of Food Microbiology, Volume 177, 2014, Pages 128-135, ISSN 0168-1605, https://doi.org/10.1016/j.ijfoodmicro.2014.02.020.

Introduction

Availability of nitrogen sources is frequently reported as a limiting factor in winemaking (Varela et al. 2004, Bell and Henschke 2005, Carrau et al. 2008), and low nitrogen content in must is a major cause of sluggish or stuck fermentation (Bisson and Butzke 2000). In order to prevent wine spoilage due to fermentation problems, a common practice in wineries is to supply must with nitrogen sources, usually in the form of ammonium salts at early stages of alcoholic fermentation (Jiranek et al. 1995). This is often done on a routine basis, and frequently without knowledge of the actual nitrogen content of grape juice, or the nitrogen requirements of the yeast strain in use. On occasions, this results in nitrogen over-supplementation, which can lead to the production of unwanted metabolites such as urea, ethyl carbamate or biogenic amines, by either fermenting yeast or spoilage microbiota (Ribéreau-Gayon et al. 2004).

During wine fermentation yeasts release many flavor active metabolites including acetic acid, fusel alcohols, esters or fatty acids (Rapp and Versini 1991, Swiegers et al. 2005, Styger et al. 2011) whose formation is closely related to nitrogen metabolism (Bell and Henschke 2005). Several studies about the effects of nitrogen supplementation on fermentation performance, production of aroma compounds, or gene expression have been recently published (Marks et al. 2003, Beltran et al. 2005, Mendes-Ferreira et al. 2007, Garde-Cerdan and Ancin-Azpilicueta 2008, Jimenez-Marti and Del Olmo 2008, Barbosa et al. 2009, Gonzalez-Marco et al. 2010, Torrea et al. 2011).

The aim of this work is to characterize the effect of ammonium supplementation and timing on growth and substrate conversion rates, under conditions mimicking optimal or excess supplementation, including the impact of nitrogen addition practices on the uptake of carbon and nitrogen sources, the release of main fermentation metabolites, and the production of aroma active compounds like esters, fusel alcohols and fatty acids.

Material and methods

Yeast strain

A single commercial wine yeast strain, *Saccharomyces cerevisiae* EC1118 (Lallemand Inc., Ontario, Canada), was used throughout this study. The strain was grown at 28 ºC and routinely maintained at 4 ºC on YPD plates (2% glucose, 2% peptone, 1% yeast extract, 2% agar) or in glycerol stocks at -80 ºC.

Culture conditions

Two basal media, SM200C and SM100, modified from Bely et al. (1990) according to Quirós et al. (2013) and containing 200 and 100 mg L^{-1} YAN (yeast assimilable nitrogen) respectively, were used in this work (Table 1). According to previous studies, SM100 is considered to be nitrogen deficient (Martinez-Moreno et al. 2012), while SM200C is nitrogen sufficient. Nitrogen supplementation assays were performed as described in section *Nitrogen supplementatio*n.

All batch cultures (300 mL initial volume) were performed in triplicate in a DASGIP parallel fermentation platform (DASGIP AG, Jülich, Germany) equipped with four SR0400SS vessels. Agitation was maintained at 250 rpm using magnetic stirrers and the temperature was kept at 28 ºC using a water bath. Medium pH was maintained at 3.5 by the automated addition of 2N NaOH. Anaerobic conditions were maintained by gassing the headspace of the bioreactors with pure N2 (4.5 sL h^{-1}). The off-gas was cooled in gas condensers (2 ºC) and the concentration of CO_2 measured with a GA4 gas analyzer (DASGIP AG). For inoculum preparation, yeast strain was grown in 25 mL of YPD and incubated at 28 ºC and 150 rpm orbital shaking. After 48 h, cells were washed twice with sterile deionized water, resuspended in 5 mL of the appropriate synthetic must and inoculated to 0.2 initial OD600.

Table 1. Composition of the two basal media used in this work.

	SM200C	SM100
C sources (g L^{-1})		
Glucose	120.0	120.0
Fructose	120.0	120.0
Malic acid	6.0	6.0
Citric acid	6.0	6.0
N sources (mg L^{-1})		
Alanine	97.0	48.5
Arginine	245.0	122.5
Aspartate	29.0	14.5
Cysteine	14.0	7.0
Glycine	12.0	6.0
Glutamine	333.0	166.5
Glutamate	80.0	40.0
Histidine	23.0	11.5
Isoleucine	22.0	11.0
Leucine	32.0	16.0
Lysine	11.0	5.5
Methionine	21.0	10.5
Phenylalanine	25.0	12.5
Proline	400.0	200.0
Serine	52.0	26.0
Threonine	50.0	25.0
Tryptophan	116.0	58.0
Tyrosine	13.0	6.5
Valine	29.0	14.5
NH_4Cl	306.0	153.0
Micronutrients and other additives		
YNB* (g L^{-1})	1.70	1.70
Myo-inositol (mg L^{-1})	20.0	20.0
$K_2S_2O_5$ (mg L^{-1})	60.0	60.0
Ergosterol (mg L^{-1})	15.5	15.5
Oleic acid (mg L^{-1})	5.5	5.5
Tween 80 (ml L^{-1})	0.5	0.5

* Yeast Nitrogen Base w/o amino acids w/o ammonium sulphate

Nitrogen supplementation

SM200C was supplemented with ammonium chloride to a final YAN content of 500 mg L^{-1} in order to mimic a nitrogen over-supplemented must (SM500). On the other hand, SM100 was supplemented with ammonium chloride to a final YAN content of 200 mg L^{-1} in order to mimic optimally supplemented must (SM200). Additions were performed at different time points: at inoculation time (E); and when nitrogen becomes a limiting nutrient by the end of yeast exponential growth phase (L). So, according to nitrogen content and supplementation, six different fermentation conditions have been used in this work: SM200C, SM100, SM200E, SM200L, SM500E and SM500L.

Determination of cell growth and biomass dry weight

Cell growth was monitored by optical density (OD600) using a Shimadzu UV-1800 spectrophotometer (Shimadzu Europe GmbH, Duisberg, Germany). When necessary, samples were diluted with deionized water to obtain OD600 values in the range of 0.1-0.4 units. OD600 data were then transformed to dry weight values using a calibration curve previously determined for *S. cerevisiae* EC1118 in SM200C. Experimental dry weight determination was made in triplicate by filtering 10 mL of the broth and washing with 10 mL distilled water through a pre-dried and pre-weighed 25 mm nitrocellulose filter with 0.45 µm pore size (Millipore, Billerica, USA). Filters were dried at 70 ºC until constant weight (12-24 h).

Analytical methods

HPLC analysis

The concentration of glucose, fructose, glycerol, ethanol and organic acids (acetic, lactic and succinic acid) were determined using a Surveyor Plus chromatograph (Thermo Fisher Scientific, Waltham, MA) equipped with refraction index and photodiode array detectors (Surveyor RI Plus and Surveyor PDA Plus, respectively) on a HyperREZTM XP Carbohydrate H+ 8µm column and guard (Thermo Fisher Scientific). The column was maintained at 50 ºC, and 1.5 mM H_2SO_4 was used as the mobile phase at a flow rate of 0.6 mL min^{-1}. Prior to injection in duplicate, samples were filtered through 0.22 µm pore size nylon filters

(Espectrocroma, Madrid, Spain) and diluted when necessary. The concentration of each amino acid was analysed in duplicate according to the method described by Gomez-Alonso et al. (2007) using an Accela 600 chromatograph (Thermo Fisher Scientific) equipped with a PDA detector and a ACE 5 C18-HL 5 µm column and guard (ACE, Aberdeen, Scotland). Ammonium was assayed spectrophotometrically using a specific R-Biopharm assay kit (Darmstadt, Germany). YAN was calculated taking into account the number of assimilable atoms of nitrogen from each amino acid according to Martinez-Moreno et al. (2012).

GC analysis

Volatile compounds were analyzed in duplicate using headspace solid-phase micro extraction coupled with gas chromatography-mass spectrometry (HS-SPME/GC-MS) by a modification of the protocol described by Ortega et al. (2001) using a Thermo Scientific Trace GC Ultra gas chromatograph equipped with a Thermo Scientific Triplus Autosampler and a Thermo Scientific ISQ mass detector. The evolution of 22 volatile compounds directly related to yeast metabolism (butanoic acid, valeric acid, isovaleric acid, hexanoic acid, octanoic acid, decanoic acid, dodecanoic acid, propanol, isobutanol, 2-methylbutanol, 3-methylbutanol, 2-phenylethanol, ethyl acetate, ethyl butanoate, ethyl isobutanoate, ethyl hexanoate, ethyl octanoate, ethyl decanoate, ethyl dodecanoate, isoamyl acetate, phenylethyl acetate, and methionol) was analyzed for each condition. One gram of sodium chloride was added to 20 mL headspace vials containing 2 mL of filtered fermentation broth and 500 µL of 25 ppm internal standard solution consisted of heptanoic acid, 2-butanol, 2-ethylhexanol, 4-methyl-2-pentanol, 1-nonanol, ethyl heptanoate and ethyl nonanoate in 1.25 % ethanol. Briefly, the vial was tightly capped with a PTFE/Silicone cap and then heated for 10 min at 70 ºC. Then, a Supelco 50/30 µm DVB/CAR/PDMS fiber was exposed to the headspace of the sample vials for 30 min and desorbed in the GC inlet for 4 min. The GC temperature program was as follows: 40 ºC (5 min hold), 3 ºC min^{-1} up to 200 ºC and 15 ºC min^{-1} up to 240 ºC (10 min hold). The 0.75 mm I.D. SPME liner was held at 180 ºC. A 30 m x 0.25 mm TG-WAXMS A fused-silica capillary column, 0.25 mm film thickness (Thermo Fisher Scientific) was employed. Helium was used as carrier gas at a flow rate of 1 mL min^{-1}, operating in split mode (ratio 30). For the MS detector, the

temperatures of transfer line and ion source were both 250 ºC, ionization mode was electron impact at a voltage of 70eV and acquisitions were performed in SIM mode (dwell time 50 ms). Instrument control, data analysis, and quantification were carried out with Xcalibur 2.1 software. Volatile compounds were identified by comparison with standards. Relative area values (the area of each compound referred to the area of the appropriate internal standard) were used for comparison between conditions.

Calculation of growth and conversion rates

Growth rate was calculated as the derivative of the natural logarithm of biomass with respect to time

$$\text{Eq. (1)} \quad \mu = dLnBM/dt$$

where μ (h^{-1}) is the specific growth rate and BM is the biomass content (expressed as OD600) for a given time point.

Conversion (consumption and production) rates (mmol gDW^{-1} h^{-1} or µmol gDW^{-1} h^{-1}) of all metabolites were calculated according to

$$\text{Eq. (2)} \quad q = (Xj-Xi) / (Bij) \bullet (Tij)$$

where q is the conversion rate, X is the amount of a metabolite at a given time point (i or j) expressed in mmol or µmol , Bij is the average of biomass content during the time period i-j expressed in grams of dry weight (gDW) and Tij is the time period (i-j) expressed in hours (h).

Statistical analysis

Principal component analysis (PCA) and Student t-Test for comparison of means were performed using SPSS 19.0 software (IBM Corp., Armonk, USA)

Results

Impact of nitrogen availability on S. cerevisiae physiology during wine fermentation.

Overall growth and conversion rates under sufficient and poor nitrogen conditions.

Time-course of the yeast uptake and production rates in SM200C for the main fermentation metabolites is shown in Figure 1. Absolute values of all conversion rates increased with increasing growth rate until a maximum value was achieved, generally about 14-16 h after inoculation (Figures 1). The continuous variation in conversion rates (which are normalized to biomass content) during this stage indicates that increasing sugar consumption is not only due to increasing biomass, but yeast cells are increasingly more efficient in substrate conversion up to 14-16 h after inoculation. Afterwards, conversion rates experienced a more or less pronounced decline until the end of fermentation. Glucose uptake rate increased faster than that of fructose and was always above it until glucose was exhausted.

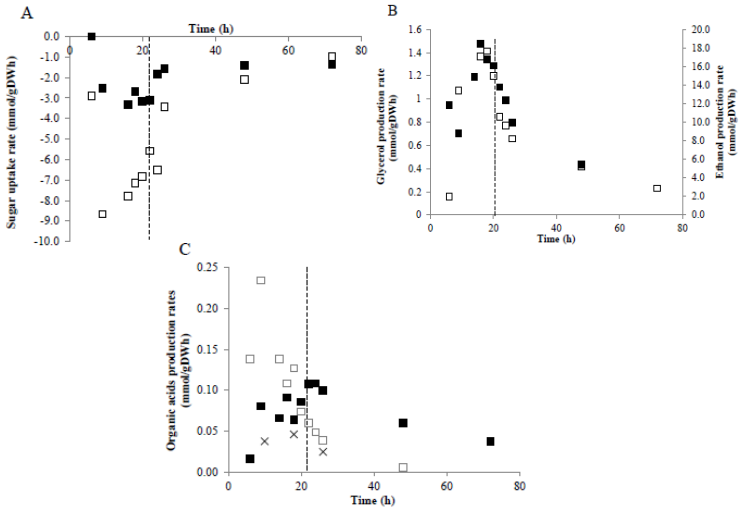

Figure 1. Consumption (A) and production rates (B and C) of different metabolites during yeast growth in SM200C expressed as mmol gDW^{-1} h^{-1}. A) (□) glucose and (■) fructose; B) (□) ethanol and (■) glycerol; C) (□) acetic acid, (■) succinic acid, and (×) lactic acid. Dashed-line indicates the moment when nitrogen was depleted. Relative standard deviation was <2% for all data.

Comparison of the CO_2 production profiles in the different fermentation conditions confirmed that SM100 was indeed a nitrogen deficient must (Figure S1).

Maximum CO_2 production level was lower than the control condition, and it was indeed the lowest of all the conditions studied (Figure S1). In addition, CO_2 production was maintained at a low rate for an extended time period, typical for sluggish fermentation, so that fermentation was not still finished after 120 h (Figure S1). The maximum growth rate for *S. cerevisiae* growing in SM100 was also lower than that calculated in SM200C, it was reached later, and the drop afterwards was more pronounced (Figure 2, panel A). Biomass content by the end of the exponential growth phase in SM200 was 1.6 times higher than for SM100 (Figure 2 panel B).

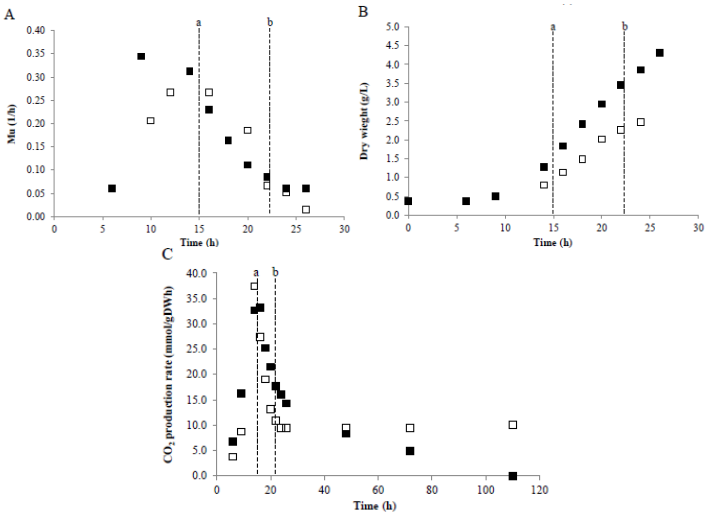

Figure 2. Evolution of different parameters during wine fermentation in poor nitrogen content must (SM100) (□) and optimal nitrogen content must (SM200C) (■): A) Growth rate (h^{-1}); B) Dry weight (g L^{-1}); and C) CO_2 production rate (mmol gDW^{-1} h^{-1}). Dashed-lines indicate the moment when nitrogen was depleted in SM100 (a) and SM200C (b). Relative standard deviation was <5% for all data.

Time for depletion of nitrogen sources was different depending on the fermentation conditions and the particular nitrogen source. In both media, lysine was the first amino acid to be exhausted, while uptake of ammonium, glycine, and tryptophan was lagging behind that of the other nitrogen sources. The order of consumption of the remaining amino acids did not show any particular trend in relation with the different ammonium addition strategies (Table 2). Nitrogen sources

(including ammonium) were depleted after 22 h of fermentation (T95) for SM200C and after 15 h for SM100. Moreover, T95 values for most amino acids where lower than ammonium in the same medium. In the case of SM200C, maximum growth and conversion rates were reached when around 90% of amino acids had already been consumed (Table S1).

Table 2. Time (h) required for the consumption of 95% of the initial content (T95) of each nitrogen source

	SM200C	SM100	SM500E	SM500L	SM200E	SM200L
Ammonium	22	15	ND*	ND*	20	4**
Aspartic acid	18	13	18	18	16	14
Alanine	20	15	22	20	16	16
Arginine	20	13	22	20	16	16
Cysteine	20	<10	18	18	18	<10
Glutamine	20	11	22	20	16	16
Glutamic acid	20	14	22	20	16	16
Glycine	22	15	22	20	18	16
Histidine	16	12	18	16	14	14
Isoleucine	18	12	18	16	16	14
Leucine	16	12	18	16	16	14
Lysine	14	<10	16	14	9	<10
Methionine	16	<10	16	16	14	<10
Phenylalanine	18	13	20	18	16	16
Serine	20	13	20	18	16	16
Threonine	18	13	20	18	16	16
Triptophan	22	15	22	22	18	16
Tyrosine	20	15	22	20	18	16
Valine	20	14	22	18	16	16

*ND: Not determined. Residual ammonium was detected in both SM500E and SM500L by the end of fermentation.
**Calculated after ammonium addition

Effects of appropriate nitrogen supplementation.

Independently of the time of addition, prior to inoculation or at the end of the exponential growth phase, proper supplementation of nitrogen-deficient must restored a CO_2 production profile similar to that of the control fermentation (Figure S1). Maximum growth rates were lower for SM200L fermentations as compared to SM200C or SM200E (Figure 3). However, these differences did not have any significant impact on the total biomass produced (Table 3). The most important differences between these three fermentation conditions were found in the production rates of certain metabolites. Addition of ammonium to nitrogen deficient must resulted in an increased production rate of succinic and lactic acid, in turn resulting in a significant increase in the content of both acids by the end of fermentation. The opposite dynamics was observed for acetic acid. The production rates of this compound were lower in SM200E and SM200L than in SM200C, and final concentrations in wine were significantly lower in supplemented musts, as shown in Table 3. Nitrogen supplementation resulted in a faster decrease on the CO_2 production rate, similar to SM200C fermentations, in contrast to the prolonged CO_2 release seen for the nitrogen deficient fermentation (Figure S1).

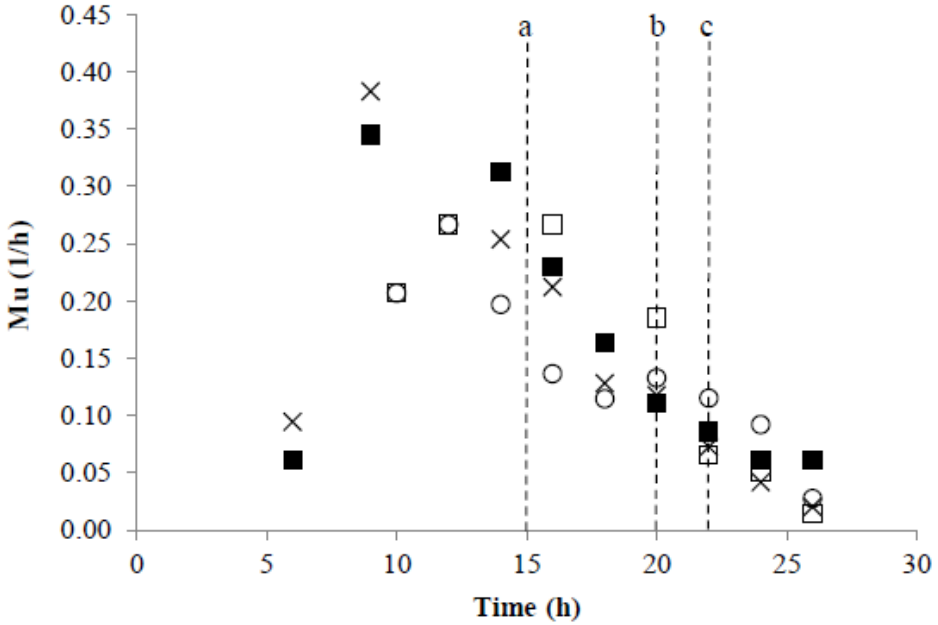

Figure 3. Evolution of Growth rate (h^{-1}) along wine fermentation in SM200E (×), SM200L (○), SM100 (□) and SM200C (■). Dashed-line indicates the moment when nitrogen was depleted in SM100 (a), SM200L (b), SM200C (c). Relative standard deviation was <5% for all data.

In all cases, nitrogen sources were completely exhausted 20 h after inoculation. In the case of SM200L, ammonium was completely consumed only 4 h after addition. Again, lysine was the first nitrogen source depleted from the medium while ammonium was the last one (Table 2).

Table 3. Concentration of the main fermentation products by the end of fermentation.

	SM200C	SM500E	SM500L	SM200E	SM200L
Glycerol (g L^{-1})	1.05±0.02^{a}	1.47±0.03^{d}	1.22±0.02^{b}	1.18±0.02^{b}	1.33±0.03^{c}
Ethanol (g L^{-1})	87.06±1.74^{b}	82.79±1.66^{a,b}	86.27±1.73^{b}	79.24±1.58^{a}	78.45±1.57^{a}
Acetic acid (g L^{-1})	0.21±0.01^{c}	0.57±0.01^{d}	0.54±0.01^{d}	0.09±0.01^{b}	0.04±0.00^{a}
Succinic acid (g L^{-1})	1.96±0.04^{b}	0.99±0.02^{a}	1.03±0.02^{a}	2.45±0.05^{c}	2.63±0.01^{c}
Lactic acid (g L^{-1})	0.23±0.01^{a}	0.35±0.01^{b}	0.48±0.01^{c}	0.34±0.68^{b}	0.43±0.01^{d}
Biomass (g L^{-1})	6.50±0.33^{a}	6.70±0.33^{a}	8.94±0.40^{b}	5.87±0.47^{a}	6.85±0.31^{a}
Time for sugar depletion (h)	96	86.5	72	100	100

Effects of ammonium over-supplementation.

Ammonium over-supplementation has been studied at two different time points during alcoholic fermentation: at inoculation time and by the end of the exponential growth phase. Although high nitrogen content did not clearly affect the maximum growth rate (Figure 4, panel A), nitrogen over-addition at the end of the yeast growth phase (SM500L) resulted in a significant increase in biomass content by the end of fermentation (Table 2). On the other hand, the maximum CO_2 production rates measured in SM500E and SM500L were lower than that determined for SM200C (Figure 4, panel C). Metabolism of organic acids (acetic, succinic and lactic acid) was also affected by nitrogen over-supplementation. Yeast growing in SM500E or SM500L presented the highest acetic acid production rate during the fermentation process and, as a consequence, these final synthetic wines showed higher acetic acid content than the control condition. However, the amount of lactic acid measured in SM500L wines was higher than in SM500E. In contrast, over-addition of nitrogen involved a significant decrease in the final content of succinic acid due to the lower production rates in SM500E and SM500L (Table 3).

After sugar was depleted, residual ammonium was still detected in both SM500E and SM500L (77.8 and 77.4 mg L^{-1} respectively). In contrast, amino acids had been totally consumed after 22 h of fermentation. Under these growth conditions lysine was the first amino acid consumed and tryptophan the last one, regardless of timing of ammonium supplementation (Tables 3 and S1).

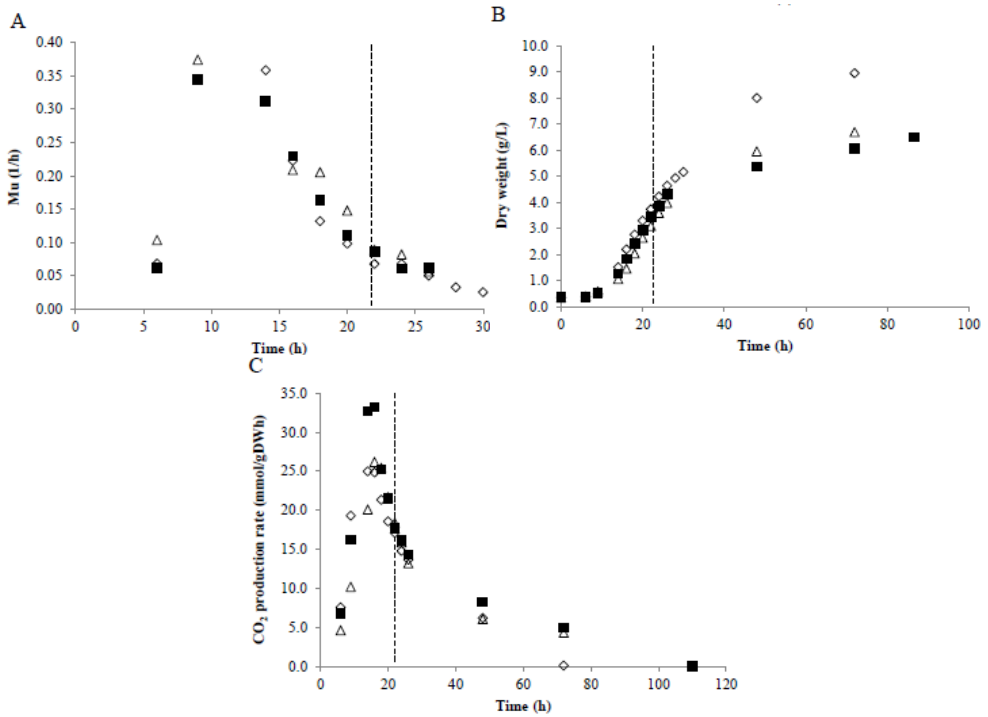

Figure 4. Evolution of different parameters along wine fermentation in SM500E (Δ), SM500L (◊) and SM200C (■): A) Growth rate (h^{-1}); B) Dry weight (g L^{-1}); and C) CO_2 production rate ($mmol^{-1}$ gDW^{-1} h^{-1}). Dashed-line indicates the moment when nitrogen was depleted in SM200C. In all cases, relative standard deviation was <5%.

Volatile compounds produced during fermentation

Major components of the volatile fraction were analyzed at different time points during fermentation experiments. Principal component analysis (PCA) showed that aroma profile at early stages of the process was mainly conditioned by fermentation time, rather than must composition (Figure 5). For all fermentation conditions component 2, mostly contributed by ethyl esters, gradually increased during the first day of fermentation, but had declined by the end of the process. Component 1, mainly contributed by phenylethyl acetate and fusel alcohols (especially 2-phenylethanol, 2-methylbutanol, and 3-methylbutanol) was clearly affected by ammonium addition, but only for over-supplemented must. While the abundance of these volatile compounds continually increased up to the end of fermentation for SM200C/E/L, such an increase was not observed for the over-supplemented experiments SM500E/L. A similar trend was observed for phenylethyl acetate (Figure S2). Finally, propanol production followed a particular pattern

(Figure S2), levels of this compound were high by the end of fermentation, but only for three samples (SM200L and SM500E/L). No other fusel alcohol showed a similar pattern among those analyzed.

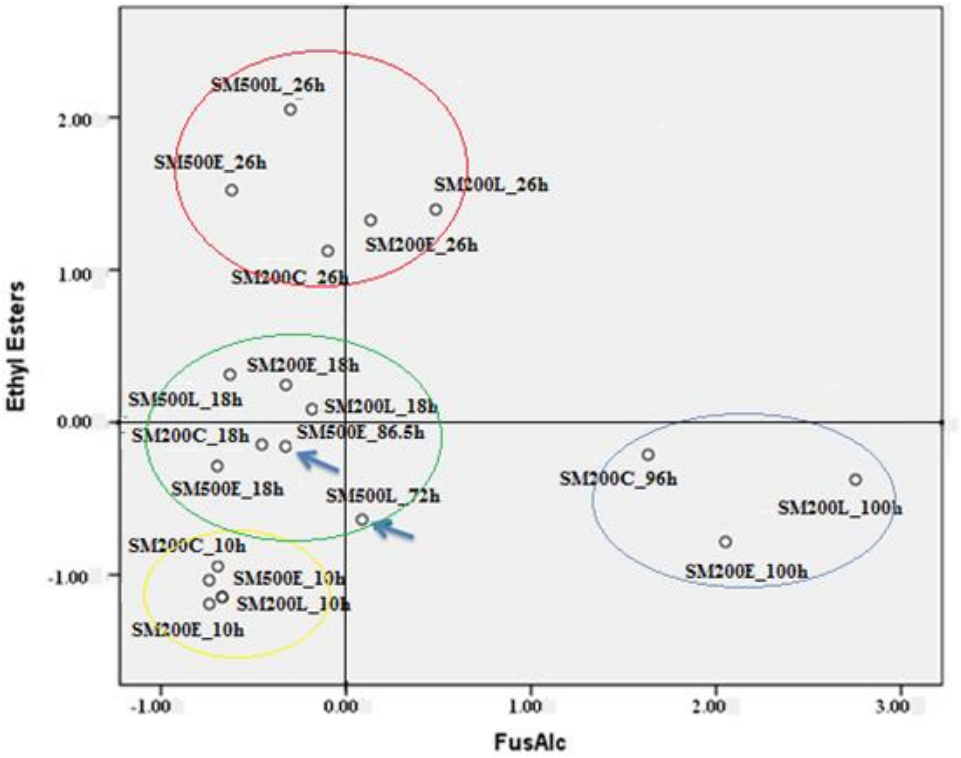

Figure 5. Principal component analysis of volatile compounds by the end of alcoholic fermentation in all the conditions studied. Component 1 (FusAlc), mainly contributed by phenylethyl acetate and fusel alcohols explained 43.56% of total variance. Component (EthylEsters), mostly contributed by ethyl esters, explained 26.24% of the variance.

Discussion

Yeast growth and fermentation kinetics in the two basal media designed for this study, SM200C and SM100, showed the expected profiles for a nitrogen sufficient grape must, or a nitrogen deficient one, respectively. Evolution of all the parameters under study for SM100 is in agreement with an aberrant fermentation profile Type III (normal initiation of fermentation, rate becoming sluggish) according to the classification proposed by Bisson and Butzke (2000). This kind of sluggish fermentation is usually related to the short supply of some nutrients.

The strong dependence of fermentation kinetics and length on nitrogen availability was confirmed in our experimental conditions (Figure S1). Fermentation length was very similar for the control must (SM200C) and those supplemented with ammonium to standard levels (SM200E/L). However it was clearly shorter (Figure S1 and Table 3) for over-supplemented musts (500 mg L^{-1} YAN).

There is a good agreement between biomass production and fermentation length in the different assays. Noticeably, the shortest fermentation time is observed for the assay with the highest final biomass content (SM500L). Indeed, the positive impact of ammonium addition on fermentation length is well established (Cantarelli 1957a, 1957b, Beltran et al. 2004, Mendes-Ferreira et al. 2004, Beltran et al. 2005). The effect of nitrogen availability on growth rate was only observed in the case of nitrogen deficiency. The highest growth rate values obtained for SM100 are clearly below those of the control or over-supplemented fermentations. This observation do not support the statement by Taillandier et al. (2007), who concluded that nitrogen supplementation had no impact on yeast growth rate in must. However, no clear differences in maximum growth rate were observed between nitrogen sufficient or over-supplemented fermentation experiments. This indicates that, even though strong nitrogen limitation might restrict yeast growth rate in grape must, it no longer limits yeast growth rate over a certain threshold (between 100 and 200 mg L^{-1} YAN for EC1118, according to this work and to previous results by Martinez-Moreno et al. (2012)). The differences in final biomass between conditions showing similar maximum growth rates (SM200C/E/L vs. SM500E/L) should be attributed to a longer growth period, due to the higher nitrogen availability in over-supplemented must. In addition to the effect on biomass production and specific growth rate, there

is a clear impact of ammonium addition on the production rates and final content of sensory relevant yeast-derived metabolites. We will pay special attention to glycerol and acetic acid, two by-products found in relatively high amounts and with high sensorial impact in wine.

The higher amounts of glycerol measured in supplemented fermentations might be related to the higher proportion of ammonium in these experiments. Nitrogen metabolism and glycerol production are closely related to cellular redox balance. Under anaerobic growth conditions, glycerol biosynthesis allows regeneration of the excess reduction equivalents resulting from biomass synthesis (Verduyn et al. 1990). The uptake and metabolism of amino acids involves a higher consumption of NADH, while pathways involved in ammonium assimilation contribute to regenerate the NADH pool (Bakker et al. 2001, Swiegers et al. 2005, Jain et al. 2012). Accordingly, the lowest glycerol formation was observed for the control condition (with the lowest proportion of ammonium). On the other side, over-supplemented must, showing the highest relative ammonium content, resulted in the highest glycerol levels. Beltran et al. (2005), also concluded that higher ammonium consumption was related to higher glycerol production.

Ammonium over-supplementation also resulted in a significant increase in the acetic acid final content. Excess volatile acidity has been reported by several authors for both nitrogen deficient and over-supplemented fermentations (Hernandez-Orte et al. 2002, Vilanova et al. 2007, Barbosa et al. 2009, Torrea et al. 2011). In contrast, we have shown that proper supplementation of a nitrogen deficient must results in a reduction of the final acetic acid content. The main difference between the control fermentation (SM200C) and SM200E/L is in the relative proportions of ammonium and amino acids, indicating that proper ammonium addition (up to 200 mg L^{-1} final YAN) has a positive impact on volatile acidity. Excess acetate production in over-supplemented fermentations might be related to increased biomass production under these conditions. The increased requirement for lipid biosynthesis, and for acetic acid as a lipid precursor, would result in an increased flux through this pathway and increased acetic acid leakage (Pigeau and Inglis 2005, Vilanova et al. 2007). Beltran et al. (2005), found ammonium consumption to stimulate acetic acid production in fermentation experiments supplemented at different time points to a final YAN of 300 mg L^{-1} (40

% of it provided as ammonium salts). Since they found residual nitrogen in all their assay conditions by the end of fermentation, this is in agreement with our results in over-supplemented fermentations (SM500E/L). Due to its positive impact on final volatile acidity and glycerol content, we conclude that ammonium addition would be a better choice than organic nitrogen in order to correct nitrogen deficiencies. However, this will hold true only when nitrogen over-supplementation is avoided.

Production of other organic acids is also influenced by nitrogen addition strategies. Succinic acid production in winemaking has been shown to be affected by several factors, including yeast strain, fermentation temperature, aeration, clarification, sugar concentration, pH, titratable acidity or sulfur dioxide concentration (Bell and Henschke 2005, Swiegers et al. 2005). At least three different pathways have been proposed for succinic acid release under anaerobic conditions. The most widely accepted is succinate formation by the oxidative branch of the tricarboxylic acid (TCA) pathway (Nordstro 1968, Oura 1977). In addition, Camarasa et al. (2003) proposed two alternative non-exclusive pathways for succinic acid biosynthesis under winemaking conditions: the reductive branch of the TCA cycle, and the reverse pathway from glutamate. The relative contribution of each pathway would show high variability depending on the nitrogen source. Our data support the influence of nitrogen sources on succinic acid production, whose final content followed the opposite trend than that described above for acetic acid. This might be related to the fact that biosynthesis of both molecules is relatively minor under anaerobic conditions, and both compete for pyruvate availability.

The effect of nitrogen supplementation on lactic acid production has not been previously studied. We found lactic acid production to be always higher in supplemented musts. Since lactic acid production under anaerobic conditions is produced by the methyl-glyoxal by-pass under overflow metabolism (Pronk et al. 1996), this results suggest that nitrogen addition would result in an increase in the glycolytic flux.

Concerning consumption patterns of the different nitrogen sources, there are some features that are shared among all conditions studied. Lysine and histidine were quickly consumed in all fermentation experiments. This fact could be related to the constitutive expression of their permeases during yeast growth under fermentative conditions (Beltran et al. 2004). In contrast, tryptophan and ammonium

were always the last nitrogen sources to be consumed. These consumption patterns are in agreement with the classification of nitrogen sources proposed by Crépin et al. (2012). However, we were unable to identify a pattern relating must composition and the uptake of the remaining nitrogen sources. On the other side, excessive addition of nitrogen during fermentation led to significant residual nitrogen, as described by other authors (Bell and Henschke 2005). Residual nitrogen consisted in ammonium, which challenges the generally accepted view of ammonium as a preferred nitrogen source, but is in agreement with the detailed description of nitrogen utilization under winemaking conditions recently published by Crépin et al. (2012). In addition, residual nitrogen is undesirable in the final wine, as it might promote wine microbial spoilage (Bell and Henschke 2005).

Yeast metabolism of sugar and nitrogen sources during wine fermentation leads to the formation of a variety of volatile compounds, including higher alcohols, fatty acids, other organic acids, esters and sulfur-compounds (Rapp and Versini 1991, Swiegers et al. 2005, Styger et al. 2011, Cordente et al. 2012). Many of these molecules directly or indirectly derive from the catabolism of amino acids. PCA of volatile compounds produced throughout the fermentation showed ethyl esters and fusel alcohols as the main compounds affected by fermentation time or ammonium addition strategies (Figure 5). For all fermentation conditions assayed, formation of ethyl esters is mainly affected by fermentation time (rather than must composition), showing a gradual increase during the first day of fermentation, but a lower value for the final samples. This final low value might be related to hydrolysis or to stripping due to the culture conditions employed. A clear effect of ammonium addition was observed, in contrast, for the formation of fusel alcohols, specifically 2-phenylethanol, 2-methylbutanol, and 3-methylbutanol. An important production of these compounds is observed in the second part of the fermentation process for SM200C/E/L. This final increase was almost undetectable for nitrogen over-supplemented fermentations (Figure 5). So, a major effect of ammonium over-supplementation is the reduction of aroma complexity by limiting the production of some fusel alcohols. This is in agreement to the conclusion by Beltran et al. (2005) who, referring to nitrogen sufficient fermentations, stated that “the closer the nitrogen concentration is to the growth-limiting level, the higher the yield of fusel alcohols is”. These compounds derive from the corresponding α-ketoacid by

reactions of the Ehrlich pathway. In turn, α-ketoacids can derive from amino acid degradation (transamination) or from de novo synthesis from sugars. Cells using ammonium as the main or only nitrogen source would require these α-ketoacids for nitrogen assimilation, withdrawing them from degradation by the Ehrlich pathway, thus limiting fusel alcohol production (Bell and Henschke 2005, Hazelwood et al. 2008). Phenylethyl acetate follows a similar production pattern to its alcohol precursor (2-phenylethanol), with very limited production in over-supplemented fermentations. Indeed, phenylethyl acetate had a similar weight to fusel alcohols for the distribution of samples shown in the PCA analysis (Figure 5).

Finally, propanol production follows a very particular production pattern (Figure S2). Propanol levels did not change from the end of the growth phase for SM200C/E, while they clearly increased from time 26 h to the end of the experiment for SM200L and SM500E/L. The common feature of the experiments in which the final increase in propanol levels was observed is that growth was exclusively supported by ammonium at least for part of the fermentation time. Since threonine can be derived from aspartic acid or asparagine, and it is the precursor of propanol biosynthesis by the Ehrlich pathway, we can speculate that increased assimilation of ammonium through asparagine biosynthesis (one of the minor entry points of ammonium in yeast anabolic pathways) would result in increased production of threonine.

Vilanova et al. (2007) suggested that wine aroma composition might be modulated by a proper design of the ammonium addition strategy, while Barbosa et al. (2009) proposed the use of timing of addition as modulator of wine aroma composition. Our data confirm that either the quality, the quantity, or the time of addition of nitrogen nutrients (ammonium in this case) will have an impact on the final volatile composition.

Conclusions

Ammonium supplementation exerts a clear effect on yeast physiology and metabolite production during winemaking, affecting fermentation length, and the production of biomass, glycerol, acetic acid and volatile aroma compounds. Some parameters are mainly dependent on the nature of the nitrogen sources, while timing of ammonium addition might have an impact for specific molecules. Fermentation length was significantly affected by ammonium over-supplementation, but only when it resulted in increased biomass production.

Our results suggest two advantages of using ammonium instead of organic nitrogen for the correction of nitrogen deficiencies in grape must. Both a slight increase in glycerol production and an important reduction in the amount of acetic acid produced can be appreciated in nitrogen sufficient fermentations with a higher proportion of ammonium. Monitoring of grape must nitrogen content is strongly advised in order to avoid nitrogen over-supplementation, and the concomitant excess of volatile acidity.

These results can contribute to help the choice of nitrogen correction strategies (timing and nature of the nitrogen source) as a tool to modulate the final aroma profile of wines.

Acknowledgements

Authors would like to thank Cristina Juez Ojeda and Miguel Ángel Fernández Recio for excellent technical assistance. This work was funded by the CDTI (Spanish Center for Technological Industrial Development) through the Ingenio 2010-CENIT Program and the AGL2009-07327 and AGL2012-32064 projects from the Spanish Governement. R.M.-M. and M.Q. are recipients of a CSIC JAE-Predoc grant and a CSIC training JAE-Doc contract respectively, both co-funded by the European Social Fund of the EU.

References

Bakker, B. M., K. M. Overkamp, A. J. A. van Maris, P. Kotter, M. A. H. Luttik, J. P. van Dijken, and J. T. Pronk. 2001. Stoichiometry and compartmentation of NADH metabolism in *Saccharomyces cerevisiae*. FEMS Microbiol. Rev. 25: 15-37.

Barbosa, C., V. Falco, A. Mendes-Faia, and A. Mendes-Ferreira. 2009. Nitrogen addition influences formation of aroma compounds, volatile acidity and ethanol in nitrogen deficient media fermented by *Saccharomyces cerevisiae* wine strains. J. Biosci. Bioeng. 108: 99-104.

Beltran, G., M. Novo, N. Rozes, A. Mas, and J. M. Guillamon. 2004. Nitrogen catabolite repression in *Saccharomyces cerevisiae* during wine fermentations. FEMS Yeast Res. 4: 625-632.

Beltran, G., B. Esteve-Zarzoso, N. Rozes, A. Mas, and J. M. Guillamon. 2005. Influence of the timing of nitrogen additions during synthetic grape must fermentations on fermentation kinetics and nitrogen consumption. J. Agric. Food Chem. 53: 996-1002.

Bely, M., J. M. Sablayrolles, and P. Barre. 1990. Automatic detection of assimilable nitrogen deficiencies during alcoholic fermentation in oenological conditions. J. Ferment. Bioeng. 70: 246-252.

Bell, S. J., and P. A. Henschke. 2005. Implications of nitrogen nutrition for grapes, fermentation and wine. Aust. J. Grape Wine Res. 11: 242-295.

Bisson, L. F., and C. E. Butzke. 2000. Diagnosis and rectification of stuck and sluggish fermentations. Am. J. Enol. Vitic. 51: 168-177.

Camarasa, C., J. P. Grivet, and S. Dequin. 2003. Investigation by 13C-NMR and tricarboxylic acid (TCA) deletion mutant analysis of pathways for succinate formation in *Saccharomyces cerevisiae* during anaerobic fermentation. Microbiology 149: 2669-2678.

Cantarelli, C. 1957a. On the Activation of Alcoholic Fermentation in Wine Making. Am. J. Enol. Vitic. 8: 113-120.

Cantarelli, C. 1957b. On the Activation of Alcoholic Fermentation in Wine Making. Part II. Am. J. Enol. Vitic. 8: 167-175.

Carrau, F. M., K. Medina, L. Farina, E. Boido, P. A. Henschke, and E. Dellacassa. 2008. Production of fermentation aroma compounds by *Saccharomyces cerevisiae* wine yeasts: Effects of yeast assimilable nitrogen on two model strains. FEMS Yeast Res. 8: 1196-1207.

Cordente, A. G., C. D. Curtin, C. Varela, and I. S. Pretorius. 2012. Flavour-active wine yeasts. Appl. Microbiol. Biot. 96: 601-618.

Crépin, L., T. Nidelet, I. Sanchez, S. Dequin, and C. Camarasa. 2012. Sequential use of nitrogen compounds by *Saccharomyces cerevisiae* during wine fermentation: a model based on kinetic and regulation characteristics of nitrogen permeases. Appl. Environ. Microb. 78: 8102-8111.

Garde-Cerdan, T., and C. Ancin-Azpilicueta. 2008. Effect of the addition of different quantities of amino acids to nitrogen-deficient must on the formation of esters, alcohols, and acids during wine alcoholic fermentation. Lwt-Food Science and Technology 41: 501-510.

Gomez-Alonso, S., I. Hermosin-Gutierrez, and E. Garcia-Romero. 2007. Simultaneous HPLC analysis of biogenic amines, amino acids, and

ammonium ion as aminoenone derivatives in wine and beer samples. J. Agric. Food Chem. 55: 608-613.

Gonzalez-Marco, A., N. Jimenez-Moreno, and C. Ancin-Azpilicueta. 2010. Influence of nutrients addition to nonlimited-in-nitrogen must on wine volatile composition. J. Food Sci. 75: S206-S211.

Hazelwood, L. A., J. M. Daran, A. J. A. van Maris, J. T. Pronk, and J. R. Dickinson. 2008. The ehrlich pathway for fusel alcohol production: A century of research on *Saccharomyces cerevisiae* metabolism. Appl. Environ. Microb. 74: 2259-2266.

Hernandez-Orte, P., J. F. Cacho, and V. Ferreira. 2002. Relationship between varietal amino acid profile of grapes and wine aromatic composition. Experiments with model solutions and chemometric study. J. Agric. Food Chem. 50: 2891-2899.

Jain, V. K., B. Divol, B. A. Prior, and F. F. Bauer. 2012. Effect of alternative NAD(+)-regenerating pathways on the formation of primary and secondary aroma compounds in a *Saccharomyces cerevisiae* glycerol-defective mutant. Appl. Microbiol. Biot. 93: 131-141.

Jimenez-Marti, E., and M. L. Del Olmo. 2008. Addition of ammonia or amino acids to a nitrogen-depleted medium affects gene expression patterns in yeast cells during alcoholic fermentation. FEMS Yeast Res. 8: 245-256.

Jiranek, V., P. Langridge, and P. A. Henschke. 1995. Amino-acid and ammonium utilization by *Saccharomyces cerevisiae* wine yeasts from a chemically defined medium. Am. J. Enol. Vitic. 46: 75-83.

Marks, V. D., G. K. van der Merwe, and H. J. J. van Vuuren. 2003. Transcriptional profiling of wine yeast in fermenting grape juice: regulatory effect of diammonium phosphate. FEMS Yeast Res. 3: 269-287.

Martinez-Moreno, R., P. Morales, R. Gonzalez, A. Mas, and G. Beltran. 2012. Biomass production and alcoholic fermentation performance of *Saccharomyces cerevisiae* as a function of nitrogen source. FEMS Yeast Res. 12: 477-485.

Mendes-Ferreira, A., A. Mendes-Faia, and C. Leao. 2004. Growth and fermentation patterns of *Saccharomyces cerevisiae* under different ammonium concentrations and its implications in winemaking industry. J. Appl. Microbiol. 97: 540-545.

Mendes-Ferreira, A., M. del Olmo, J. Garcia-Martinez, E. Jimenez-Marti, A. Mendes-Faia, J. E. Perez-Ortin, and C. Leao. 2007. Transcriptional response of *Saccharomyces cerevisiae* to different nitrogen concentrations during alcoholic fermentation. Appl. Environ. Microb. 73: 3049-3060.

Nordstro, K. 1968. Yeast growth and glycerol formation. II. Carbon and redox balances. J. Inst. Brew. 74: 429-432.

Ortega, C., R. Lopez, J. Cacho, and V. Ferreira. 2001. Fast analysis of important wine volatile compounds Development and validation of a new method based on gas chromatographic-flame ionisation detection analysis of dichloromethane microextracts. J. Chromatogr. A 923: 205-214.

Oura, E. 1977. Reaction products of yeast fermentations. Process Biochem. 12: 19-21.

Pigeau, G. M., and D. L. Inglis. 2005. Upregulation of ALD3 and GPD1 in *Saccharomyces cerevisiae* during icewine fermentation. J. Appl. Microbiol. 99: 112-125.

Pronk, J. T., H. Y. Steensma, and J. P. vanDijken. 1996. Pyruvate metabolism in *Saccharomyces cerevisiae*. Yeast 12: 1607-1633.

Quirós, M., R. Martínez-Moreno, J. Albiol, P. Morales, F. Vázquez-Lima, A. Barreiro-Vázquez, P. Ferrer, and R. Gonzalez. 2013. Metabolic flux analysis during the exponential growth phase of *Saccharomyces cerevisiae* in wine fermentations. PLOS ONE 8: e71909.

Rapp, A., and G. Versini. 1991. Influence of nitrogen compounds in grapes on aroma compounds of wines, pp. 156-164, Proceedings of the International Symposium on Nitrogen in Grapes and Wine, Kos, Grece.

Ribéreau-Gayon, P., D. Dubourdieu, B. Donèche, and A. Lanvaud. 2004. Traité d'oenologie. Micobiologia du vin: Vinofocation, 5e édition ed. La vigne, Paris.

Styger, G., B. Prior, and F. F. Bauer. 2011. Wine flavor and aroma. J. Ind. Microbiol. Biotechnol. 38: 1145-1159.

Swiegers, J. H., E. J. Bartowsky, P. A. Henschke, and I. S. Pretorius. 2005. Yeast and bacterial modulation of wine aroma and flavour. Aust. J. Grape Wine Res. 11: 139-173.

Taillandier, P., F. R. Portugal, A. Fuster, and P. Strehaiano. 2007. Effect of ammonium concentration on alcoholic fermentation kinetics by wine yeasts for high sugar content. Food Microbiol. 24: 95-100.

Torrea, D., C. Varela, M. Ugliano, C. Ancin-Azpilicueta, I. Leigh Francis, and P. A. Henschke. 2011. Comparison of inorganic and organic nitrogen supplementation of grape juice - Effect on volatile composition and aroma profile of a Chardonnay wine fermented with *Saccharomyces cerevisiae* yeast. Food Chem. 127: 1072-1083.

Varela, C., F. Pizarro, and E. Agosin. 2004. Biomass content governs fermentation rate in nitrogen-deficient wine musts. Appl. Environ. Microb. 70: 3392-3400.

Verduyn, C., E. Postma, W. A. Scheffers, and J. P. Vandijken. 1990. Physiology of *Saccharomyces cerevisiae* in anaerobic glucose-limited chemostat cultures. J. Gen. Microbiol. 136: 395-403.

Vilanova, M., M. Ugliano, C. Varela, T. Siebert, I. S. Pretorius, and P. A. Henschke. 2007. Assimilable nitrogen utilisation and production of volatile and non-volatile compounds in chemically defined medium by *Saccharomyces cerevisiae* wine yeasts. Appl. Microbiol. Biot. 77: 145-157.

Supplementary material

Tabla S 1. Evolution of YAN (expressed in mg L^{-1}).

	SM200C			SM500E			SM500L		
Time (h)	YAN AA	YAN NH_4	YAN T	YAN AA	YAN NH_4	YAN T	YAN AA	YAN NH_4	YAN T
0	123.51	82.34	205.85	123.51	390.44	513.95	123.51	82.34	205.85
6	116.77	82.1	198.87	110.38	390.63	501.01	120.52	80.35	200.87
9	94.07	75.11	169.18	95.36	385.42	480.78	90.38	70.27	160.65
10	-	-	-	-	-	-	-	-	-
11	-	-	-	-	-	-	-	-	-
12	-	-	-	-	-	-	-	-	-
13	-	-	-	-	-	-	-	-	-
14	45.31	48.13	93.44	55.31	377.15	432.46	47.65	40.02	87.67
15	-	-	-	-	-	-	-	-	-
16	10.49	21.52	32.01	12.49	358.74	371.23	7.36	14.96	22.32
18	0.27	4.41	4.68	0.86	338.42	339.28	0	0.53	0.53
20	0	0.19	0.19	0	332.96	332.96	0	302.48	302.48
22	0	0	0	0	311.25	311.25	0	279.63	279.63
24	-	-	-	0	292.2	292.2	0	257.53	257.53
26	-	-	-	0	273.15	273.15	0	230.86	230.86

	SM200E			SM200L			SM100		
Time (h)	YAN AA	YAN NH_4	YAN T	YAN AA	YAN NH_4	YAN T	YAN AA	YAN NH_4	YAN T
0	75.14	142.73	217.87	75.14	40.37	115.51	75.14	40.38	115.52
6	78.15	138.16	216.31	-	-	-	-	-	-
9	48.03	135.11	183.14	-	-	-	-	-	-
10	-	-	-	30.69	20.35	51.04	34.2	24.25	58.45
11	-	-	-	-	-	-	22.63	19.94	42.57
12	-	-	-	8.23	9.96	18.19	10.01	12.13	22.14
13	-	-	-	-	-	-	2.52	1.14	3.66
14	1.45	89.27	90.72	0	0.25	0.25	0.42	1.02	1.44
15	-	-	-	-	-	-	0	0	0
16	0	44.83	44.83	0	106.54	106.54	-	-	-
18	0	0.76	0.76	0	67.94	67.94	-	-	-
20	0	0	0	0	16.89	16.89	-	-	-
22	-	-	-	0	0.38	0.38	-	-	-
24	-	-	-	0	0	0	-	-	-
26	-	-	-	-	-	-	-	-	-

YAN AA: YAN from amino acids; YAN NH_4: YAN from ammonium;
YAN T: YAN Total = YAN AA + YAN NH_4. Relative standard deviation in all cases was lower than 10%

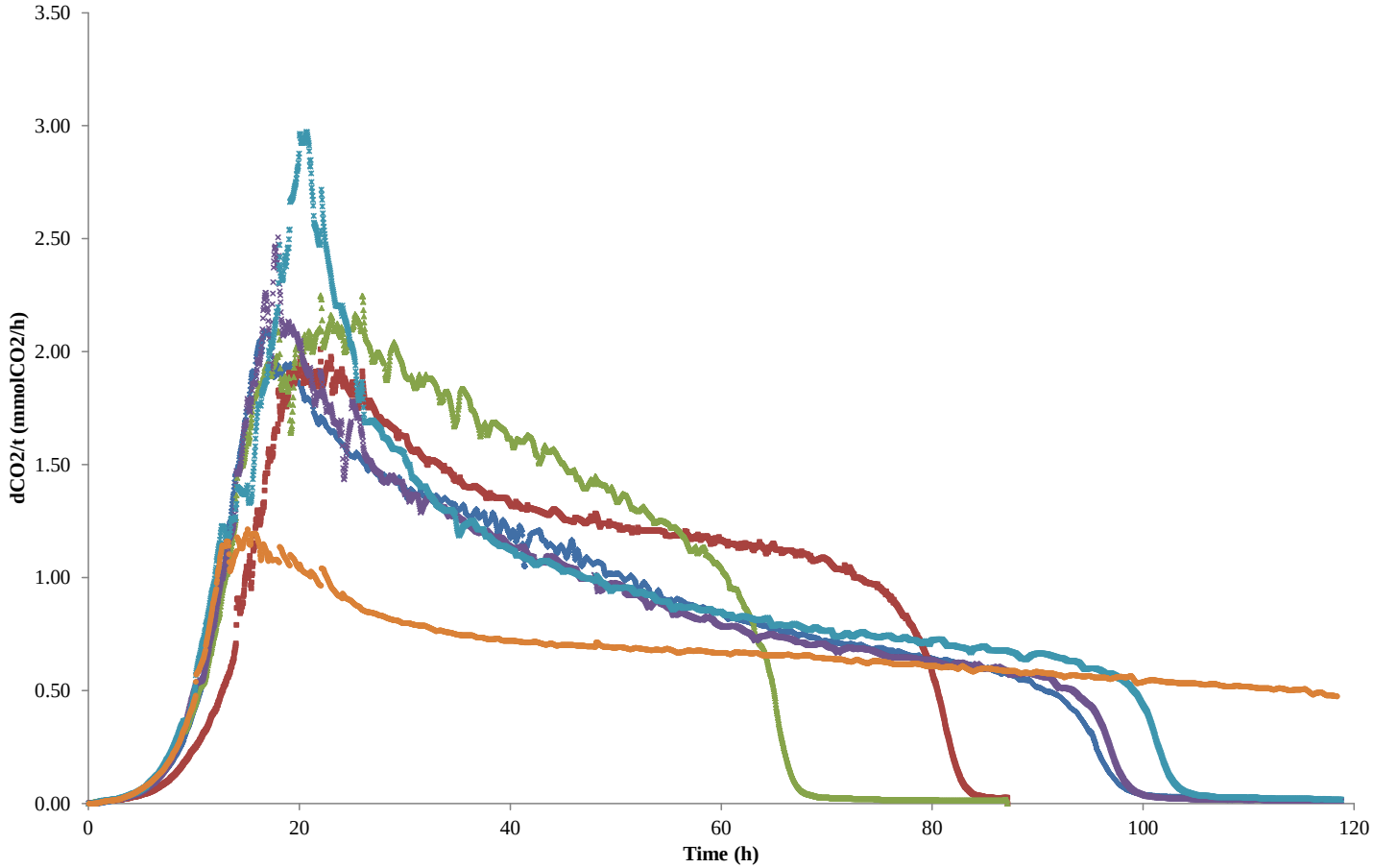

Figure S 1. Real-time CO2 production during fermentations performed with different nitrogen content. Dark blue: SM200C; Orange: SM100; Purple: SM200E; Light blue: SM200L; Red: SM500E; Green: SM500.

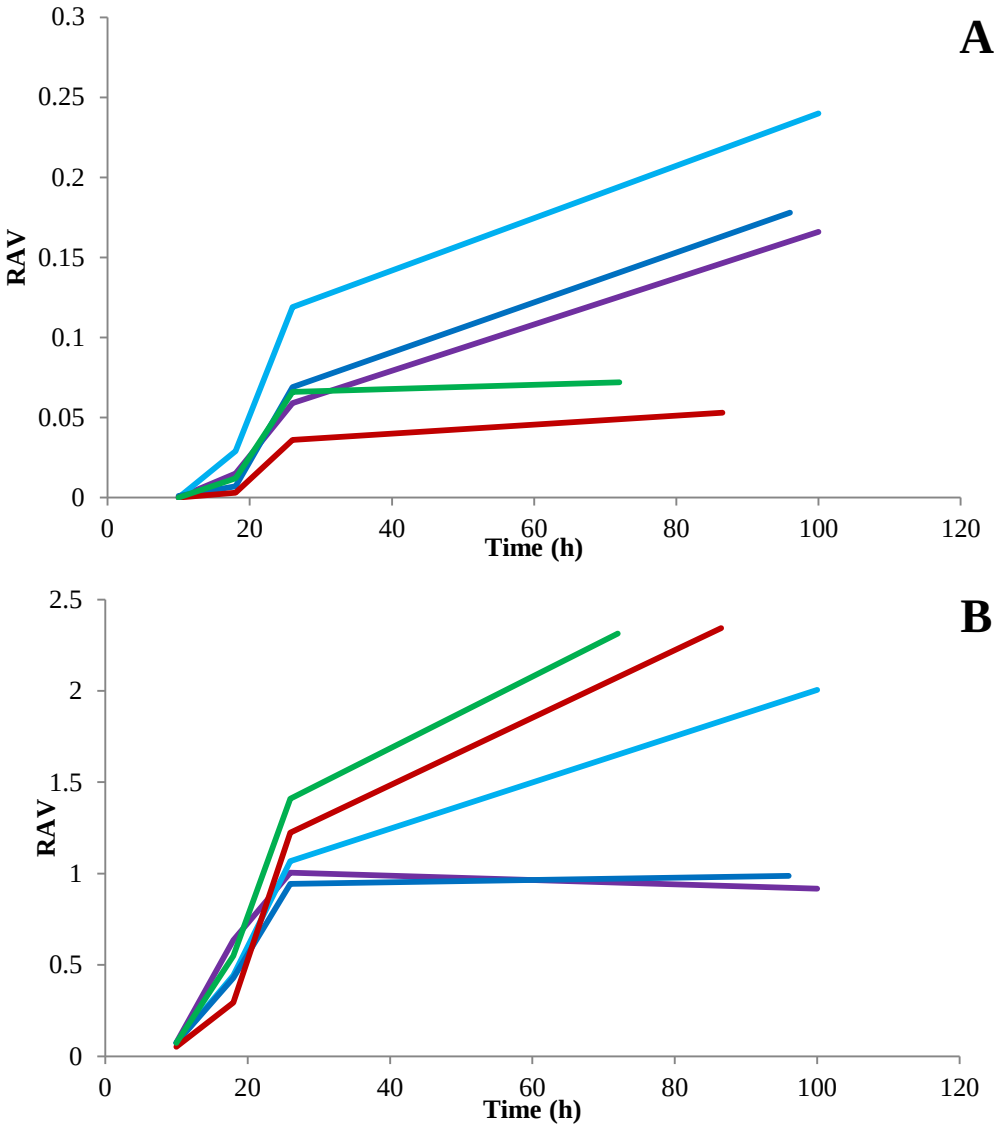

Figure S 2. Relative abundance of A) phenylethyl acetate and B) propanol. RAV: Relative Area Value. Dark blue: SM200C; Purple: SM200E; Light blue: SM200L; Red: SM500E; Green: SM500L.

Chapter V

♦

Carbon fate and macromolecular composition of Saccharomyces cerevisiae wine yeasts in response to nitrogen management

CHAPTER V

Carbon fate and macromolecular composition of *Saccharomyces cerevisiae* wine yeasts in response to nitrogen management

Abstract

Saccharomyces cerevisiae is the most relevant yeast species responsible for the alcoholic fermentation that transforms grape juice into wine. Nitrogen is usually considered as a limiting factor for yeast growth during winemaking. Therefore, assimilable nitrogen is usually measured in wineries and its levels are adjusted by adding ammonium salts in order to prevent stuck or sluggish fermentation. However, this addition has to be controlled considering that an excess of nitrogen sources could result in the production of undesirable yeast metabolites during wine fermentation.
The main goal of this work is to study the effect of ammonium supplementation on the macromolecular composition of wine yeast cells and on carbon fate. Yeasts were grown under different continuous culture conditions where feeds were specifically designed in order to mimic different supplementations of must with ammonium salts. We found significant differences in production rate of several metabolites (biomass, organic acids…) depending on the proportion amino acids:ammonium available in the medium.

Manuscript in preparation

Introduction

Grape juice potentially contains all the nutrients needed to support yeast growth and to ensure complete fermentation. However, while the carbon sources (glucose and fructose) present in the grape juice greatly exceed yeast requirements, nature and concentration of nitrogen sources are highly variable and often become limiting-factors (Pretorius 2000). Nitrogen composition of must affects yeast growth, fermentation performance and duration and, under some conditions, could be the cause of sluggish and/or stuck fermentations. In order to prevent these problems, winemakers usually supplement must with ammonium salts (Bisson and Butzke 2000, Bell and Henschke 2005). As a consequence of these practices, the composition of yeast assimilable nitrogen (YAN) of grape juice could be severely affected. This fact could affect fermentation rate or other fermentation parameters but also the production of other compounds derived from yeast metabolism such as glycerol, acetic acid or fusel alcohols (Albers et al. 1996, Beltran et al. 2005, Gonzalez-Marco et al. 2010).

Continuous culture is a powerful tool of cultivation to obtain accurate data for analyzing the physiology of a biological system (yeast, bacteria…). The concentrations of all compounds present in the medium remain constant in the steady states. Moreover, the growth rate of the biological system also stays constant as well as the rates of all the internal reactions (Hoskisson and Hobbs 2005). Data obtained from continuous culture are useful for analyzing the global distribution of carbon fluxes by using black-box models (Wang and Stephanopoulos 1983) among other like metabolic flux analysis or flux balancing analysis (Calik and Ozdamar 2002, Kauffman et al. 2003, Hoskisson and Hobbs 2005), or the macromolecular composition of the system (Lange and Heijnen 2001).

The main goal of this work is to study the effect of ammonium supplementation on yeast metabolism during the transition stage from exponential to stationary growth phase. We have used data obtained from continuous cultures mimicking different environmental conditions resulting from ammonium supplementation. Both the effect of the concentration of nitrogen sources and the composition of the nitrogen sources have been analyzed.

Material and methods

Yeast strain

The reference industrial wine yeast strain *Saccharomyces cerevisiae* EC1118, isolated from the Champagne region (France) and produced and commercialized by Lallemand Inc. (Ontario, Canada), was used in this work. The strain was routinely maintained at 4 ºC on YPD plates and in glycerol stocks (20 % v v^{-1}) at -80 ºC

Experimental approach

Firstly, a thorough characterization of batch cultures using synthetic musts with different nitrogen supplementations was performed in duplicate. These cultures allowed us to determine the evolution of yeast specific growth rate and conversion rates of the main metabolites (e.g. glucose, glycerol, ethanol, CO_2, biomass, and acetic, lactic and succinic acid) along the whole fermentative process. Secondly, and on the basis of these results, different feed formulations and dilution rates were defined in order to properly mimic the physiological state of yeast cells in the transition from exponential to stationary growth phase of wine fermentations with different nitrogen content using continuous cultures.

Batch and chemostat cultivation conditions

A chemically defined synthetic must previously described by Bely et al. (1990) and modified by Quirós et al. (2013), represents the basis for the formulation of all media used in the present work. This medium, referred to as BM1 and whose composition is detailed in Table 1, was used both for the batch cultures performed for the physiological characterization of the yeast strain and the batch phase of two of the conditions mimicked using continuous cultures (see below). An additional synthetic must, referred to as BM2 and containing the exact same composition as BM1 but half of the concentration of each nitrogen source, was used for the batch phase of the continuous cultures mimicking a must with poor nitrogen content that is supplemented with ammonium salts to reach 200 mg L^{-1} YAN (Table 1).

Table 1. Media used in this work.

	Media formulation for batch cultures		Feed formulation for continuous cultures		
	BM1	BM2	CSM	SM450	SM100
C sources (g L^{-1})					
Glucose	120.0	120.0	120.0	120.0	120.0
Fructose	120.0	120.0	120.0	120.0	120.0
Malic acid	6.0	6.0	6.0	6.0	6.0
Citric acid	6.0	6.0	6.0	6.0	6.0
N sources (mg L^{-1})					
Alanine	97.0	48.5	29.1	29.1	0.0
Arginine	245.0	122.5	73.5	73.5	0.0
Aspartate	29.0	14.5	8.7	8.7	0.0
Cysteine	14.0	7.0	4.2	4.2	0.0
Glycine	12.0	6.0	3.6	3.6	0.0
Glutamine	333.0	166.5	99.9	99.9	0.0
Glutamate	80.0	40.0	24	24	0.0
Histidine	23.0	11.5	6.9	6.9	0.0
Isoleucine	22.0	11.0	6.6	6.6	0.0
Leucine	32.0	16.0	9.6	9.6	0.0
Lysine	11.0	5.5	3.3	3.3	0.0
Methionine	21.0	10.5	6.3	6.3	0.0
Phenylalanine	25.0	12.5	7.5	7.5	0.0
Proline	400.0	200.0	120	120	0.0
Serine	52.0	26.0	15.6	15.6	0.0
Threonine	50.0	25.0	15	15	0.0
Tryptophan	116.0	58.0	34.8	34.8	0.0
Tyrosine	13.0	6.5	3.9	3.9	0.0
Valine	29.0	14.5	8.7	8.7	0.0

Continued on next page

	Media formulation for batch cultures		Feed formulation for continuous cultures		
	BM1	BM2	CSM	SM450	SM100
NH_4Cl	306.0	153.0	137.7	1582	382.5
Micronutrients and other additives					
YNB* (g L^{-1})	1.70	1.70	1.70	1.70	1.70
Myo-inositol (mg L^{-1})	20.0	20.0	20.0	20.0	20.0
$K_2S_2O_5$ (mg L^{-1})	60.0	60.0	60.0	60.0	60.0
Ergosterol (mg L^{-1})	15.5	15.5	15.5	15.5	15.5
Oleic acid (mg L^{-1})	5.5	5.5	5.5	5.5	5.5
Tween 80 (ml L^{-1})	0.5	0.5	0.5	0.5	0.5
	BM1	BM2	CSM	SM450	SM100
Total YAN	200	100	72	450	100
Organic YAN (%)	60	60	50	8	0
Inorganic YAN (%)	40	40	50	92	100

* YNB w/o amino acids w/o ammonium sulfate

All fermentations were carried out at 28 ºC in a DASGIP parallel fermentation platform (DASGIP AG, Jülich, Germany) equipped with four SR0400SS vessels. Agitation was set to 250 rpm and anaerobic conditions maintained by gassing the headspace of the bioreactors with 4.5 sL h^{-1} of pure nitrogen gas. The effluent fermentation gas was measured every 30 s in order to determine the concentration of CO_2 with a GA4 gas analyzer (DASGIP AG). pH of the medium was kept constant (pH 3.5) during batch and continuous cultures by the automatic addition of 2 N NaOH.

Pre-cultures of EC1118 strain were grown in 25 mL of YPD broth, incubated at 28 ºC and 150 rpm orbital shaking for 48 h. Cells were then washed twice in sterile deionized water, resuspended in 5 mL of sterile distilled water and inoculated to an initial OD_{600} 0.2. Batch cultures were performed in duplicate using 300 mL as the initial working volume. Continuous cultures were performed in duplicate at a constant volume of 200 mL and a dilution rate (D) of 0.08 h^{-1}, mimicking yeast growth rate during the transition from exponential to stationary phase in wine

fermentations. Steady states were sampled only after all continuous cultures had been running for at least 5 residence times and the CO_2 production rate, and the concentration of biomass and the main metabolites were constant.

Feed formulation for continuous cultures

In order to mimic yeast physiology during the transition from exponential to stationary phase in wine fermentations with different nitrogen content, three different feed formulations, with variations in the nature and concentration of N sources were employed. All variations stated below are referred to the BM1 synthetic must indicated above and whose formulation is described in Table 1.

According to results from batch fermentations, in order to mimic N-limited conditions found on a control must containing an N concentration of 200 mg L^{-1} YAN, the organic and inorganic N content of the feed was reduced by 70 and 55 %, respectively (Table I). This condition will be referred to as CSM (Control Synthetic Must) throughout the text. In order to simulate N-limited conditions found on a must naturally containing an initial poor nitrogen content (100 mg L^{-1} YAN) that is supplemented with inorganic ammonium salts prior to the onset of fermentation, the feed was prepared by removing all organic nitrogen sources and adjusting the concentration of NH_4Cl to 382.5 mg L^{-1}. This condition will be referred to as SM100 throughout the text. Finally, for conditions mimicking a must containing an adequate nitrogen content of 200 mg L^{-1} YAN yet oversupplemented with inorganic ammonium salts prior to fermentation, the feed was formulated reducing the concentration of amino acids present in the BM1 must by 70 % and adjusting the concentration of NH_4Cl to 1.58 g L^{-1} (which involves continuous culture running under non N-limited conditions). This condition will be referred to as SM450 throughout the text. The detailed composition of these three media is shown in Table 1.

Analytical methods

Biomass concentration

Cell growth was monitored by OD_{600} measurement during the course of batch fermentations. Samples were diluted in duplicate with deionized water to obtain values in the linear range of 0.1-0.4. OD_{600} values were then transformed to

biomass dry cell weight (g L^{-1}) using a calibration curve previously determined for *S. cerevisiae* EC1118 in BM1 synthetic must. In the steady state, biomass dry weight was determined in triplicate by filtering 10 mL of the cultures through pre-dried and pre-weighed 0.45 µm pore size nitrocellulose filters (Millipore, Billerica, USA). Filters were heat dried at 70 °C until constant weight (24-48 h).

Biomass composition

Approximately 150 mL of each culture in the steady state were centrifuged at 10,000 rpm for 5 minutes and cells washed three times in sterile distilled water. The recovered pellet was immediately frozen by immersion in liquid nitrogen and lyophilized during 72 h. Once lyophilized, cell pellets were additionally dried at 65 °C for 24 h.

Biomass macromolecular components were determined as follows. To determine total carbohydrate content, an aqueous solution of lyophilized biomass was prepared at a concentration of 0.1 g L^{-1} and subjected in triplicate to the phenol-sulphuric acid method as described by Segarra et al. (1995) using a standard curve of glucose (Sigma-Aldrich). Total protein content and amino acid composition of cell protein were determined following the protocol described by Carnicer et al. (2009). Finally, the lipid fraction was determined by a modification of the protocol described by Hara and Radin (1978) as described by Carnicer et al. (2009).

For elemental composition analysis, 1 mg of lyophilized biomass was analyzed in an EA 1110 CHNS-O elemental analyzer (CE-Instruments/Thermo Fisher Scientific) coupled to an E3200 autosampler and a thermoconductivity detector. Biomass ash content was determined as the weight difference after calcinating a known amount of lyophilized biomass in a muffle furnace at 800 °C for 24 h.

Extracellular metabolites

The concentrations of glucose, glycerol, ethanol and lactic, acetic and succinic acid were determined in duplicate by HPLC using a Surveyor Plus chromatograph (Thermo Fisher Scientific, Waltham, MA) equipped with a refraction index and a photodiode array detector (Surveyor RI Plus and Surveyor PDA Plus,

respectively) on a 300 × 7.7 mm HyperREZTM XP Carbohydrate H+ (8µm particle size) column and guard (Thermo Fisher Scientific) as described elsewhere (Quirós et al. 2013). The concentration of each amino acid was analyzed in duplicate according to the method of Gomez-Alonso et al. (2007) using an Accela 600 chromatograph (Thermo Fisher Scientific) equipped with a PDA detector and a 250 × 4.6 mm ACE C18-HL ID (5 µm particle size) column and guard (ACE, Aberdeen, Scotland). The concentration of ammonium was determined enzymatically using the R-Biopharm assay kit (Darmstadt, Germany).

Consistency check, data reconciliation and statistical analysis

Data obtained during continuous cultures were checked for consistency and reconciled based on a χ^2-test ($p \leq 0.05$) as proposed by Wang and Stephanopoulos (1983). The test proposed by Lange and Heijnen (2001) was used for verification of consistency and reconciliation of macromolecular and elementary biomass compositional data. This test allowed estimating the nucleic acids content.

The physiological parameters and metabolic fluxes obtained in all conditions were compared by means of Student's t-test at 95 % confidence level. Principal Components Analysis (PCA) was performed in order to identify relevant experimental condition effects using the SPSS win 19.0 software (IBM Corp., Armonk, USA).

Software

All numerical calculations were performed using Matlab 2010b (MathWorks Inc., Natick, MA, USA).

Results and discussion

Conversion (consumption and production) rates (Table 2) were experimentally obtained from two independent biological replicates for each condition (see Material and Methods) and represent the basis for all the calculations performed in this work. Carbon, nitrogen and redox balances closed with >95% recovery in all cases. Conversion rates determined for each steady state condition were within the range of rates estimated during the transition from exponential to

stationary phase in the batch cultivations performed aiming to emulate fermentations with different content on nitrogen sources (data not shown, see "Experimental approach" in the Material and Methods section).

Table 2. Consumption and production rates of metabolites measured in the steady states.

	CSM		SM450		SM100	
	C-mmol gDW^{-1} h^{-1}	sd	C-mmol gDW^{-1} h^{-1}	sd	C-mmol gDW^{-1} h^{-1}	sd
Glucose	-38.108	2.408	-36.441	1.296	-39.174	2.093
Fructose	-16.405	1.061	-16.000	1.496	-16.606	1.626
Glycerol	3.738	0.827	3.115	0.482	4.298	0.743
Ethanol	31.094	0.439	30.095	0.300	31.359	0.337
Succinic	0.367	0.081	0.120	0.019	0.266	0.046
Acetic	0.052	0.011	0.049	0.008	0.105	0.018
Lactic	0.075	0.017	0.248	0.038	0.108	0.019
Biomass	2.887	0.622	3.002	0.438	2.865	0.473
CO_2	16.413	0.219	15.839	0.149	16.540	0.168
2MButOH	0.049	0.011	0.017	0.003	0.057	0.011
3MButOH	0.095	0.022	0.036	0.006	0.058	0.011
PropOH	0.063	0.014	0.143	0.024	0.050	0.009
IbutOH	0.115	0.026	0.038	0.006	0.058	0.011
2PheEtOH	0.090	0.021	0.008	0.001	0.015	0.003
Ammonium	-0.181	-0.039	-0.451	-0.075	-0.412	-0.068
Aspartate	-8.79E-03	-1.95E-03	-5.75E-03	-8.89E-04		
Glutamate	-4.12E-02	-9.11E-03	-1.96E-02	-3.03E-03		
Serine	-2.12E-02	-4.69E-03	-1.02E-02	-1.57E-03		
Glutamine	-1.31E-01	-2.90E-02	-6.35E-02	-9.82E-03		
Histidine	-1.46E-03	-3.24E-04	-1.36E-03	-2.10E-04		

Continued on next page

	CSM		SM450		SM100	
	C-mmol gDW^{-1} h^{-1}	sd	C-mmol gDW^{-1} h^{-1}	sd	C-mmol gDW^{-1} h^{-1}	sd
Glycine	-4.39E-03	-9.72E-04	-2.16E-03	-3.35E-04		
Threonine	-2.43E-02	-5.38E-03	-1.17E-02	-1.82E-03		
Arginine	-1.33E-01	-2.94E-02	-6.71E-02	-1.04E-02		
Alanine	-4.65E-02	-1.03E-02	-2.25E-02	-3.49E-03		
Tyrosine	-1.17E-02	-2.60E-03	-5.79E-03	-8.95E-04		
Valine	-2.34E-02	-5.17E-03	-1.34E-02	-2.08E-03		
Methionine	-3.35E-03	-7.43E-04	-1.23E-03	-1.90E-04		
Cysteine	-1.18E-03	-2.62E-04	-3.96E-03	-6.12E-04		
Isoleucine	-1.44E-02	-3.18E-03	-6.92E-03	-1.07E-03		
Tryptophan	-1.62E-02	-3.59E-03	-1.25E-02	-1.94E-03		
Leucine	-1.86E-02	-4.12E-03	-9.03E-03	-1.40E-03		
Phenylalanine	-1.87E-02	-4.14E-03	-9.17E-03	-1.42E-03		
Lysine	-6.49E-03	-1.44E-03	-3.21E-03	-4.96E-04		

2MButOH: 2-Methylbutanol; 3MButOH: 3-Methylbutanol; PropOH: Propanol; IbutOH: Isobutanol; and 2PheEtOH: 2-Phenylethanol.

Physiology of S. cerevisiae during growth with different nitrogen concentrations

First, physiological differences among the three conditions were investigated. Significant changes in the biomass concentration at the steady states were observed. While CSM and SM100 supported a biomass of 1.53 and 1.62 g L^{-1}, respectively, biomass concentration in SM450, the condition simulating nitrogen over supplementation reached 3.16 g L^{-1} (Table 3). Biomass is a key variable during winemaking, as it is well know that its concentration determines fermentation rate (Varela et al. 2004). High biomass concentrations ensure fermentation completion and, therefore, imply a lower risk for the appearance of stuck or sluggish fermentative processes. Concentrations of glucose and fructose, the main carbon sources under these growing conditions, were significantly lower in the steady state of SM450 that in the control condition or SM100, while the concentration of ethanol, glycerol and lactic acid, the main resulting products, were significantly higher (Table

3). Nitrogen over supplementation therefore allows higher conversion rates of biomass, ethanol and CO_2 (expressed in mmol h^{-1}, Figure 1), that under batch conditions would result in an earlier completion of fermentation.

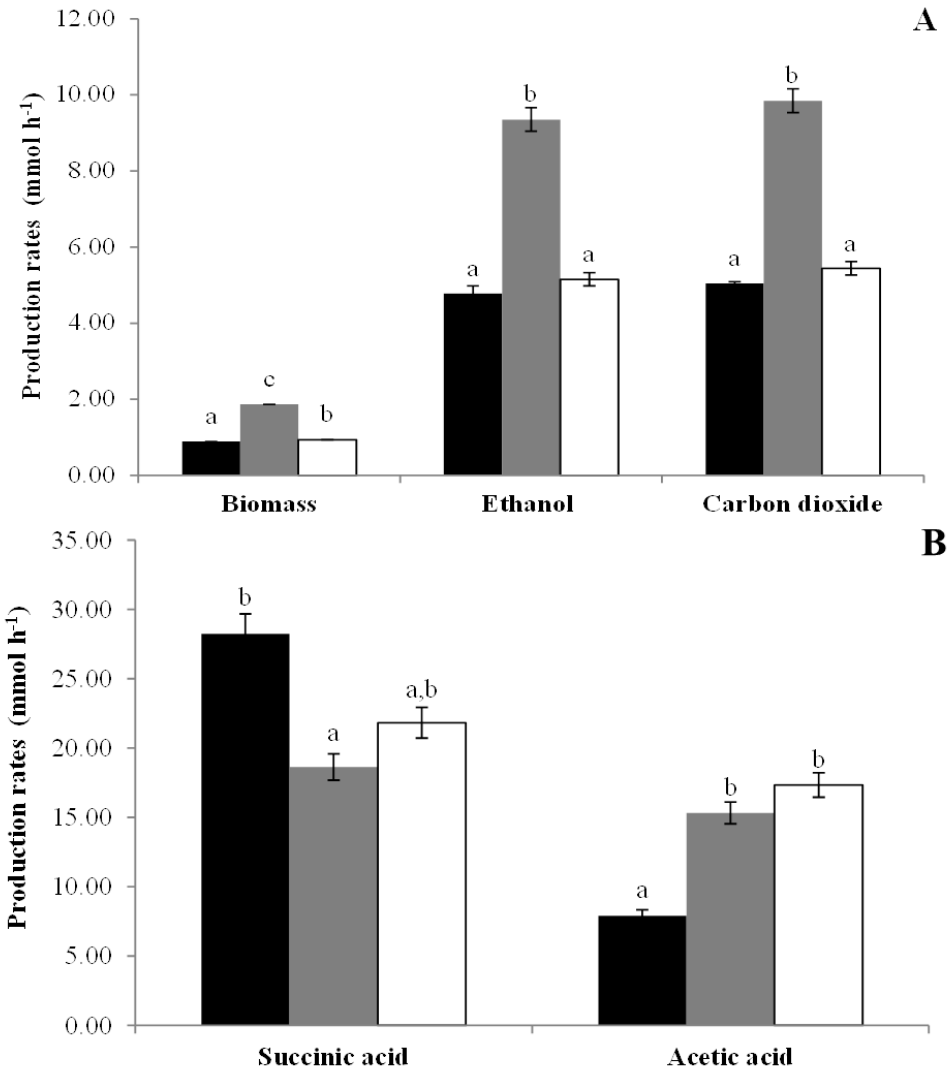

Figure 1. Production rates of A) Biomass, ethanol and CO2; and B) Succinic and acetic acid. Black bars indicates CSM, grey bars SM450 and white bars SM100. Letters indicate significant differences.

On the other hand, production rate of acetic acid was influenced by the nature of nitrogen sources (amino acids or ammonium-). Conditions containing a mixture of amino acids and ammonium (CSM and SM450) supported significantly lower production rates for this acid than SM100, where ammonium was the sole nitrogen source. Moreover, as shown in Figure 1 panel B, the production rate for this organic acid increases proportionally to the contribution of ammonium to the total pool of nitrogen sources. SM100 presented the highest concentration of acetic acid of all steady states (Table 3).

With respect to succinic acid, an inverse relationship between nitrogen availability and succinic acid production rate (both expressed as C-mmol g DW^{-1} h^{-1} or as mmol h^{-1}, Table 2 and Figure 1, respectively) is observed. In this way, SM450 supported the lowest succinic acid production rate of all conditions.SM450 showed statistically lower concentration of succinic acidthan CSM and MS100 in the steady states (Table 3).

Table 3. Steady-state nutrient concentrations in continuous cultures.

	CSM	SM450	SM100
Glucose (g L^{-1})	105.85 ± 1.44^{b}	82.35 ± 1.61^{a}	104.65 ± 0.94^{b}
Fructose (g L^{-1})	118.13 ± 1.73^{b}	104.65 ± 2.01^{a}	118.00 ± 1.16^{b}
Glycerol (g L^{-1})	2.20 ± 0.20^{a}	3.70 ± 0.10^{b}	2.70 ± 0.17^{a}
Ethanol (g L^{-1})	12.40 ± 0.33^{a}	25.83 ± 0.96^{b}	14.42 ± 0.32^{a}
Biomass (g L^{-1})	1.53 ± 0.07^{a}	3.16 ± 0.05^{b}	1.62 ± 0.03^{a}
Lactic acid (mg L^{-1})	43.55 ± 1.32^{a}	289.53 ± 5.77^{b}	66.81 ± 0.24^{a}
Succinic acid (mg L^{-1})	208.34 ± 4.07^{b}	137.56 ± 2.69^{a}	161.12 ± 2.02^{b}
Acetic acid (mg L^{-1})	29.74 ± 0.68^{a}	57.51 ± 0.58^{b}	65.04 ± 0.35^{c}

Superscripts indicate significant differences.

General carbon distribution: Yields on substrate (Y_S)

Ammonium addition did not severely affect the general carbon distribution (Table 4). However, slight differences were observed specially for minor metabolites that will be analyzed below based on the internal distribution of fluxes. Independently of the nitrogen source available in medium, between 85.9 and 87.6 % of carbon uptake was consumed in energy production (measured as ethanol and CO_2). The carbon derived towards glycerol production varied between 5.9 and 7.7 % while carbon used for biomass production ranged from 5.1 to 5.7 %. The remaining carbon (0.5-1.3 %) was directed towards the production of other metabolites including acetic acid, lactic acid or succinic acid (Table 4).

Table 4. Yields on substrate (Y_S) of main metabolites produced during chemostats.

Y_S(Cmol Cmol sugar^{-1})	CSM	SM450	SM100
Glycerol	0.069	0.059	0.077
Ethanol	0.570	0.574	0.562
Succinic	0.007	0.002	0.005
Acetic	0.001	0.001	0.002
Lactic	0.001	0.005	0.002
Biomass	0.053	0.057	0.051
CO_2	0.301	0.302	0.297
Total	1.002	1.001	0.996

Cmol sugar = Cmol Glucose + Cmol Fructose

Similarity on the percentage of carbon derived to ethanol and CO_2 production found between conditions (< 2% variation) are in agreement with the strong regulation of pathways related to energy production described by other authors (Pronk 1991, Rodrigues et al. 2006). In contrast, the variations on carbon derived towards the production of glycerol, biomass and organic acids (acetic, lactic and succinic acid) showed a high variability between conditions (23.4, 10.5 and 61.5 % respectively). The biosynthesis of all of these compounds is linked to the internal redox state of the cell and could therefore present higher variability

depending on growth conditions and nitrogen availability (Overkamp 2002, Jain et al. 2012).

Effect of nitrogen on yeast biomass composition

A precise measurement of the macromolecular composition of cells is essential to calculate an accurate flux of carbon to biomass, especially, if the macromolecular composition changes with the culture conditions (Nissen et al. 1997). In this work, the macromolecular composition of biomass was therefore determined in all the conditions studied.

In agreement with previous studies (Verduyn et al. 1990, Albers et al. 1996, Schulze et al. 1996b, Nissen et al. 1997, Varela et al. 2004, Hazelwood et al. 2009, Quirós et al. 2013), proteins and carbohydrates were the main macromolecular constituents of biomass, always representing around 80 % (w w^{-1}). However, this macromolecular composition of the biomass was affected by nitrogen availability in the medium (Table 5). Carbohydrates content was significantly higher in conditions presenting the lowest nitrogen availability (CSM and SM100). Our data support previous observations which indicate that reserve carbohydrates (glycogen and trehalose) are accumulated under nitrogen-limited and excess of glucose conditions (Schulze et al. 1996b, Schulze et al. 1996a, Varela et al. 2004, Hazelwood et al. 2009). The lowest flux to carbohydrates biosynthesis was observed in the absence of nitrogen limitation (SM450). This fact could be due to the higher biomass formation detected in SM450. So, according to current literature, most of the carbohydrates present in SM450 would be structural molecules (Albers et al. 1998, Lange and Heijnen 2001, Varela et al. 2004, Quirós et al. 2013).

Table 5. Macromolecular composition of biomass expressed in molar percentage.

	CSM	SM450	SM100
Proteins*	32.50[a]	51.01[b]	31.52[a]
Carbohydrates*[#]	48.93[b]	32.17[a]	46.56[b]
Lipids*	5.87[a]	7.82[a]	7.55[a]
Nucleic acids**[#]	12.70[b]	9.01[a]	14.37[b]

*Relative standard deviation was <5% in the measured data.
**Calculated by difference.
[#]Reconciliated data was used for calculations.
Letter indicates significant differences in the content of each macromolecular component in the biomass

Protein content was significantly lower in the conditions with the lowest amount of nitrogen available in the medium (CSM and SM100). The excess of ammonium in SM450 would allow the synthesis of amino acids supporting a higher synthesis of proteins (Schulze et al. 1996a). The different nitrogen composition of the medium did not significantly affect to amino acid composition of proteins. The most interesting difference was observed for proline, whose contribution to protein in CSM was higher than in SM100 and SM450, probably due to the proportionally higher uptake of arginine from the medium (Table 6). In general, these results are in agreement with data presented by Albers et al. (1996), where cells growing in media with different nitrogen composition presented the same protein content, although protein content analyze by Albers and co-workers (1996) were performed at the end of fermentation while our data correspond to an intermediate stage during wine fermentation.

Table 6. Amino acid composition of protein (% mol mol^{-1}).

	CSM	SM100	SM450
Aspartate+Asparagine	10.64	10.83	10.53
Serine	7.13	7.25	7.30
Glutamate+Glutamine	11.05	10.91	10.71
Glycine	7.49	8.24	7.86
Histidine	2.09	2.23	2.33
Arginine	4.81	4.28	4.45
Threonine	6.09	6.19	6.07
Alanine	8.41	8.59	11.04
Proline	7.40^{b}	4.30^{a}	4.22^{a}
Cysteine	0.30^{b}	0.36^{b}	0.20^{a}
Tyrosine	2.55	2.45	2.47
Valine	6.30	7.06	6.79
Methionine	1.47	1.49	1.55
Lysine	7.62	7.96	7.82
Isoleucine	4.89	5.48	4.90
Leucine	8.01	8.42	7.99
Phenylalanine	3.74	3.97	3.74
Triptophan	0.01	0.02	0.03

Relative standard deviation was <5%.
Superscripts indicate significant differences in the content of each amino acid in the protein. Absence of letter indicates that significant differences were not found in the content of each amino acid in the protein

Conclusions

Our results show that both the concentration and the composition of the nitrogen sources could affect yeast metabolism. However, the latter factor seems to exert a strong influence on carbon fate and macromolecular composition of yeast during the transition from exponential growth phase to stationary phase and has played a key role in the production of metabolites with oenological interest like acetic acid, glycerol or biomass.

Data obtained in this work will be run in genome-scale models developed for mimicking this stage of wine fermentation. The result of these tests will contribute to determine the effect of both nitrogen amount of the medium and the composition of the nitrogen on metabolic flux distribution of yeast. Moreover, we expect to obtain more detailed conclusions about of the effect on yeast physiology of different strategies of nitrogen supplementation of must.

Acknowledgements

Authors would like to thank Cristina Juez Ojeda and Miguel Ángel Fernández Recio for technical support. This work was funded by the CDTI (Spanish Center for Technological Industrial Development) through the Ingenio 2010-CENIT Program. R.M.-M. and M.Q. are recipients of a CSIC JAE-pre grant and a CSIC training JAE-Doc contract respectively, both co-funded by the European Social Fund of the EU.

References

Albers, E., L. Gustafsson, C. Niklasson, and G. Liden. 1998. Distribution of C-14-labelled carbon from glucose and glutamate during anaerobic growth of *Saccharomyces cerevisiae*. Microbiol.-UK 144: 1683-1690.

Albers, E., C. Larsson, G. Liden, C. Niklasson, and L. Gustafsson. 1996. Influence of the nitrogen source on *Saccharomyces cerevisiae* anaerobic growth and product formation. Appl. Environ. Microb. 62: 3187-3195.

Beltran, G., B. Esteve-Zarzoso, N. Rozes, A. Mas, and J. M. Guillamon. 2005. Influence of the timing of nitrogen additions during synthetic grape must fermentations on fermentation kinetics and nitrogen consumption. J. Agric. Food Chem. 53: 996-1002.

Bely, M., J. M. Sablayrolles, and P. Barre. 1990. Automatic detection of assimilable nitrogen deficiencies during alcoholic fermentation in oenological conditions. J. Ferment. Bioeng. 70: 246-252.

Bell, S. J., and P. A. Henschke. 2005. Implications of nitrogen nutrition for grapes, fermentation and wine. Aust. J. Grape Wine Res. 11: 242-295.

Bisson, L. F., and C. E. Butzke. 2000. Diagnosis and rectification of stuck and sluggish fermentations. Am. J. Enol. Vitic. 51: 168-177.

Calik, P., and T. H. Ozdamar. 2002. Bioreaction network flux analysis for industrial microorganisms: A review. Rev. Chem. Eng. 18: 553-596.

Carnicer, M., K. Baumann, I. Toplitz, F. Sanchez-Ferrando, D. Mattanovich, P. Ferrer, and J. Albiol. 2009. Macromolecular and elemental composition analysis and extracellular metabolite balances of *Pichia pastoris* growing at different oxygen levels. Microb. Cell Fact. 8: 65.

Gomez-Alonso, S., I. Hermosin-Gutierrez, and E. Garcia-Romero. 2007. Simultaneous HPLC analysis of biogenic amines, amino acids, and ammonium ion as aminoenone derivatives in wine and beer samples. J. Agric. Food Chem. 55: 608-613.

Gonzalez-Marco, A., N. Jimenez-Moreno, and C. Ancin-Azpilicueta. 2010. Influence of nutrients addition to nonlimited-in-nitrogen must on wine volatile composition. J. Food Sci. 75: S206-S211.

Hara, A., and N. S. Radin. 1978. Lipid extraction of tissues with a low-toxicity solvent. Anal. Biochem. 90: 420-426.

Hazelwood, L. A., M. C. Walsh, M. A. H. Luttik, P. Daran-Lapujade, J. T. Pronk, and J. M. Daran. 2009. Identity of the growth-limiting nutrient strongly affects storage carbohydrate accumulation in anaerobic chemostat cultures of *Saccharomyces cerevisiae*. Appl. Environ. Microb. 75: 6876-6885.

Hoskisson, P. A., and G. Hobbs. 2005. Continuous culture - making a comeback? Microbiol.-Sgm 151: 3153-3159.

Jain, V. K., B. Divol, B. A. Prior, and F. F. Bauer. 2012. Effect of alternative NAD(+)-regenerating pathways on the formation of primary and secondary aroma compounds in a *Saccharomyces cerevisiae* glycerol-defective mutant. Appl. Microbiol. Biot. 93: 131-141.

Kauffman, K. J., P. Prakash, and J. S. Edwards. 2003. Advances in flux balance analysis. Curr. Opin. Biotechnol. 14: 491-496.

Lange, H. C., and J. J. Heijnen. 2001. Statistical reconciliation of the elemental and molecular biomass composition of *Saccharomyces cerevisiae*. Biotechnol. Bioeng. 75: 334-344.

Nissen, T. L., U. Schulze, J. Nielsen, and J. Villadsen. 1997. Flux distributions in anaerobic, glucose-limited continuous cultures of *Saccharomyces cerevisiae*. Microbiol.-UK 143: 203-218.

Overkamp, K. 2002. Mitochondrial oxidation of cytosolic NADH in yeast: physiological analysis and metabolic engineering. PhD Thesis., Delft University of Technology Delft, The Nederlands.

Pretorius, I. S. 2000. Tailoring wine yeast for the new millennium: Novel approaches to the ancient art of winemaking. Yeast 16: 675-729.

Pronk, J. T. 1991. Physiology of the acidophilic thiobacilli. PhD Thesis., Delft University of Technology Delft, The Nederlands.

Quirós, M., R. Martínez-Moreno, J. Albiol, P. Morales, F. Vázquez-Lima, A. Barreiro-Vázquez, P. Ferrer, and R. Gonzalez. 2013. Metabolic flux analysis during the exponential growth phase of *Saccharomyces cerevisiae* in wine fermentations. PLOS ONE 8: e71909.

Rodrigues, F., P. Ludovico, and C. Leão. 2006. Sugar metabolism in yeasts: An overview of aerobic and anaerobic glucose catabolism, pp. 101-121, Biodiversity and Ecophysiology of Yeasts. Springer Berlin Heidelberg, New York, USA.

Schulze, U., G. Liden, and J. Villadsen. 1996a. Dynamics of ammonia uptake in nitrogen limited anaerobic cultures of *Saccharomyces cerevisiae*. J. Biotechnol. 46: 33-42.

Schulze, U., G. Liden, J. Nielsen, and J. Villadsen. 1996b. Physiological effects of nitrogen starvation in an anaerobic batch culture of *Saccharomyces cerevisiae*. Microbiol.-UK 142: 2299-2310.

Segarra, I., C. Lao, E. Lopez-Tamames, and M. C. De La Torre-Boronat. 1995. Spectrophotometric methods for the analysis of polysaccharide levels in winemaking products. Am. J. Enol. Vitic. 46: 564-570.

Varela, C., F. Pizarro, and E. Agosin. 2004. Biomass content governs fermentation rate in nitrogen-deficient wine musts. Appl. Environ. Microb. 70: 3392-3400.

Verduyn, C., E. Postma, W. A. Scheffers, and J. P. Vandijken. 1990. Physiology of *Saccharomyces cerevisiae* in anaerobic glucose-limited chemostat cultures. J. Gen. Microbiol. 136: 395-403.

Wang, N. S., and G. Stephanopoulos. 1983. Application of macroscopic balances to the identification of gross measurement errors. Biotechnol. Bioeng. 25: 2177-2208.

AKNOLEDGEMENTS/AGRADECIMIENTOS

Me gustaría agradecer a las instituciones que han hecho posible el desarrollo de este trabajo. A los socios del proyecto Deméter, al Consejo Superior de Investigaciones Científicas (CSIC), que ha financiado mi trabajo a través del programa JAE_Predoc, y al Instituto de Ciencias de la Vid y el Vino (ICVV), mi "segunda vivienda" durante 4 años.

Sin embargo, este apoyo institucional no hubiera resultado en esta tesis sin todo el equipo humano que ha trabajado conmigo codo con codo durante todo este tiempo. Me gustaría agradecer:

- A mis directores de tesis, Ramón González, Pilar Morales y Manuel Quirós, su dedicación y su implicación en este proyecto.
- A todo el grupo de Biotecnología Enológica de la Universitat Rovira i Virgili por su magnífica acogida durante los cuatro meses que estuve con ellos, muy especialmente a Gemma Beltrán y a Albert Mas.
- A todo el grupo de Microbiología Industrial de la Universidad Técnica de Delft por hacerme una estancia tan agradable y provechosa, especialmente a Jack Pronk, Pascale Daran-Lapujade, Markus Bisschops y Tim Vos.
- A todos los compañeros de la Universitat Autònoma de Barcelona, por todo lo que me habéis enseñado en esas estancias breves pero intensas. Sin vuestra aportación esta tesis nunca hubiera visto la luz. Muchas gracias Pau. Muchas gracias Joan.
- A todo el personal y todos los compañeros/as del ICVV. Ha sido un placer conoceros y trabajar con vosotros. Muchas gracias por hacer mi trabajo un poco más fácil y agradable cada día.
- A todo el personal de la Universidad Pública de Navarra por su eficiencia y profesionalidad. Especialmente a Gerardo Pisabarro y Jesús Murillo.
- A mis amigos. Muchas gracias por vuestro apoyo. Particularmente a los que estabais ahí todos los jueves arreglando el mundo (Mai "The teacher", Rober "The fisherman", Txen, Jerome, Nieves y José).
- A mi familia. Especialmente a mi madre, Victoria y a mi hermano, Abimael. Y, cómo no, a mis abuelos Juana y Ramón, que aunque creo que no

entienden muy bien que es eso de “la tesis”, no importa, ellos siempre me animado en todo.

- A Valvanera Caballero. La ÚNICA y VERDADERA responsable de que esta tesis haya visto la luz. Sin tu apoyo, todo esto ni hubiera sido posible ni hubiera tenido sentido. Muchas gracias por todo.
- En general, gracias a todos los que habéis creído en mí y me habéis apoyado.

LIST OF PUBLICATIONS/LISTA DE PUBLICACIONES

Felícitas Vázquez-Lima, Paulina Silva, Antonio Barreiro, **Rubén Martínez-Moreno**, Pilar Morales, Manuel Quirós, Ramón González, Joan Albiol, Pau Ferrer (2013) Use of chemostat cultures mimicking different phases of wine fermentations as a tool for quantitative physiological analysis. Microbial Cell Factories. (Submitted).

Rubén Martínez-Moreno, Manuel Quirós, Pilar Morales, Ramon Gonzalez (2013) New insights into the advantages of ammonium as winemaking nutrient. International Journal of Food Microbiology. (Under revision).

Manuel Quirós, **Rubén Martínez-Moreno**, Joan Albiol, Pilar Morales, Felícitas Vázquez-Lima, Antonio Barreiro-Vázquez, Pau Ferrer and Ramon Gonzalez (2013) Metabolic flux analysis during the exponential growth phase of *Saccharomyces cerevisiae* in wine fermentations. PLOS ONE 8: e71909. doi:10.1371/journal.pone.0071909.

Rubén Martínez-Moreno, Pilar Morales, Ramón Gonzalez, Albert Mas and Gemma Beltran (2012), Biomass production and alcoholic fermentation performance of Saccharomyces cerevisiae as a function of nitrogen source. FEMS Yeast Research, 12: 477–485. doi: 10.1111/j.1567-1364.2012.00802.